Investigation of Factors Affecting Web Fractures in Shear Links

by

Pedro Gálvez, BCE

Thesis

Presented to the Faculty of the Graduate School of

The University of Texas at Austin

in Partial Fulfillment

of the Requirements

for the Degree of

Master of Science in Engineering

The University of Texas at Austin

May 2004

Investigation of Factors Affecting
Web Fracture in Shear Links

Approved by
Supervising Committee:

Michael D. Engelhardt

Karl H. Frank

Acknowledgements

May 2004

Table of Contents

List of Tables

List of Figures

xiii

CHAPTER 1

Introduction

1.1 GENERAL

This thesis documents the results of a research program investigating the cause of web fractures in links of eccentrically braced frames (EBFs). In recent laboratory tests, EBF links have, in some cases, failed prematurely due to fracture of the link web (Arce 2002, Ryu 2004). This chapter provides background information on EBFs, on recent testing of links, and describes the objectives and scope of this research program.

1.2 BACKGROUND ON EBFs

Eccentrically braced frames (EBF) are seismic lateral force resisting systems that combine the ductility of moment resisting frames with the elastic stiffness of concentrically braced frames. EBF's are particularly ductile because the yielding takes place at the link elements in the frame. The plastic deformations in the frame will take place in the link while the rest of the the frame will remain elastic. Figure 1.1 shows three different arrangements of links in EBF's. Link lengths are denoted by the letter "e."
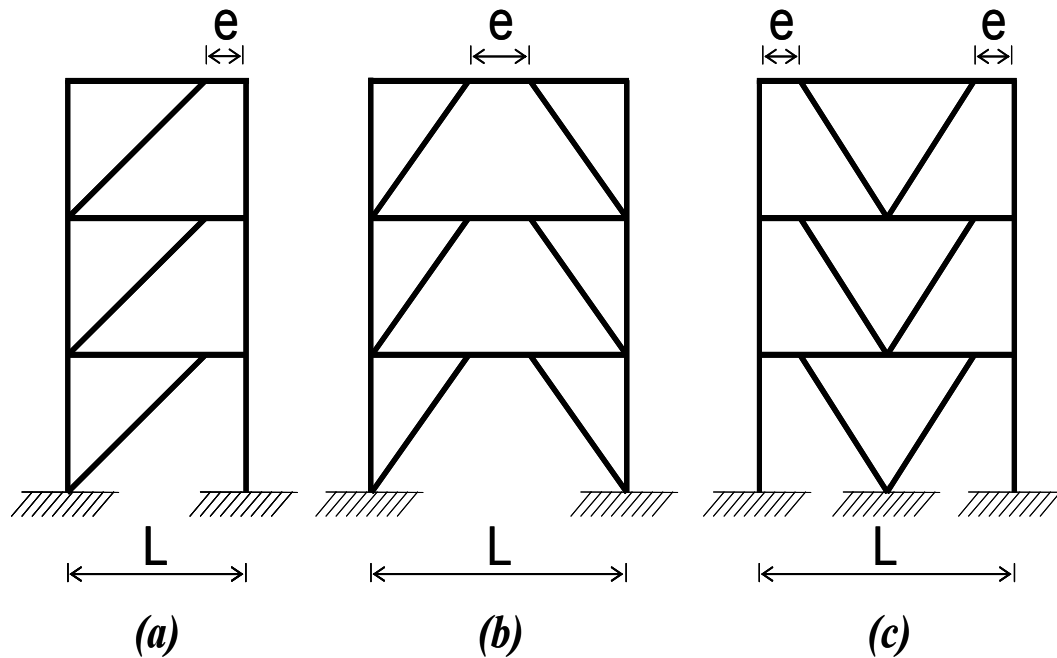
Figure 1.1 Examples of eccentrically braced frames (EBF)

Links in eccentrically braced frames can be classified depending on their length and predominant mode of inelastic behavior. For example, short links will yield primarily in shear while long links will yield primarily in flexure. Meanwhile, intermediate length links yield by a combined effect of shear and flexure.

Links can be divided into three length ranges according to the *AISC Seismic Provisions for Structural Steel Buildings (2002)*:

▪ Long (flexural) yielding links:

$$e \geq 2.6 \frac{M_p}{V_p}$$

- Intermediate length (shear + flexural yielding) links:

$$1.6\frac{M_p}{V_p} < e < 2.6\frac{M_p}{V_p}$$

- Short (shear yielding) links:

$$e \leq 1.6\frac{M_p}{V_p}$$

In the above equations, the plastic shear capacity (V_p) of the link section is calculated as $V_p = 0.6F_y\,(d-2t_f)\,t_w$ and the plastic Moment (M_p) can be calculated as $M_p = ZF_y$. In these equations, Z is the plastic modulus of the section, d is the section's depth, t_f is the flange thickness and t_w is the thickness of the web.

The plastic link rotation achieved by an EBF link, "γ_p", varies depending on link length. Shear links are required to achieve a plastic rotation of at least 0.08 radians, $\gamma_P = \pm\ 0.08$ radian, as specified by the *2002 AISC Seismic Provisions*. Long links, can achieve plastic rotations, γ_P, only on the order of ±0.3 radians (Engelhardt and Popov, 1989). Therefore, shear links are preferable since they provide the best ductility, stiffness and overall strength. Past tests on shear links, conducted primarily in the 1980s, showed that the ultimate failure mode for shear links was inelastic buckling of the web followed by fracture of the web. This failure occurred only after the link achieved plastic rotations of at least ± 0.08 radian, as required by the *AISC Seismic Provisions*. However, in recent research

many shear links failed to achieve the required plastic rotation, γ_p, due to premature fracture of the web.

1.3 RECENT RESEARCH ON SHEAR LINKS

1.3.1 Arce (2002)

Under cyclic loading tests, Arce (2002) observed frequent occurrences of premature fractures in the web of links. These fractures initiated at the termination of fillet welds connecting stiffeners to the link web, at the top and bottom of stiffeners. The fractures then normally propagated horizontally, running parallel to the flanges and ultimately causing failure of the specimens. Shear yielding links (e $\leq 1.6M_p/V_p$) seemed to be especially affected by this problem. Further, these fractures typically occurred prior to web buckling, and in many cases, before the link achieved the required plastic rotation of 0.08 radian. These fractures, originating at the top and bottom of the stiffeners in the links, were not reported in earlier EBF research conducted in the 1980s. The photo in Figure 1.2 shows an example of the cracks in the web of a shear link observed by Arce. Arce attempted to prevent these web fractures by moving the stiffener weld termination further away from the k-area of the link section. The objective was to reduce the stress concentration at the end of the stiffener induced when the stiffener termination is too close to the flange. The purpose was also to move the weld termination away from the k-area of the W-Shape link section, where

4

material toughness and ductility may be low. To examine the effectiveness of this approach, three specimens were tested by Arce. Specimens 4A, 4B and 4C were constructed from A992 steel W10X33 sections from the same heat with a length of 23 inches. The stiffeners in each specimen were welded by the Shielded Metal Arc (SMAW) process with an E7018 electrode. However, the distance between the k-area and the termination of the fillet weld in the stiffener was changed in each specimen. Figure 1.3 shows the details of the welding and arrangement of stiffeners on each of the three specimens. The specimens were tested using the loading protocol specified in appendix S of the *AISC Seismic Provisions 2002.*
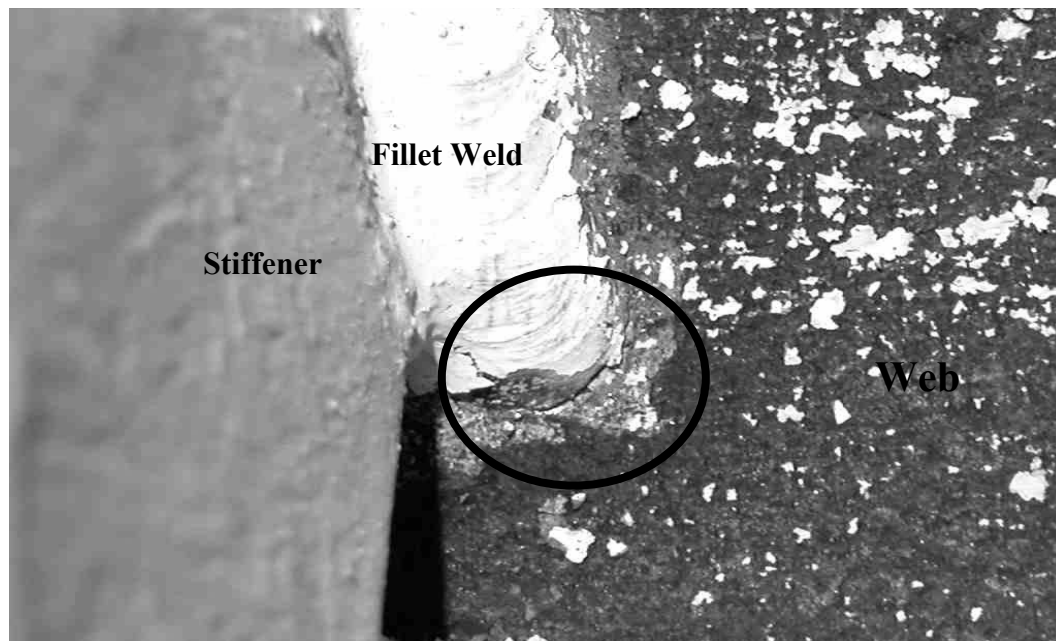
Figure 1.2 Crack observed at the toe of the weld in one of the stiffeners of a shear link tested by Arce (2002).

It was found that by increasing the distance between the termination of the stiffener weld and the flange, the inelastic rotation in the specimens was improved. The results showed that by moving the welding away from the k-line web fractures could be delayed, but not prevented. Based on these results, Arce recommends terminating the stiffener welds a distance of at least five times the link web thickness from the k-line of the section.
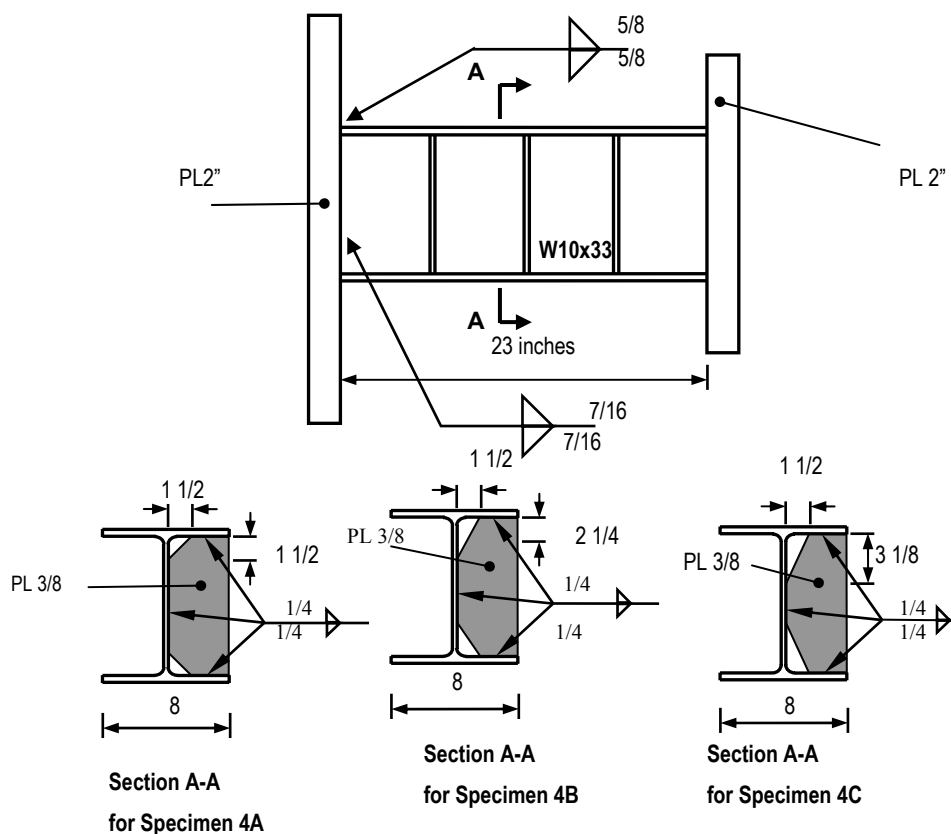
Figure 1.3 Welding detailing on link stiffeners in specimens 4A, 4B and 4C tested by Arce (2002)

1.3.2 Richards and Uang (2002)

Richards & Uang (2002) suggested that the fractures observed by Arce had three possible causes. First, many of the links tested in earlier research programs had stiffeners spaced further apart than currently required by *the AISC Seismic* Provisions or as provided in the specimens tested by Arce. For example, Malley and Popov (1984) conducted a series of tests on shear links using W18X40 and W18X60 sections. They recommended spacing stiffeners at a minimum distance of 20tw for shear links and warned that "close stiffener spacing can lead to abrupt failures before the initiation of web buckling". However, no tests were reported where the spacing between the stiffeners was less than 20tw. According to the *AISC Seismic Provisions,* links of lengths $1.6M_p/V_p$ or less are to be provided with stiffeners spaced at intervals not exceeding (30tw-d/5) for a link rotation of 0.08 radian. Richards and Uang (2002) suggest that the tighter spacing provided for stiffeners in the current provisions may change the controlling mode of failure from web buckling to web fracture. Second, the material properties of the k-area in the wide flange sections are suspected of being part of the cause of the web fractures described above. The *2002 AISC Seismic Provisions* warns of the poor material properties at the k-area. Third, the current loading protocol specified in Appendix S of the *2002 AISC Seismic Provisions* is more severe that loading protocols used to test shear links in past years. Therefore, Richards and Uang developed a revised loading protocol to test shear links.

7

1.3.3 Ryu (2004)

Ryu (2004) extended the test program of Arce (2002) in order to further investigate the causes of the premature link web fractures observed by Arce. The loading protocol used by Arce was considered too severe and was suspected to be one of the causes of the web fractures. Therefore, Ryu used the new loading protocol developed by Richards & Uang (2002). Ryu repeated tests on link sections previously tested by Arce, but used the new loading protocol developed by Richards and Uang. For example, Ryu repeated Arce's Specimens 4A and 4C using the revised loading protocol. The plastic rotation achieved by these specimens using the new loading protocol significantly exceeded the plastic rotation achieved by the original specimens. Further, using the new loading protocol, the specimens were capable of achieving and exceeding the shear link plastic rotation requirement of 0.08 radian. However, even though these links met the rotation requirements of the *AISC 2002 Seismic Provisions* when tested under the new loading protocol, they still exhibited the same fractures at the stiffener weld terminations and failed in a similar fashion to Arce's specimens. Consequently, the work by Ryu (2004) showed that the loading protocol used to test shear links has a large effect on rotation capacity. However, the shear links still ultimately exhibited web fracture prior to web buckling. Thus differences in loading protocol cannot explain the fact that links tested in earlier programs in the 1980s did not exhibit web fractures of the type seen in more recent tests.

1.4 BACKGROUND ON MATERIAL PROPERTIES IN THE K-AREA

The k-area of rolled wide-flange shapes is defined as the region "extending from mid-point of the radius of the fillet from the flange into the web, approximately 1 to 1-1/2 inches beyond the point of tangency between the fillets and web" (section 3.3.2.3, FEMA-350). Figure 1.4 shows the k-area in a typical wide flange beam. This area is characterized by lower toughness and higher hardness, as compared to properties in other areas of the wide-flange cross-section. It is suspected that these properties might make the k-area prone to fracture when welds are placed in this region.

Area of Potential Lower Notch Toughness in Rotary-Straightened W-Shapes
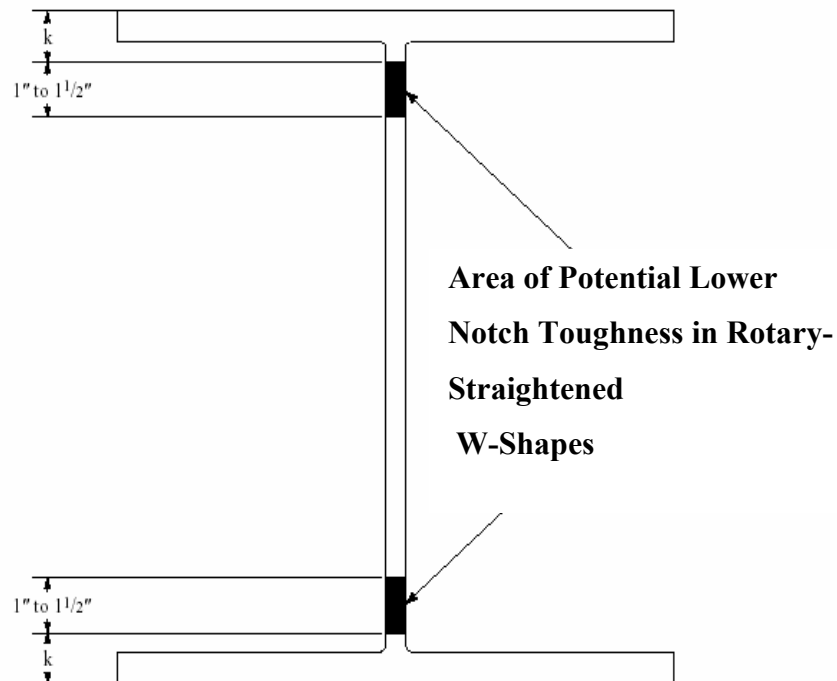
Figure 1.4 "k" Area as shown in the 2002 AISC Seismic Provisions

Miller (1999) suggested that the roller straightening process, used by steel mills to straighten members within required ASTM tolerances, introduced high hardness and reduced the ductility of the material in the k area. However, straightening practices vary among mills and it is difficult to identify steel that has gone through the rolled-straightening process. Therefore, FEMA-350 recommends treating all rolled sections as if they were rotary-straightened.

Poor material properties in the k-area are suspected as a possible cause of the link web fractures observed in tests by Arce (2002) and Ryu (2004). Material testing conducted on these sections (Arce 2002) did, in fact, show very high hardness and low ductility in the k-area of the sections. Changes in mill straightening practices over the years, and resulting changes in k-area material properties, may in part explain why the link web fractures frequently seen in recent tests were not seen in link tests conducted in the 1980s. Nonetheless, the role of k-area material properties in the observed link web fractures is not clear. The correlation of k-area material properties and shear link performance is an issue examined more closely in this thesis.

1.5 OBJECTIVES AND SCOPE OF THE RESEARCH

The overall goal of this research project is to extend previous work by Arce (2002) and Ryu (2004) in investigating factors affecting the occurrence of web fractures in shear links. The goal is to obtain a better understanding of the

factors causing these factors, and possible approaches for delaying or eliminating these fractures. More specifically, the following issues are examined in this research project.

1. *Correlation of k-area material properties and overall shear link performance.*

   As discussed above, it has been postulated that poor material properties of steel in the k-area is a factor responsible for the occurrence of link web fracture. One objective of this project is to collect additional data to determine if the overall performance of a shear link correlates with material properties in the k-area. To examine this correlation, cyclic tests were conducted on different link specimens that were nominally identical, except for their k-area properties. Specimens for this portion of the project were constructed using steel wide-flange sections from three different mills.

2. *Effect of one-sided vs. two sided stiffeners on link web fracture.*

   In recent work by Arce (2002) and Ryu (2004) investigating link web fracture, all shear link specimens were constructed with web stiffeners welded on only one-side of the web. However, for some

cases, the *AISC Seismic Provisions* require stiffeners be provided on both sides of the web. There is a possibility that that links with two-sided stiffeners will fail by web fracture at lower rotation levels than links with one-sided stiffeners. The use of two-sided stiffeners results in additional welding in the k-area of the link section, and may also result in higher local stress concentrations at the termination of the stiffener welds. To determine if the use of two-sided stiffeners exacerbates the fracture problem, tests were conducted on link specimens that were nominally identical, except for the use of stiffeners on one side of the web only, versus the use of stiffeners on both sides of the web.

3. *Effect of other stiffener details on link web fracture.* The *AISC Seismic Provisions* require that link stiffeners be welded to the web of the link section, as well as to both flanges of the link section. A further objective of this research program is to determine if link web fracture can be avoided or delayed by welding the stiffeners only to the web, or welding the stiffeners only to the flanges.

4. *Effect of increased stiffener spacing on link web fracture.* As discussed above, Richards and Uang (2002) noted that most links

tested in the 1980s used stiffeners spaced further apart than currently required by the *AISC Seismic Provisions*. They suggested that this smaller stiffener spacing may change the controlling link failure mode from web buckling to web fracture. To investigate this possibility, a link specimen was tested with stiffeners spaced farther apart than required by the *AISC Seismic Provisions* for a shear link with 0.08 radian of plastic rotation.

5. *Effect of welding process on link web fracture.* In recent work by Arce (2002) and Ryu (2004) investigating link web fracture, stiffeners were welded to link specimens using the shielded metal arc welding (SMAW) process. However, in actual fabrication practice, stiffeners can be welded using a variety of other processes. Other welding processes may provide for higher heat input, and may therefore have a larger effect, and potentially more adverse effect, on the material properties in the heat-affected zone of the link web at the termination of the stiffener weld in the k-area. Consequently, an additional objective of this project was to determine if the process used to weld stiffeners to a link has an effect on the occurrence of link web fracture. To investigate this possibility, a link was tested in which the stiffeners were welded by the SMAW process. This was

compared to a nominally identical link in which the stiffeners were welded using the self-shielded flux cored arc welding (FCAW) process.

6.

The issues described above were investigated in an experimental research program described herein. The following chapter provides a description of the setup, specimens and loading protocols used to test the specimens. This is followed by a detailed description of the cyclic loading performance of each test specimen. The results of the test program are then discussed, along with the design implications of the research.

CHAPTER 2

Experimental Setup and Test Specimens

2.1 INTRODUCTION

This chapter describes the test setup, the shear link test specimens and the loading protocols used in this experimental investigation. In addition, the results of hardness tests and tensile coupon tests for the wide flange sections used in the test specimens are presented.

The test setup is described along with the instrumentation used to gather the data for each specimen. Descriptions are provided for each specimen along with drawings that show key details used for stiffeners and welding. Test specimens were constructed using wide flange sections from three different steel mills, to examine the influence of material property variations on overall link performance. Material test data is presented for each of the three mill sections. Finally, the loading protocols used to test the specimens are presented at the end of the chapter.

2.2 TEST SETUP

2.2.1 Description of Overall Test Setup

The test setup used in these experiments was designed to reproduce the forces and deformations that will occur in a link in a single diagonal EBF. Figure 2.1 shows the key features and dimensions of the setup.

The test setup was previously designed and built by Okazaki (2004) and Arce (2002) for investigations on the experimental performance of links and link-to-column connections. It was originally designed to accommodate links with lengths ranging from 23" up to 73". The shaded region shown in Figure 2.1 is the link specimen, and is the portion of the test setup which is changed for each experiment. For the investigation reported herein, all specimens were built with a link length of 23-inches. A link specimen placed in the test setup is subjected to constant shear throughout its length and to reverse curvature bending. The moment introduced at the south end of the link (column end of link) in the elastic range of behavior is larger than the moment at the north end (Beam end of link), similar to the elastic moments developed in the link of a typical single diagonal EBF. Figure 2.2 compares the distribution of forces in a single EBF and the test setup.

e = 23",36.6",48" or 73"

200"

e

95.19"

Column:
W12x120

Horizontal Beam: W18x76

100 kip Load Cell

96"

Link Specimen:
W10x33,
W10X19,W16X36
Or W10X68

99.93"

150 kip Load Cell

99.93"

300 kip Load Cell

100kip Load Cell

17

Hydraulic
Loading Ram
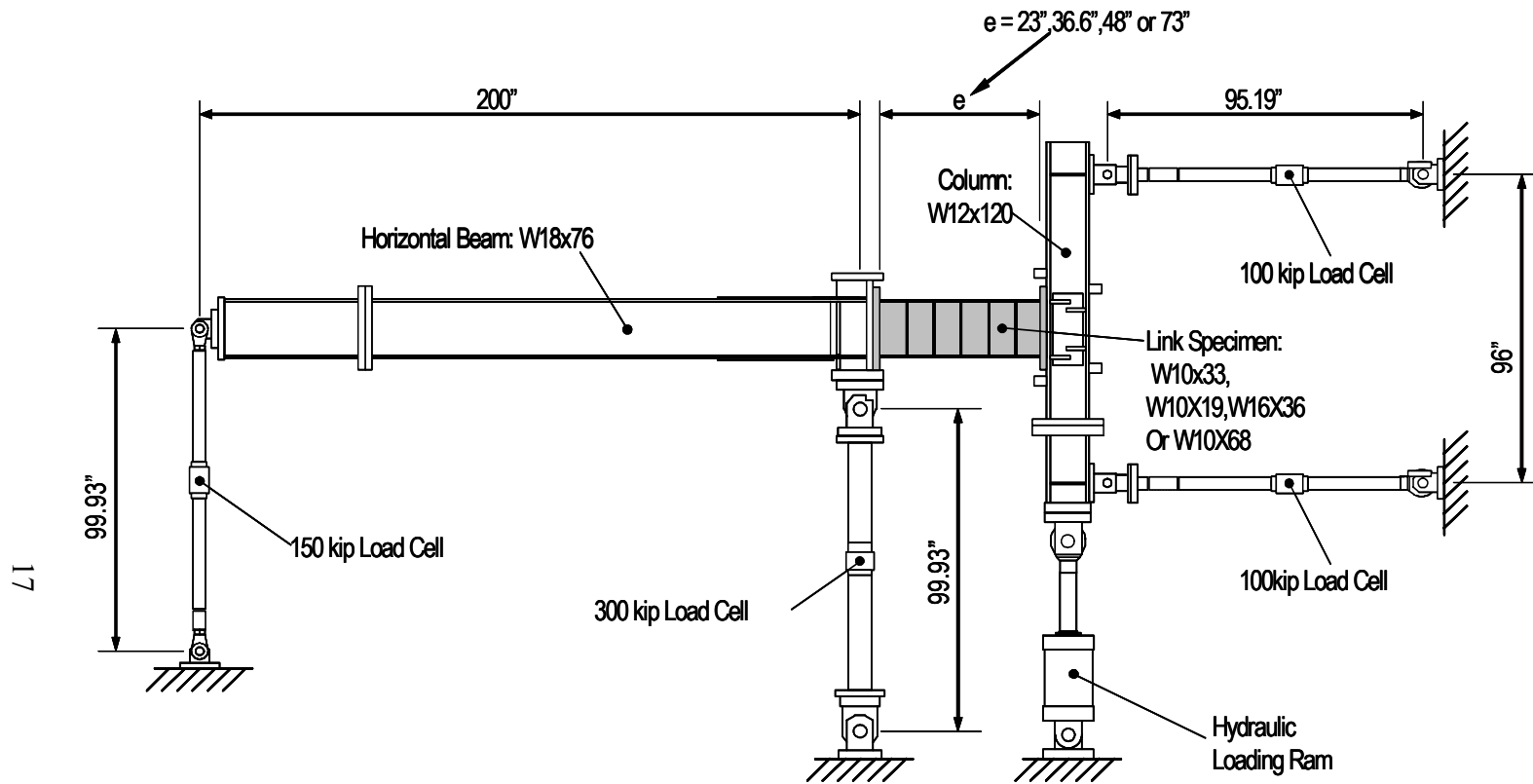
Figure 2.1 Details and dimensions of the test setup
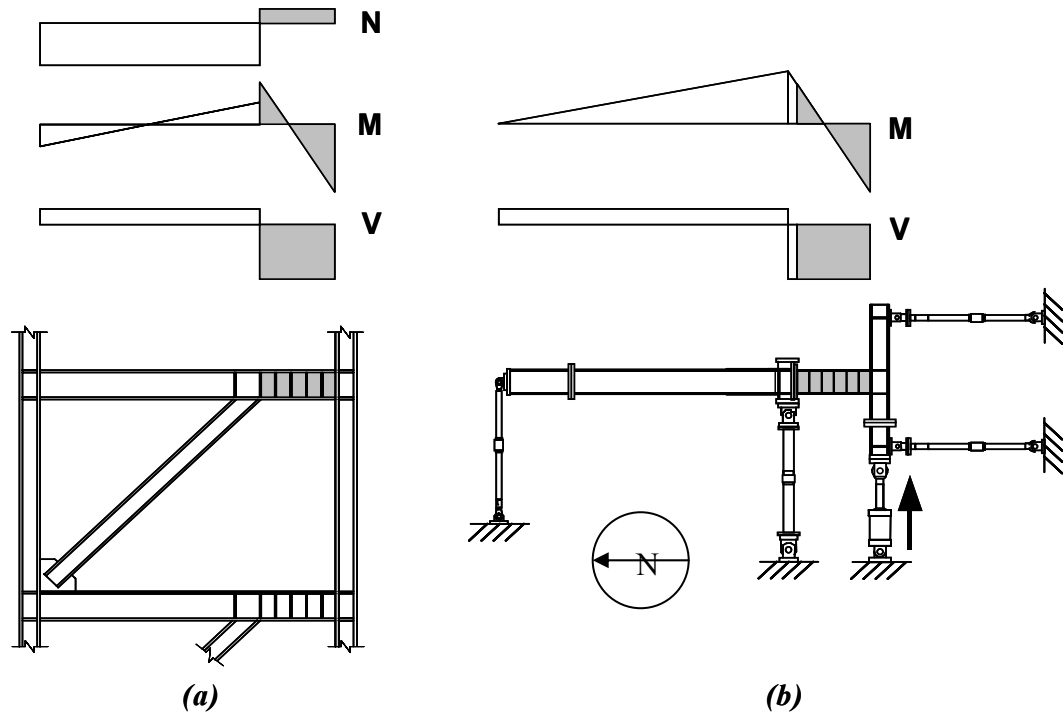
Figure 2.2 Force distributions in (a) typical single diagonal EBF and (b) in the test setup

The setup is designed so that axial forces introduced in the link can be considered negligible. Link rotation was achieved by quasi-statically displacing the W12X120 column segment of the test setup, until a target rotation was achieved as required by the loading protocol. The ends of the link specimens were welded to 2" thick end plates which were then bolted on to the beam and the column segment of the test setup using eight 1 ¼" A490 bolts at each side. In addition, a fastening mechanism was in place to prevent the plates from slipping under shear loading.

2.2.2 Lateral Bracing System

Figure 2.3 presents the detailing of the bracing used to prevent out-of plane movement of the test setup. The frame was provided with a support system to provide lateral stability throughout the testing process. Lateral support was provided at four points in the frame as shown in the figure. The bracing system was designed so that it would not interfere with the free in-plane movement of the system. Contact surfaces between the lateral braces and the test frame were coated with Teflon to minimize friction associated with in-plane movement.

Reaction Wall

Link to Beam Connection
Lateral Support

N

Column Top Lateral
Support

Beam Lateral
Support

Column Bottom Lateral
Support

20

Strong
Floor
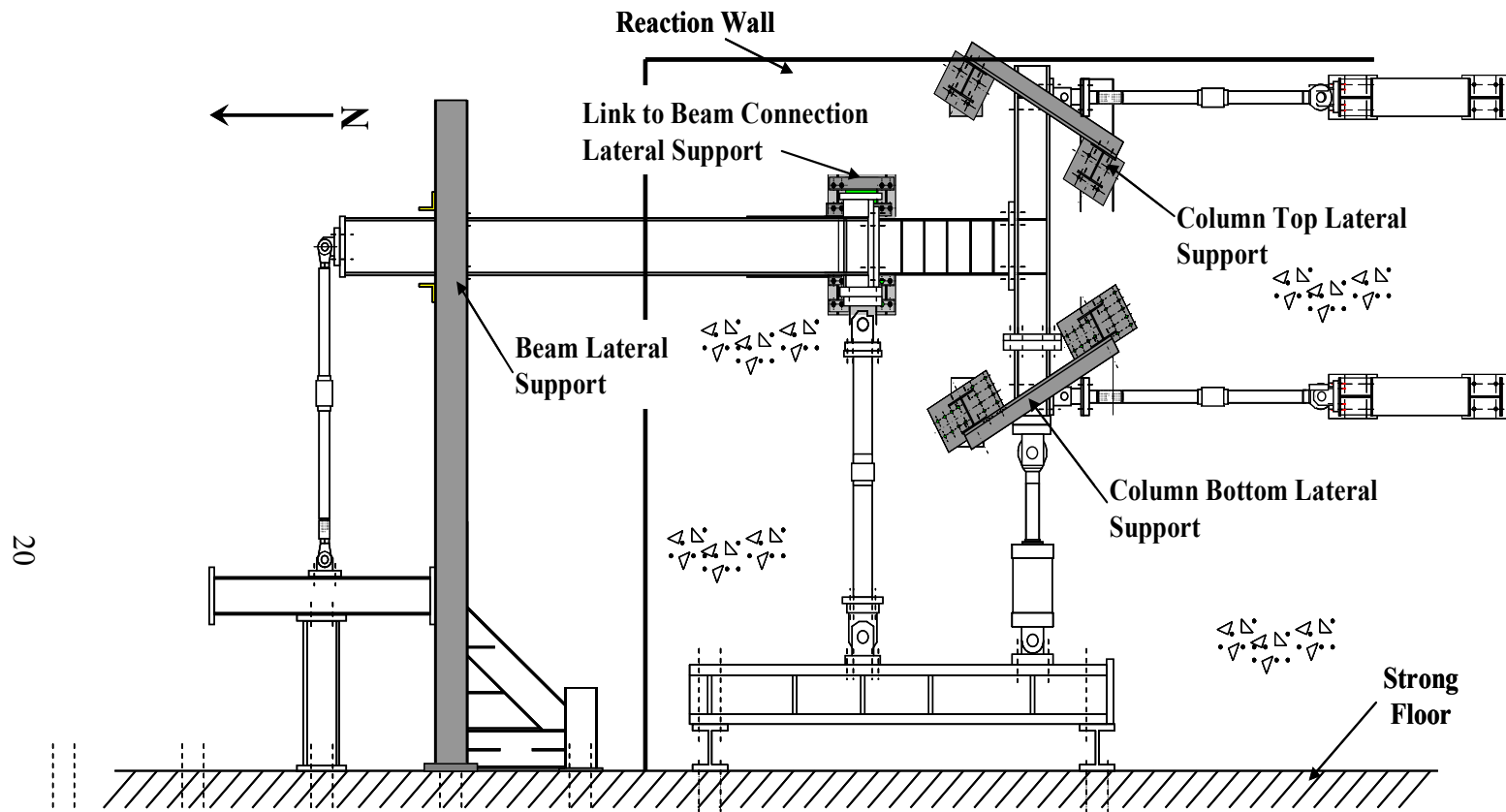
Figure 2.3Lateral support system

2.2.3   Instrumentation

The test setup was instrumented to permit calculation of all force components in the link specimen (shear, end moments, and axial force) and also to permit calculation of link deformations. Link forces were derived from forces measured at the load cells shown in Figure 2.1 Link deformations were computed from the array of displacement and rotation transducers shown in Figure 2.4. The deformation parameter of greatest interest in these experiments is the link rotation. Link rotation is defined as the relative vertical displacement of the link ends divided by the link length. Consequently, the specimens were instrumented to permit accurate measurement of the vertical displacement at each end of the link. Link horizontal displacements and link end rotations were also measured to provide additional data on link response.

All data was recorded by a data acquisition system. The data acquisition system used for these tests was relatively slow. Consequently, loading was stopped whenever instrument reading were recorded by the data acquisition system. When a specimen was yielding during the loading process, and the loading was stopped for reading data, the load on the specimen typically dropped a small amount. These load drops are attributed to strain rates effects, as the strength of the specimen reduces from a dynamic yield value to a static yield value. Normally, about a five-second interval was used between the time the

loading was stopped and when the data readings were taken to allow most of the load relaxation to occur.

More complete details on the design, fabrication and instrumentation of the test setup can be found in Arce (2002) and Okazaki (2004).
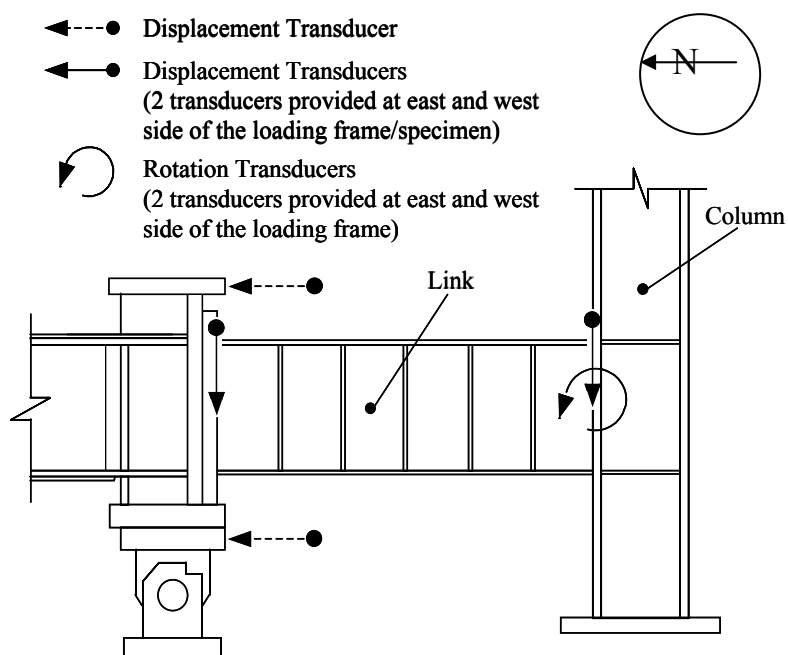
Figure 2.4 Location of transducers used to monitor the link displacement

2.3   TEST SPECIMENS

2.3.1   Section Dimensions and Section Properties

All specimens in this test program were constructed using W10X33 sections of ASTM A992 steel. The W10x33 section was used in recent test programs investigating shear link behavior (Arce 2002, Ryu 2004) and frequently exhibited failure by fracture of the link web. In order to provide a basis of comparison with these previous test programs, the W10x33 section was also chosen for this current investigation.

For this test program, shear link specimens were constructed using W10x33 sections produced by three different steel mills. In this report, the mills will be referred to as "A", "B" and "C". Tables 2.1 and 2.2 compare the nominal dimensions of the W10x33 section with the measured dimensions for the sections used in the test specimens.

Table 2.3 lists nominal cross-section properties for the W10x33. In this table, V_p is the plastic shear capacity of the section, and is computed per the 2002 *AISC Seismic Provisions*, as $0.6F_y(d-2t_f)t_w$. Table 2.3 also lists M_p, the plastic moment capacity of the W10x33 cross-section, computed as Z_xF_y. The values of V_p and M_p listed in Table 2.3 are based on $F_y = 50$ ksi and on nominal section dimensions.

23

Finally, Table 2.4 lists cross-section properties based on measured dimensions and measured yield stress values. Tension coupon tests are described later in Section 2.4. For the properties listed in Table 2.4, dynamic yield stress values were used.

Table 2.1 Nominal Section Dimensions

Section	d (in)	t_w(in)	t_f(in)	b_f(in)
W10x33	9.73	0.29	0.435	7.96

Table 2.2 Measured Section Dimensions

Section	Mill	d (in)	t_w(in)	t_f(in)	b_f(in)
W10x33	A	9.65	0.325	0.420	8.05
W10x33	B	9.7	0.302	0.435	8.0
W10x33	C	9.7	0.32	0.423	8.1

Table 2.3 Nominal Section Properties

Section	Z_x (in^3)	V_P (Kip)	M_P (Kip-in)	$\dfrac{M_P}{V_P}$
W10x33	38.8	77.1	1947	25.3

Table 2.4 Calculated Section Properties Based on Dynamic Yield Values

Section	Mill	V_P (Kip)	M_P (Kip-in)	$\left(\dfrac{M_P}{V_P}\right)_{actual}$
W10x33	A	93.6	2207	23.6
W10x33	B	99.7	2313	23.2
W10x33	C	92.1	2235	24.3

Table 2.5 Calculated Section Properties Based on Static Yield Values

Section	Mill	V_P (Kip)	M_P (Kip-in)	$\left(\dfrac{M_P}{V_P}\right)_{actual}$
W10x33	A	91.0	2072	22.8
W10x33	B	93.3	2165	23.2
W10x33	C	90.4	2107	23.3

where,

$$V_P = 0.6 \cdot (d - 2t_f) \cdot t_w \cdot F_{yw}$$

$$M_P = Z_{flange}F_{yf} + Z_{web}F_{yw} + Z_{fillets}F_{yw}$$

Z_{flange} = Plastic section modulus of the flanges based on measured section dimensions

F_{yf} = Average yield stress of coupons F2 and F3

Z_{web} = Plastic section modulus of the web based on measured section dimensions

F_{yw} = Yield stress of coupon W

25

Z_{fillet} = nominal plastic section modulus of the fillets

2.3.2   Test Specimen Parameters and Details

In this research program 10 shear link specimens were fabricated and tested. All specimens were of the same length, e = 23-inches, and all were constructed using a W10x33 section. Tables 2.6 and 2.7 list various parameters and details of each specimen. Some of the key parameters changed in the specimens are: material (producing mill), stiffeners on one side of web versus stiffeners on both sides, welding process used for stiffeners, spacing between stiffeners and other stiffener details. Drawings of each specimen are shown in Figures 2.5 to 2.14.

Listed in Table 2.6 is the nondimensional length of each link, $e/(M_p/V_p)$, based on the estimated actual values of M_p and V_p in Table 2.4. All specimens have a nondimensional length of about 1.0 M_p/V_p. Links with a length less than 1.6 M_p/V_p are classified as shear yielding links. Consequently, all specimens tested in this program are classified as shear links. Even though all links had the same length of 23-inches, the nondimensional link length varies slightly among the specimens. This is due to variations of yield stress among the three different mill steels used in the test program. These variations in yield stress result in variations in M_p and V_p, and therefore result in variations in $e/(M_p/V_p)$. Table 2.6 also lists the spacing of intermediate web stiffeners for each specimen.

26

Table 2.7 provides additional information on each specimen. This table lists if intermediate stiffeners were provided on one side or both sides of the web, and if the stiffeners were welded to the flanges and web, to the flanges only, or to the web only. Also listed is the welding process used to connect the stiffeners to the link section. Finally, Table 2.7 also lists the loading protocol used for each specimen.

Table 2.6 Test Specimen Details

SPECIMEN	MILL	e/$(M_p/V_p)_{actual}$	Spacing at intermediate stiffeners	Series
1	A	0.98	3 @ 5.75"	
2	B	0.99	3 @ 5.75"	**1**
3	C	0.95	3 @ 5.75"	
4	B	0.99	3 @ 5.75"	
5	B	0.99	3 @ 5.75"	
6	B	0.99	3 @ 5.75"	**2**
7	B	0.99	3 @ 5.75"	
8	B	0.99	3 @ 5.75"	
9	B	0.99	3 @ 5.75"	**3**
10	B	0.99	2 @ 7.67"	

Table 2.7 Further Test Specimen Details

SPECIMEN	Stiffeners on one side or both sides	Welding procedure for the stiffeners	Stiffener Welding detail	Loading Protocol	Series
1	One side	SMAW	F & W	SLP	
2	One side	SMAW	F & W	SLP	1
3	One side	SMAW	F & W	SLP	
4	Both sides	SMAW	F & W	SLP	
5	Both sides	SMAW	F	SLP	
6	Both sides	FCAW	F & W	SLP	2
7	one side	SMAW	W	SLP	
8	Both sides	SMAW	F	RLP	
9	Both sides	FCAW	F & W	RLP	3
10	One side	SMAW	W	RLP	

SMAW = Shielded Meatal Arc Welding procedure with E-7018 electrode.

FCAW = Self Shielded Flux Cored Arc Welding with E70T-6 electrode.

F & W = Stiffeners are welded to both flanges and the web of the link.

W = Stiffeners are welded to the web of the link only.

F = Stiffeners are welded to both flanges of the link, but not to the web.

SLP = Severe Loading Protocol (Table 2.10)

RLP = Revised Loading Protocol (Richards & Uang, 2002) (Table 2.11)

29

2.3.3   Discussion of Test Specimen Design

As indicated in Tables 2.6 and 2.7, the ten specimens tested in this research program were divided into three test series. For each test series, the specimens were designed and detailed to investigate various issues related to the occurrence of web fractures in shear links. The three test series are discussed below.

2.3.3.1 Series 1: Effect of K-Area Properties

One of the objectives of this research program was to investigate the influence of k-area material properties on the development of web fractures in shear links. As discussed in Chapter 1, previous researchers have cited the high hardness and low ductility of the material in the k-area of wide flange links as a possible contributor to the development of web fractures. The three specimens in the first test series were designed to provide additional data on the correlation between k-area material properties and the overall performance of shear links. In this first series, three nominally identical links were fabricated using three different heats of W10x33 sections. That is, essentially the only difference between Specimens 1, 2 and 3 was that the W10x33 sections used to construct the specimens came from three different mills. In developing this test series, it was hoped that the W10x33 sections coming from three different steel mills would

exhibit somewhat different material properties in the k-areas of the sections. This, in turn, would then allow a comparison of cyclic loading performance for three different links that are nominally identical except for k-area properties.

As indicated in Table 2.6, the W10x33 sections used for Specimens 1, 2 and 3 came from Mills A, B and C respectively. Mills A and B were US mills, whereas Mill C was outside of the US. Section 2.4 presents the results of material tests on samples of W10x33 from each mill, including material tests in the k-area.

Specimens 1 to 3 were provided with stiffeners designed in accordance with the 2002 *AISC Seismic Provisions.* Each specimen was provided with three 3/8-inch thick stiffeners on one side of the web only, spaced 5 ¾" away from each other. Using the shielded Metal Arc (SMAW) process with E7018 electrodes, the stiffeners were fillet welded to the web and both flanges of the link. Further details of the first 3 specimens and other details on the stiffening of each specimen are provided in Figures 2.5, 2.6 and 2.7. As indicated in these figures, the corners of the stiffeners were cut so that the termination of the stiffener to link web weld occurred at a distance of one-inch from the inside face of the flange. Hardness measurements made for the test sections (see Section 2.4) showed a significant variation of hardness at this location among the three sections.

Specimen 1 (Mill A) showed the highest hardness at the location of the stiffener weld termination. Specimen 2 (Mill B) showed the lowest hardness at this location. Finally, Specimen 3 (Mill C) showed hardness close to, but somewhat less than the hardness for Specimen 1.

2.3.3.2 Series 2: Effects of Different Arrangements of Stiffeners and Welding Procedures

In the second test series (Specimens 4 to 7) the effects of different arrangements of stiffeners and different stiffener welding procedures were investigated. All specimens in this series were constructed using a W10x33 section from Mill B. Results from the first test series showed that the overall performance of Specimens 1 to 3 was quite similar, but that Specimen 2 (Mill B) exhibited failure by web fracture somewhat earlier in the loading sequence than Specimens 1 (Mill A) or Specimen 3 (Mill C). Consequently, the remainder of the test specimens in the program, both for Series 2 and Series 3, were constructed of W10x33 sections from Mill B, as this section appeared to be most vulnerable to web fracture.

Specimen 4 was nominally identical to Specimen 2, except that Specimen 4 was provided with stiffeners on both sides of the link, whereas Specimen 2 had stiffeners on only one side of the link. All shear link specimens tested in recent

research programs where the web fracture problem was first observed and subsequently investigated (Arce 2002, Ryu 2004, Okazaki 2004) had stiffeners welded on only one side of the link. The 2002 *AISC Seismic Provisions* require stiffeners on only one side of the link for wide flange link sections less than 25-inches in depth. For deeper sections, stiffeners are required to be placed on both sides. Since all of the recent test programs used link sections less than 25-inches in depth, stiffeners were provided on only one side of the link specimens in accordance with the requirements of the 2002 *AISC Seismic Provisions*. Thus, whereas all recent test specimens have been fabricated with one-sided stiffeners, many links in actual building construction, where link sections greater than 25-inches in depth are possible, will be provided with two-sided stiffeners. This raises the question of whether the web fracture problem is more severe when stiffeners are welded on both sides of the web rather than on only one side. Welding stiffeners on both sides is a potentially more severe case due to the additional welding in the k-area of the link section, and potentially higher local stress concentrations at the termination of the stiffener welds. Specimen 4 was included in this test program to investigate this issue.

As noted above, all link specimens tested in recent research programs used stiffeners on only one side of the web. Similarly, all link specimens in recent research programs were fabricated by welding the stiffeners to the links using the

shielded metal arc welding (SMAW) process with E7018 electrodes. In actual building fabrication practice, other welding processes are often used. Other welding processes may provide for higher heat input than SMAW, and may therefore have a potentially more adverse effect on the material properties in the heat-affected zone of the link web at the termination of the stiffener weld in the k-area. The use of welding processes other than SMAW may therefore affect the occurrence of web fractures in shear links. To investigate this possibility, Specimen 6 was constructed to be nominally identical to Specimen 4, except for the welding process used for the stiffeners. The stiffeners in Specimen 4 were welded by SMAW using E7018 electrodes. The stiffeners for Specimen 6 were welded using the self shielded flux cored arc welding (FCAW) process with an E70T-6 electrode. Welding by FCAW is expected to produce a higher heat input than welds made by SMAW.

The 2002 *AISC Seismic Provisions* require that stiffeners be welded to the web of a link section, as well as to both flanges. Consequently, all link test specimens in recent research programs had stiffeners welded to the web and to both flanges. Specimens 5 and 7 were built to determine if web fractures could be prevented by welding stiffeners only to the flanges (and not to the web); or by welding stiffeners only to the web (and not the flanges).

Specimen 5 was constructed by welding stiffeners only to the flanges, but not to the web. Stiffeners were provided on both sides of the link web, and were installed so that the edges of the stiffeners were touching the web of the link, but were not welded to the web of the link (Figure 2.09). The intent was to restrain out of plane movement of the web at the location of the stiffeners by essentially "trapping" the web between stiffeners on both sides of the web. Previous tests (Arce 2002, Ryu 2004 and Okazaki 2004) have shown that web fractures consistently initiate at the termination of the stiffener to link web fillet welds. By completely avoiding stiffener to link web welds, it is hoped that web fractures can also be avoided or delayed. Stiffeners in shear links are provided to control shear buckling of the link web. It is unclear if the stiffeners will still function properly in this capacity if they are not welded to the link web. Specimen 5 was intended to serve as a pilot test of this concept. To the knowledge of this researcher, no shear link test reported in the literature has ever used this detail. This innovative approach for controlling the web fracture problem in shear links was suggested by Malley (2003).

In Specimen 7, yet another approach was attempted for controlling link web fracture. In this specimen, stiffeners were welded only to the web, and not to the flanges, as shown in Figure 2.11. In testing of shear links where the stiffeners are welded to the web and to the flanges, significant bending of the stiffeners is

often observed. The bending of the stiffeners is a result of cross-sectional warping of the link. Under large inelastic shear loading, the link cross-section exhibits significant warping. That is, plane sections do not remain plane. When a stiffener is welded to the web and to the flanges, the warping deformations of the link produce bending of the stiffener, since the stiffener starts as a "plane section" and therefore resists warping of the link. It is postulated that this warping induced bending of the stiffener may increase the local stress concentration at the termination of the stiffener to link web welds. By not welding the stiffener to the flanges, the stiffener no longer significantly restrains warping, and therefore no longer significantly bends. This, in turn, may reduce stress concentrations at the termination of the stiffener to link web welds, and may therefore prevent or delay web fracture. Specimen 7 was designed to investigate this possibility.

2.3.3.3   Series 3: Link Testing Under the Revised Loading Protocol

Appendix S of the 2002 *AISC Seismic Provisions* specify a loading protocol to be used when testing links. This loading protocol was used in the test program by Arce (2002) where the occurrence of premature link web fracture was first observed. Subsequent investigation of the premature failure of shear links suggested that the loading protocol used to test these links was too severe and not representative of rotation demands expected in actual earthquakes. As a result of

concerns raised regarding the rationality of the current link loading protocol, a research project was conducted at the University of California at San Diego to establish a rational loading protocol for shear links. This study established that the link loading protocol currently in the 2002 *AISC Seismic Provisions* was, in fact, too severe. This study also developed a new loading protocol for shear links, using a methodology similar to that used for moment frame connection testing, as developed under the FEMA/SAC program. The development of the revised loading protocol for shear links in EBFs is reported by Richards and Uang (2003). This revised loading protocol has been proposed for adoption in the upcoming 2005 *AISC Seismic Provisions*, and will therefore serve as the basis for acceptance testing of shear links in the future. That is, links will be considered acceptable if they can develop the required plastic rotation capacity (0.08 radian for shear links) when tested under the revised loading protocol developed by Uang and Richards.

Link specimens in Series 1 and 2 described above were all tested using a loading protocol that is significantly more severe than the current loading protocol in either the 2002 *AISC Seismic Provisions* or the revised loading protocol proposed for the 2005 *AISC Seismic Provisions*. This very severe loading protocol was chosen to increase the likelihood of web fracture, so that the effect of different variables on the occurrence of web fracture could be studied. However,

since the specimens were tested using a very severe, nonstandard loading protocol, it was not possible to determine if these specimens actually satisfied the plastic rotation requirements in the *AISC Seismic Provisions.*

Specimens in the final test series of this research program (Specimens 8 to 10) were tested using the revised loading protocol proposed for the 2005 *AISC Seismic Provisions.* The purpose of this test series was to determine if links with selected stiffener details would be considered acceptable per the *AISC Seismic Provisions.* That is, the purpose was to determine if these shear link specimens could develop a plastic rotation of at least 0.08 radian under the revised loading protocol. Further details of the loading protocols are described later in Section 2.5.

In this final test series, Specimen 8 was nominally identical to Specimen 5 with the exception of the loading protocol. As described above, the stiffeners in Specimen 5 were welded only to the link flanges and not to the link web. The performance of Specimen 5 under the severe loading protocol was promising. Consequently, this same detail was tested under the revised loading protocol in Specimen 8 to determine if a link where the stiffeners are not welded to the web is capable of meeting the plastic rotation requirements of the *AISC Seismic Provisions.*

Similarly, Specimen 9 in Series 3 was nominally identical to Specimen 6 in Series 2, with the exception of the loading protocol. Specimen 6 was constructed by welding the stiffeners using the FCAW process. Results of testing of Specimen 6 using the severe loading protocol showed that web fracture occurred much earlier in the loading process when FCAW was used for the stiffeners. Since FCAW is commonly used in actual building fabrication practice, the concern was raised as to whether a link fabricated using FCAW could actually meet the plastic rotation requirements of the *AISC Seismic Provisions*. Specimen 9 was designed to investigate this question.

As discussed in Chapter 1, Richards and Uang (2002) noted that most links tested in the 1980s used stiffeners spaced further apart than currently required by the 2002 *AISC Seismic Provisions*. They suggested that this smaller stiffener spacing may change the controlling link failure mode from web buckling to web fracture. To investigate this possibility, Specimen 10 was constructed using stiffener spacing larger than required by the *AISC Seismic Provisions* for a shear link with 0.08 radian of plastic rotation. The intent of this specimen was to determine if the use of larger stiffener spacing precluded the development of link web fracture. To develop the maximum permissible plastic rotation of 0.08 radian in shear links, the 2002 *AISC Seismic Provisions* require that the space between stiffeners not exceed $30t_w - d/5$, where t_w in the link web thickness and *d* is the

depth of the link section. For the W10x33 section, this formula gives a maximum stiffener spacing of 6.75-inches, using nominal values for web thickness and depth. For the 23-inch link length of the test specimens, this required the use of three equally spaced stiffeners, with a spacing of 5.75-inches. This stiffener spacing was used for the first nine specimens in this investigation. For Specimen 10, only two equally spaced stiffeners were provided, with a spacing of 7.67-inches. Consequently, the stiffener spacing provided in Specimen 10 was somewhat more representative of links tested in the 1980s, where the web fracture problem was not observed.
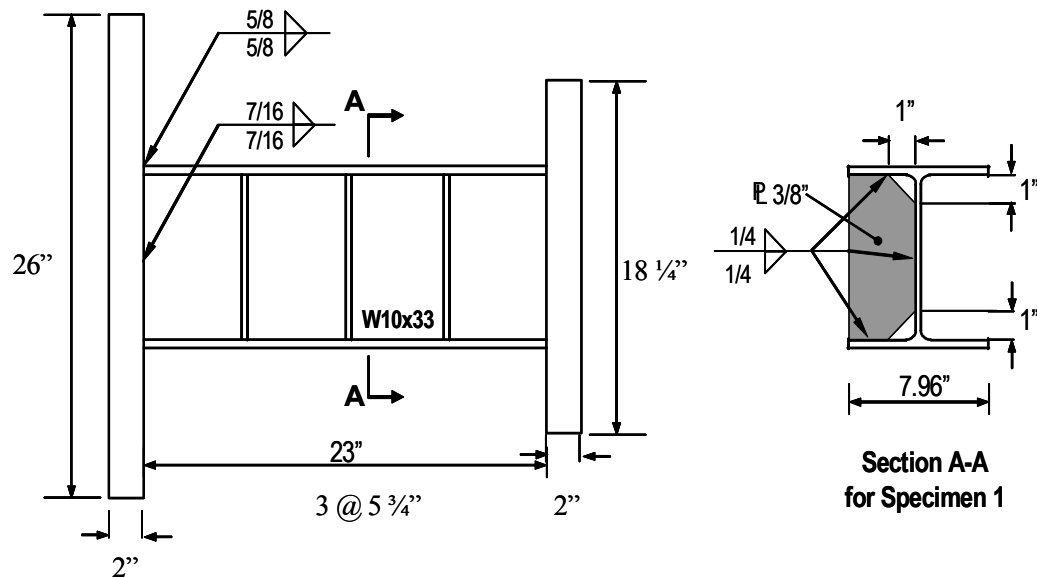
Figure 2.5 Welding and stiffener details for Specimen 1
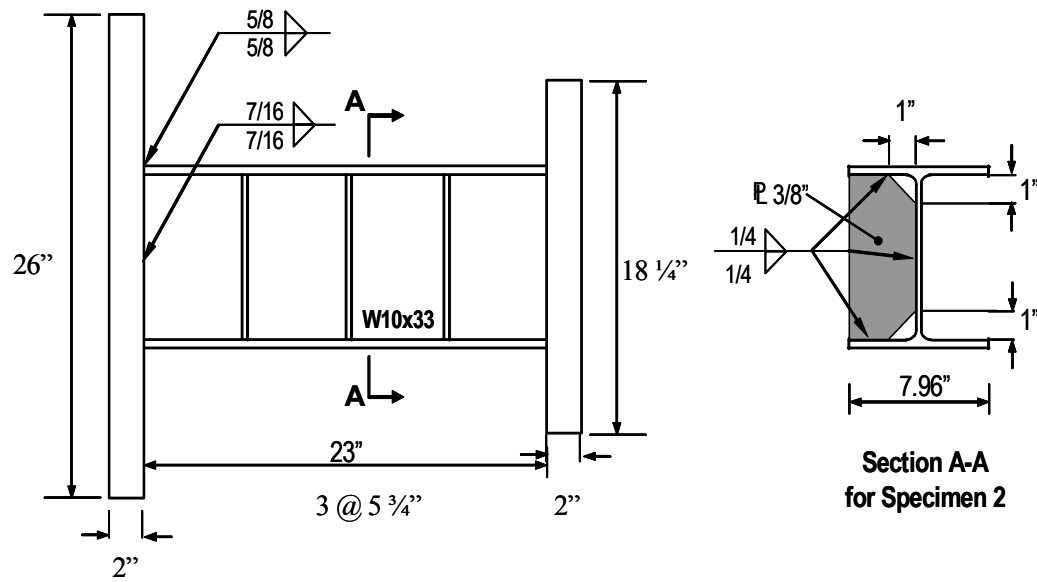
Figure 2.6 Welding and stiffener details for Specimen 2
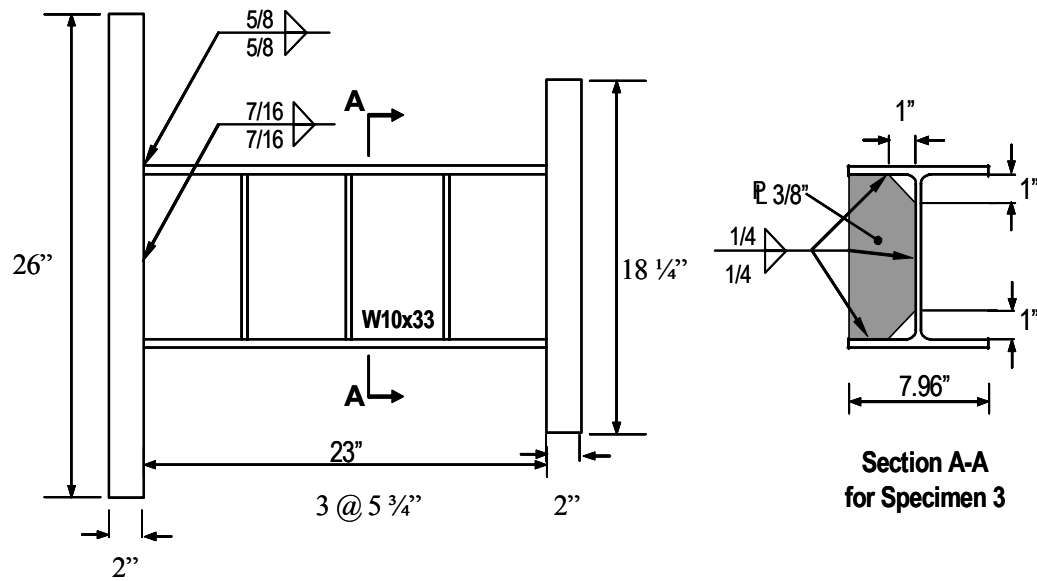
Figure 2.7 Welding and stiffener details for Specimen 3

41
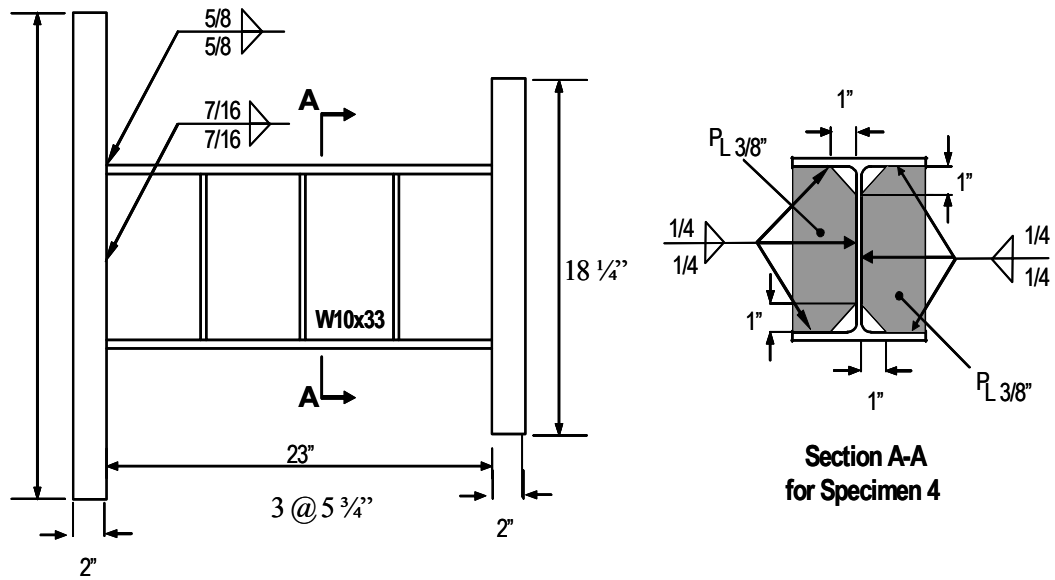
Figure 2.8 Welding and stiffener details for Specimen 4
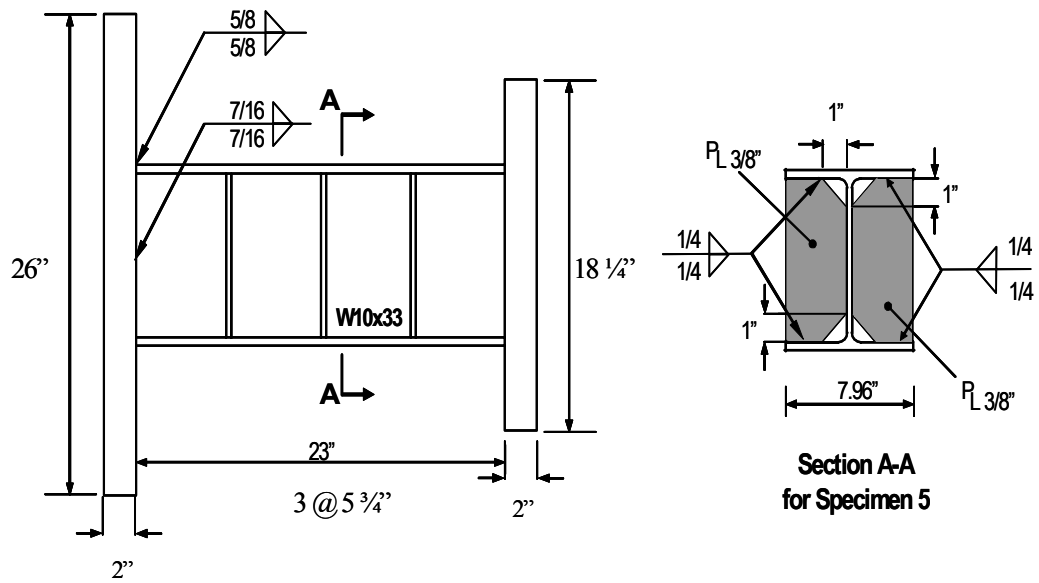
Figure 2.9 Welding and stiffeners details for Specimen 5
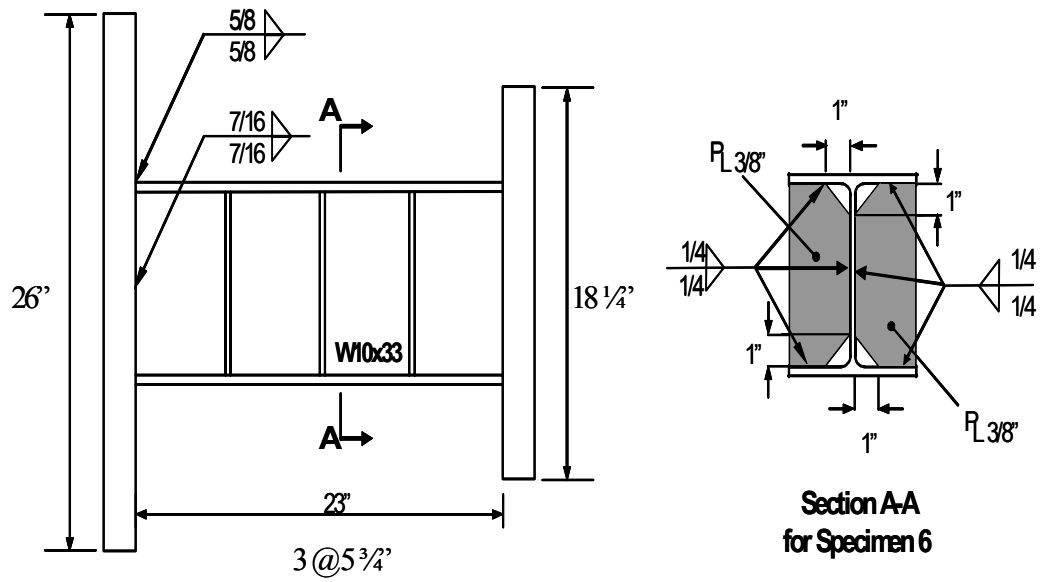
Figure 2.10 Welding and stiffener details for Specimen 6
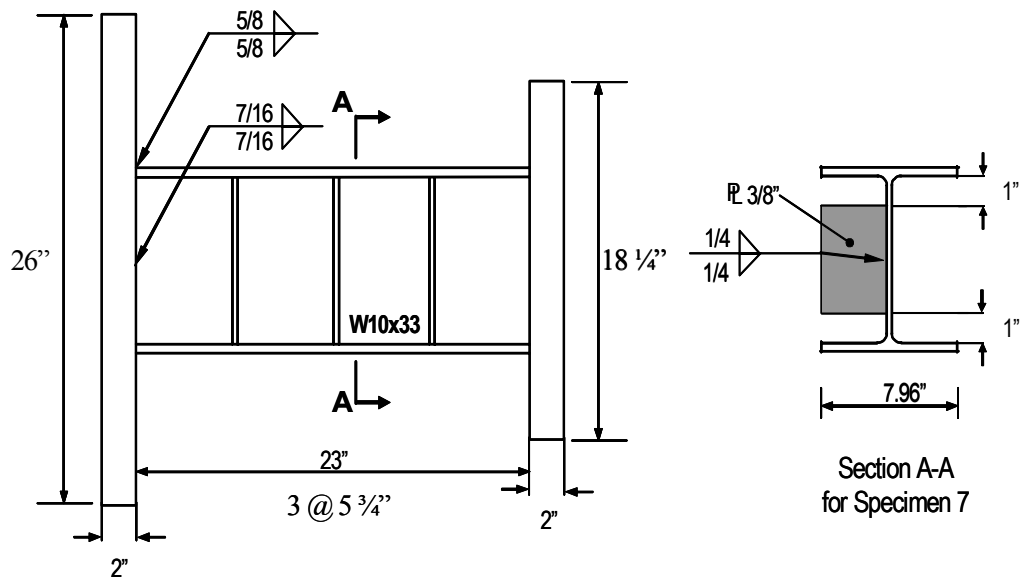
Figure 2.11 Welding and stiffener details for Specimen 7

43
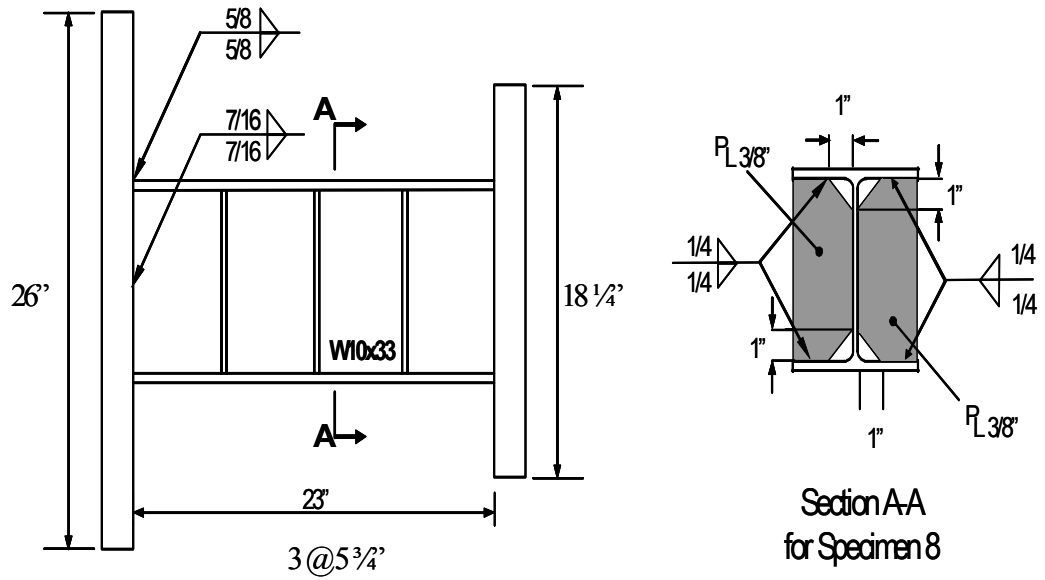
Figure 2.12 Welding and stiffener details for Specimen 8
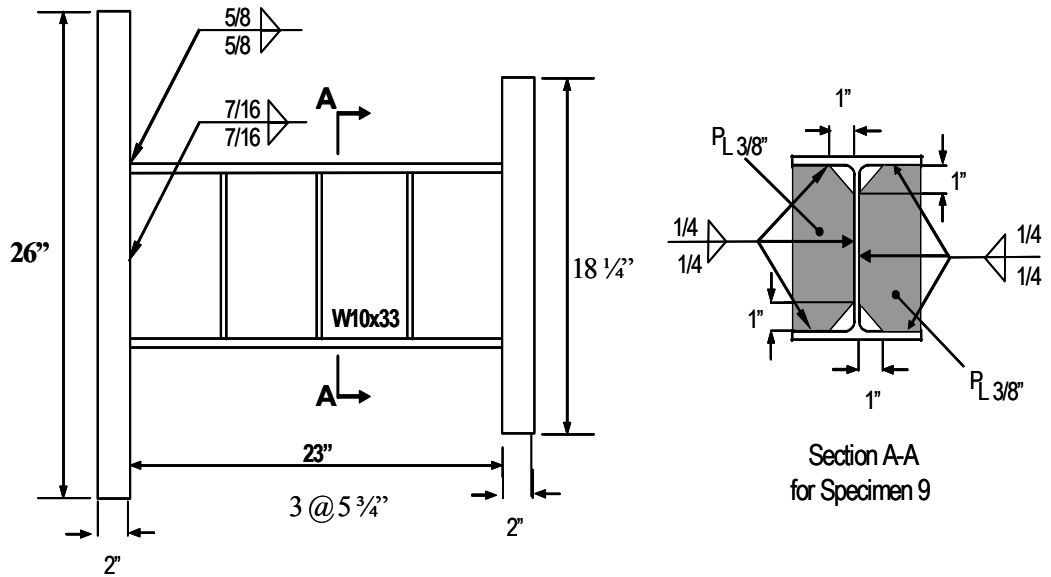
Figure 2.13 Welding and stiffener details for Specimen 9

44
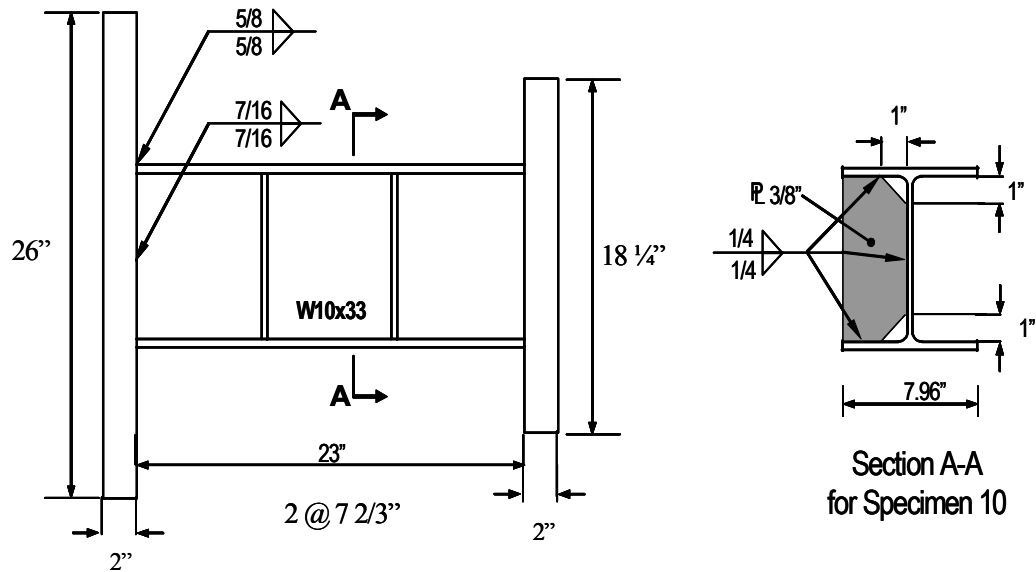
Figure 2.14 Welding and stiffener details for Specimen 10

2.4 MATERIAL PROPERTIES

2.4.1 Hardness Tests

One of the objectives of this research was to study steel with different levels of hardness in the k-area. As discussed earlier, it has been postulated that high hardness in the k-area may play a role in the web fractures observed in shear links. Al specimens in this test program were constructed from W10x33 sections that came from three different steel mills, designated as Mill A, B and C. Samples of W10x33 sections from these three mills were examined using the Rockwell Hardness test using the B Scale. The specimens were prepared and tested following the procedure described in ASTM E18.

45

From a sample of W10x33 from each mill, a 0.5–inch thick slice of the section was prepared. The section was divided into two "T" shaped specimens from the top and bottom of the cross-section. Each "T" shaped sample included the entire flange and approximately 4-inches of the web. The entire cross-section was divided into these smaller "T" sections to permit easier handling in the hardness testing machine.

For each "T" sample, hardness readings were taken at 0.2-inch intervals along the centerline of the web, with the measurements extending from the outer face of the flange and continuing along the web centerline for a distance of about 3.6 inches. These measurements therefore included the portion of the web within the k-area. Hardness measurements were also taken at 0.2-inch intervals along the center line of the flange, and extended across the entire width of the flange.

Figure 2.15 shows the results of the hardness tests across the width of the flange of W10x33 samples taken from all three mills. Hardness numbers are quite uniform across the width of the flanges and are very consistent for the three mills. The average hardness is approximately 85 HRB, and the difference in hardness between the three specimens is less than 4 HRB units.

Figure 2.16 shows hardness readings along the centerline of the web for the first "T" specimen from each mill. Similarly, Figure 2.17 shows hardness readings along the centerline of the web for the opposite "T" specimen from each mill. All

specimens show high hardness in the k-area, although there are differences in k-area hardness levels among the three mill samples. The peak hardness for each sample occurs at a distance of about 0.6-inches to 1-inch from the outer face of the flange. The flange of the W10x33 is about 0.43-inches thick and the "k" dimension (distance from outer face of the flange to the end of the web-flange fillet) is about 1-inch. Consequently, the peak hardness is, in fact, occurring within the flange-web fillet area of the cross-section. Mills A and C showed the largest peak hardness values, which were in the range of about 96 to 98 HRB. Mill B showed a lower peak hardness of about 93 to 95 HRB.

After reaching their peak values, the high hardness readings along the web centerline decrease. Beyond a distance of about 2.5-inches from the face of the flange, the hardness readings remain constant at a level about 83 to 85 HRB, similar to the flange readings. As shown in Figures 2.16 and 2.17, the k-area hardness levels are similar for Mills A and C, although the hardness for Mill C is slightly smaller. However, the k-area hardness levels are significantly smaller for Mill B.

The largest differences in hardness readings among the samples from Mills A, B and C was estimated to occur at about 1.4-inches away from the outer face of the flange, as shown in Figure 2.16. Therefore, it was decided that in order to have a better understanding of the role of k-area properties in link web fracture,

47

the fillet welds joining the stiffeners to the link web would be terminated 1.4-inches away from the outer face of each flange, as previously shown in Figures 2.5 to 2.14.
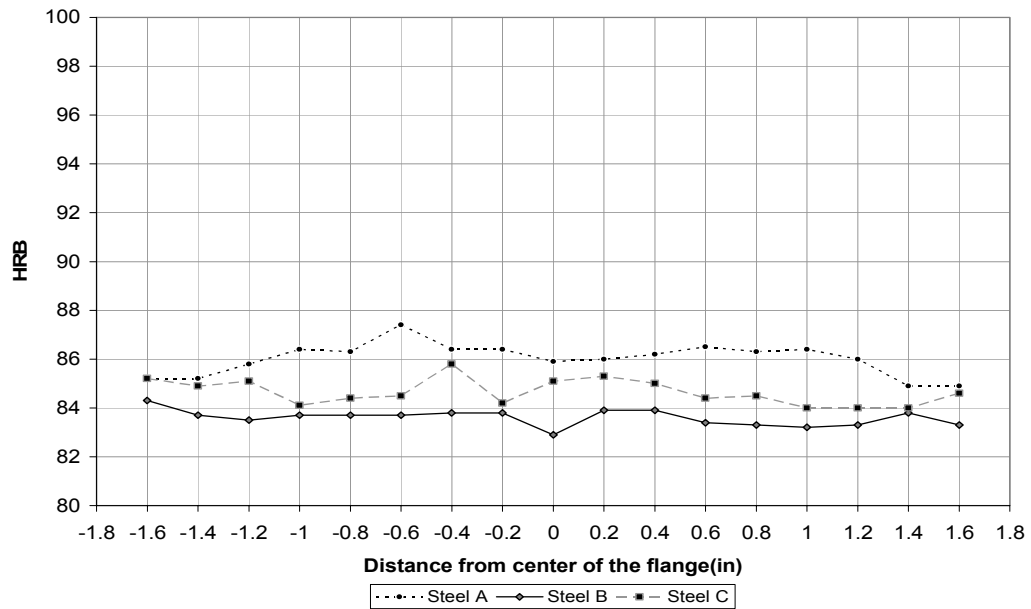
Figure 2.15 Hardness results at the center line of the flange for Mills A, B and C. (zero distance is the center line of the web of the section)
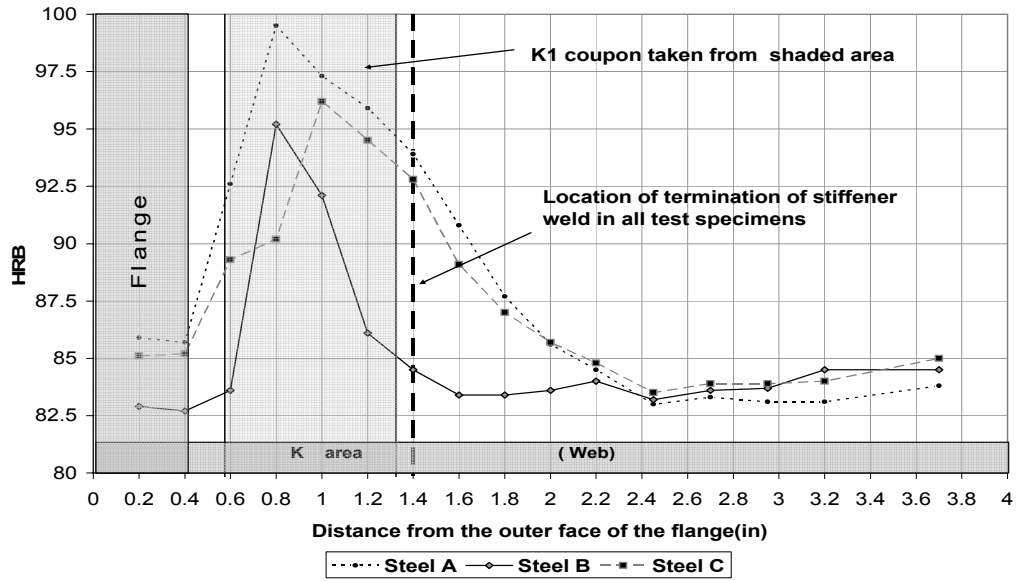
Figure 2.16 Hardness results at the center line of the web of the first "T" for Mills A, B and C (zero distance is measured from the outer face of the flange of the specimen)
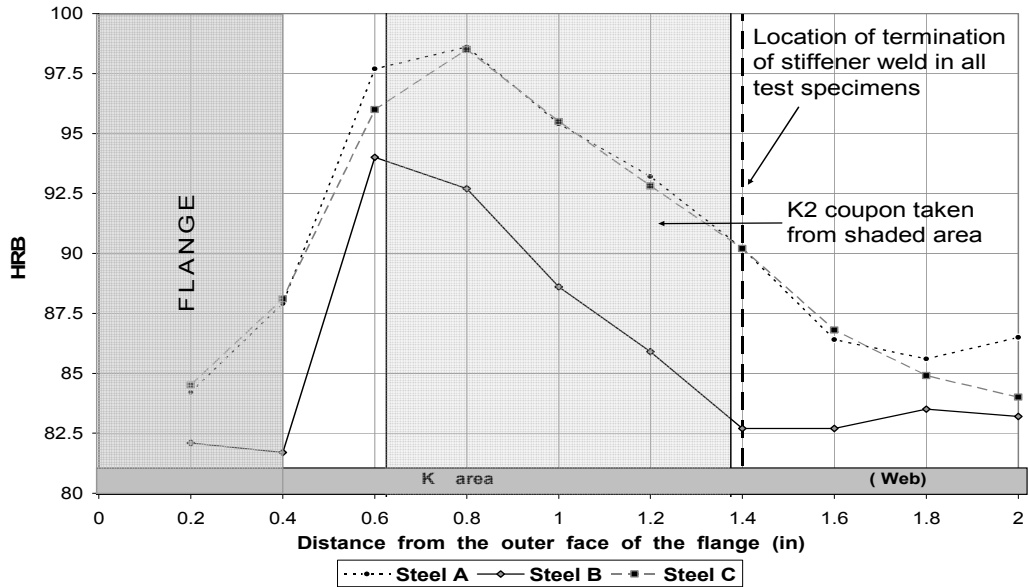
Figure 2.17 Hardness results at the center line of the web of the second "T" for Mills A, B and C (zero distance is measured from the outer face of the flange of the Specimen)

49

2.4.2 Tensile Coupon Tests

Tensile coupon tests were conducted on samples removed from various parts of the W10x33 section from each of the three mills. The coupons were prepared following the specifications of ASTM A370. However, ½-in sheet-types were used instead of 1 1/2 in plate types. A total of 5 coupons were prepared from each of the three sections of steel used to build all the specimens. All 5 coupons were taken from the same location of each section of each of the three mills used to build the specimens. The location of the 5 coupons is illustrated in Figure 2.18.
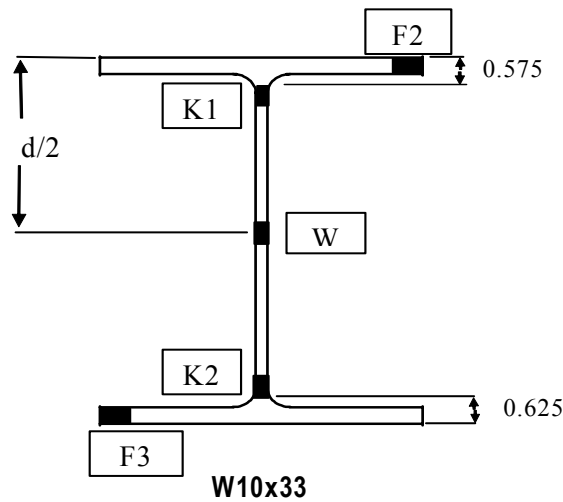
Figure 2.18 Location of tensile coupons

Two coupons were taken from the flanges: one from the top flange, F2, and one from the bottom flange, F3. One coupon was taken from the center of the web, designated as W. Finally, coupons were taken from the k-area at the top and bottom flanges, and designated K1 and K2. The results of the coupon tests are

50

summarized in Table 2.9. Figures 2.19 to 2.25 show measured stress-strain curves.

The sections from all three mills show very similar properties in the flange, with a static yield stress of about 55 ksi and a tensile strength of about 75 ksi. The web coupons (taken at mid-depth of the web) are also reasonably consistent, with static yield stress values of about 53 to 58 ksi (static yield stress was not available for the web coupon for Mill A, but is estimated at about 53 ksi), and tensile strength values of about 73 to 77 ksi.

The tensile coupon data from the k-areas show significantly different mechanical properties as compared to the flanges and web. For the k-area coupons from Mill A, the yield stress and tensile strength values are highly elevated. Further, the elongation of the material in the k-area is only about 10-percent, as compared to 30-percent in other parts of the cross-section. Also, as shown Figure 2.23, the stress-strain curves for the k-area coupons from Mill A exhibit no yield plateau. The k-area coupon from Mill C shows similar high yield and tensile strengths and low elongations, as for Mill A.

The k-area coupons from Mill B show somewhat better mechanical properties than those from Mills A and C. The yield and tensile strengths in the k-area of Mill B are only slightly elevated compared to the yield and tensile strength at mid-depth of the web. The elongation of the k-area coupons for Mill B is about

51

20 to 23-percent. This is smaller than the elongation at mid-depth of the web of Mill B, which was about 31-percent. However, the elongation of the k-area coupon for Mill B was approximately double the elongation values in the k-areas for Mills A and C.

In general, the results obtained from the k-area coupon tests show a correlation with the results obtained from hardness tests. Steels from Mills A and C exhibited higher hardness at the k-area and also showed higher yield stress, higher ultimate stress and lower elongation. The steel from Mill B showed somewhat lower hardness in the k-area, and correspondingly had lower yield stress, lower ultimate stress, and higher elongation.

2.4.3   Steel Chemical Analysis

Chemical analysis of steel used for the test specimen, as reported in the Mill certificate, is shown in Table 2.8. The Mill certificate for steel from Mill C provided no data on chemical analysis.

Table 2.8 Chemical Analysis for Steel from Mills A and B

Steel	C Cr	Mn Mo	P Sn	S Al	Si V	Cu Nb	Ni	CE
A	.0690 .0330	.8390 .0160	.0105 .0074	.0209 .0007	.2270 .0028	.1290 .0284	0.039	0.2304
B	.09 .14	1.11 .031	.007 .010	.034 .005	.29 .002	.34 .015	.11	.34

Table 2.9 Tensile Coupon Data

Steel	Location of Coupon	F_y dynamic (ksi)	F_y Static (ksi)	F_u (ksi)	$(F_{y\text{-}dynamic})/$ Fy=50ksi	Elongation (%) 2" gage
A	F2	58.5	54.8	75.4	1.17	30.20
	F3	57.8	53.6	75.3	1.16	28.10
	K1	**93**	**91.5**	**99.7**	**1.86**	**10.36**
	K2	**82.5**	**80.9**	**90.3**	**1.65**	**12.85**
	W	54.5	53.0**	72.9	1.09	31.92
B	F2	59.7	56.4	75.3	1.19	32.32
	F3	57.5	53.3	74.8	1.15	32.99
	K1	**65.5**	**64.5**	**79.4**	**1.31**	**19.84**
	K2	**62.1**	**61.2**	**77.9**	**1.24**	**23.40**
	W	62.3	58.3	76.9	1.25	31.22
C	F2	57.3	55.4	74.9	1.15	30.00
	F3	58.8	53.1	75.2	1.18	26.04
	K1	**87.8**	**88.9**	**96.2**	**1.76**	**12.00**
	K2*	-	-	-	-	-
	W	54.2	53.2	72.9	1.08	32.06

where,

$F_{y\ dynamic}$ = dynamic yield strength measured at a cross-head rate of 0.02in/min.

$F_{y\ static}$ = static yield strength measured with cross-heads stationary for one minute (the value reported in the table is the average of three static yield strength measurements)

F_u = Dynamic ultimate tensile strength measured at cross-head rate of 0.125 in/min.

*K2 not reported because of problems with testing machine

** Static yield estimated because load pauses occurred before plateau was reached

Note: Based on Mill certificate:

Steel A: Fy = 53.6   Fu = 66.78   Elongation = 24.89%

Steel B: Fy = 57.5   Fu = 75.3   Elongation = 25.5%
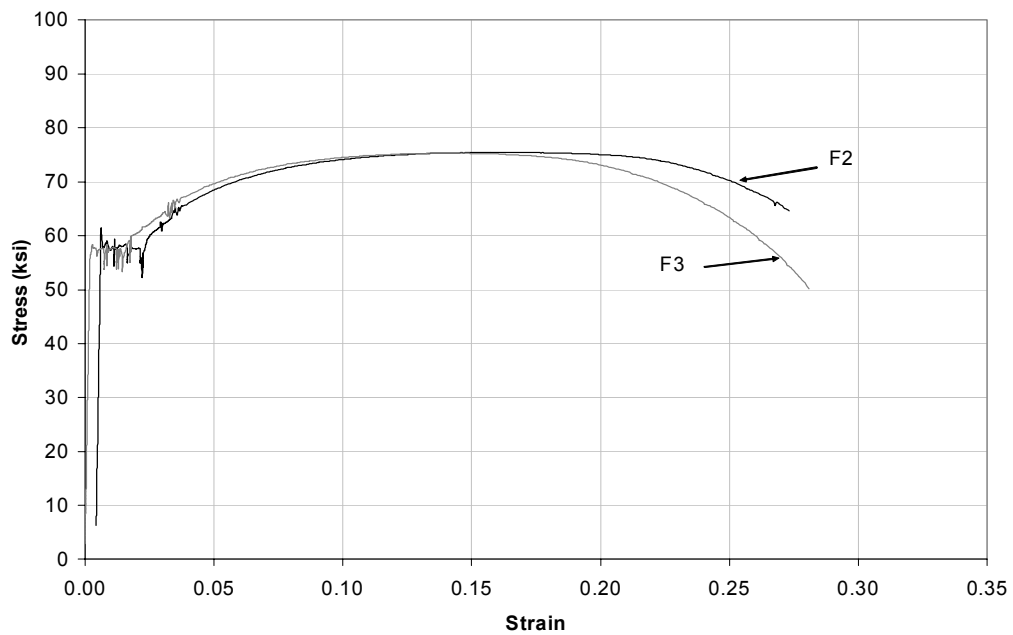
Figure 2.19 Tensile test results for F2 and F3 from steel A
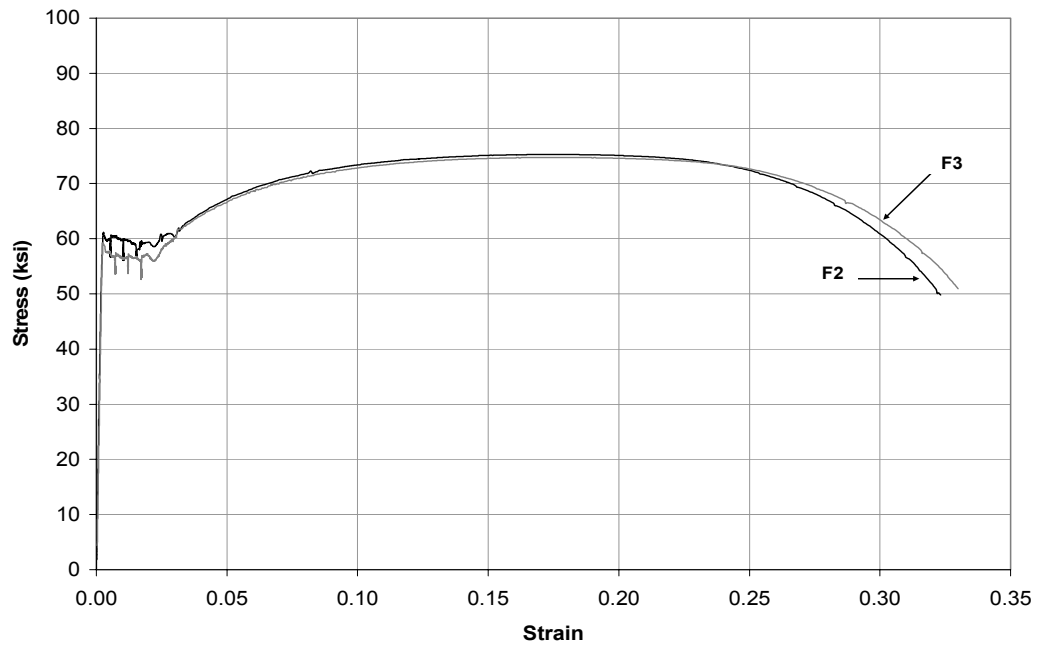
Figure 2.20 Tensile test results for F2 and F3 from steel B
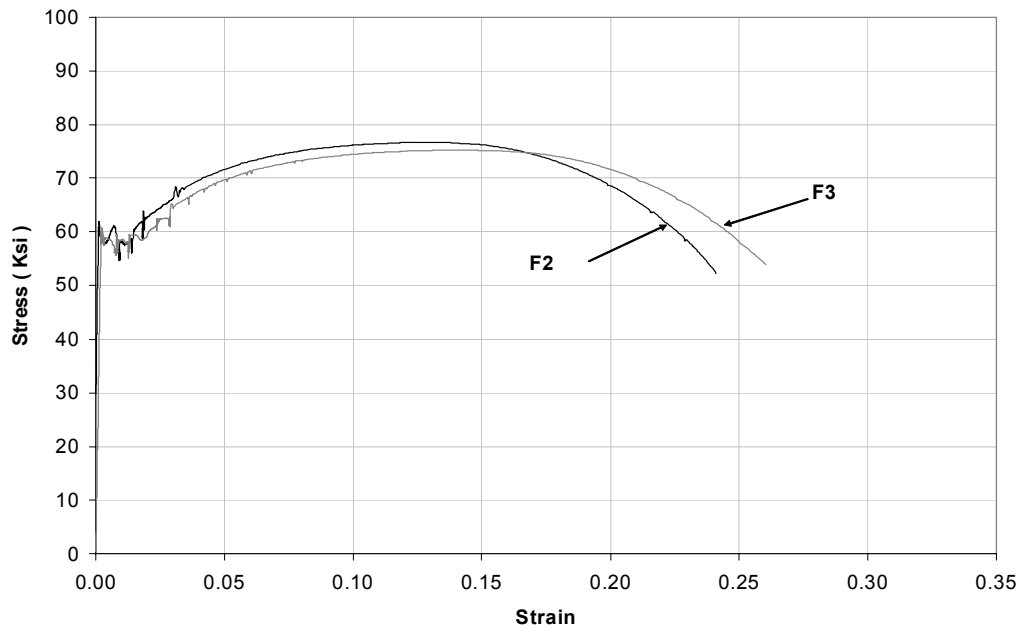
Figure 2.21 Tensile test results for F2 and F3 from steel C

55
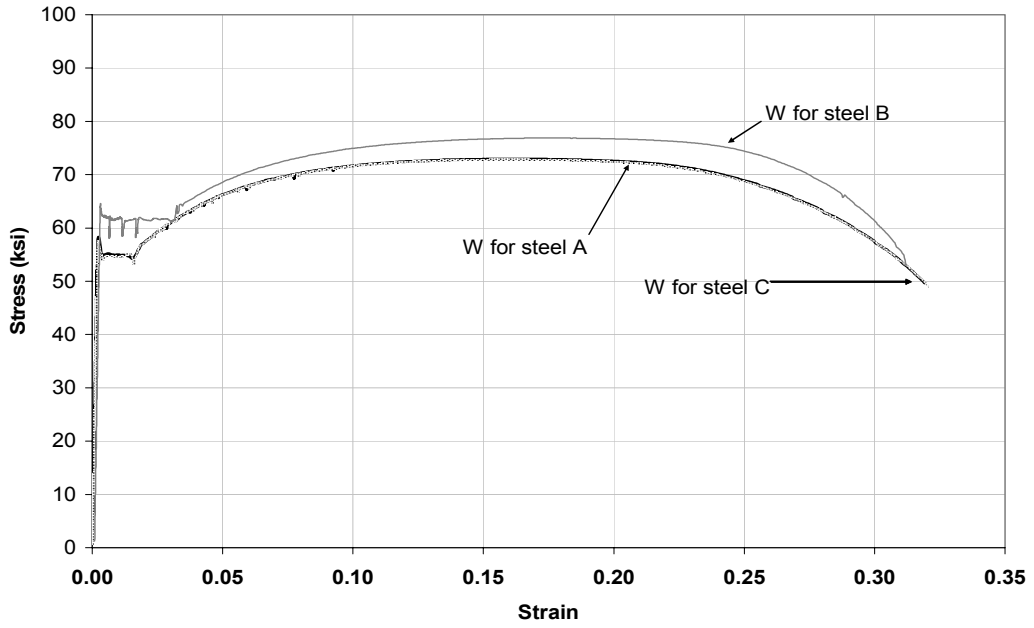
Figure 2.22 Tensile test results for W from steel A, steel B and steel C
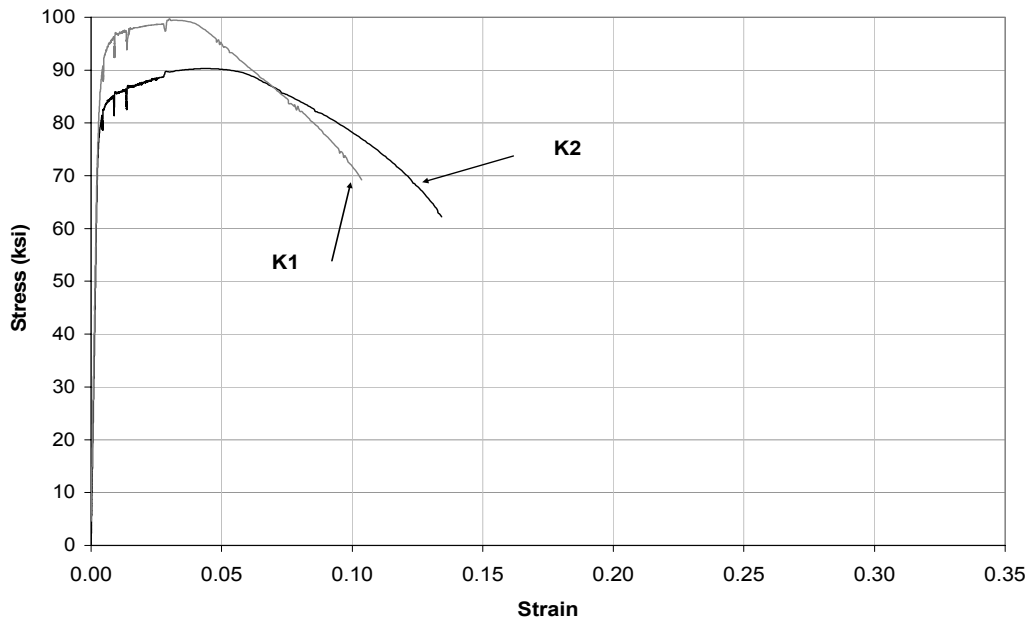
Figure 2.23 Tensile test results for coupons K1 and K2 from steel A
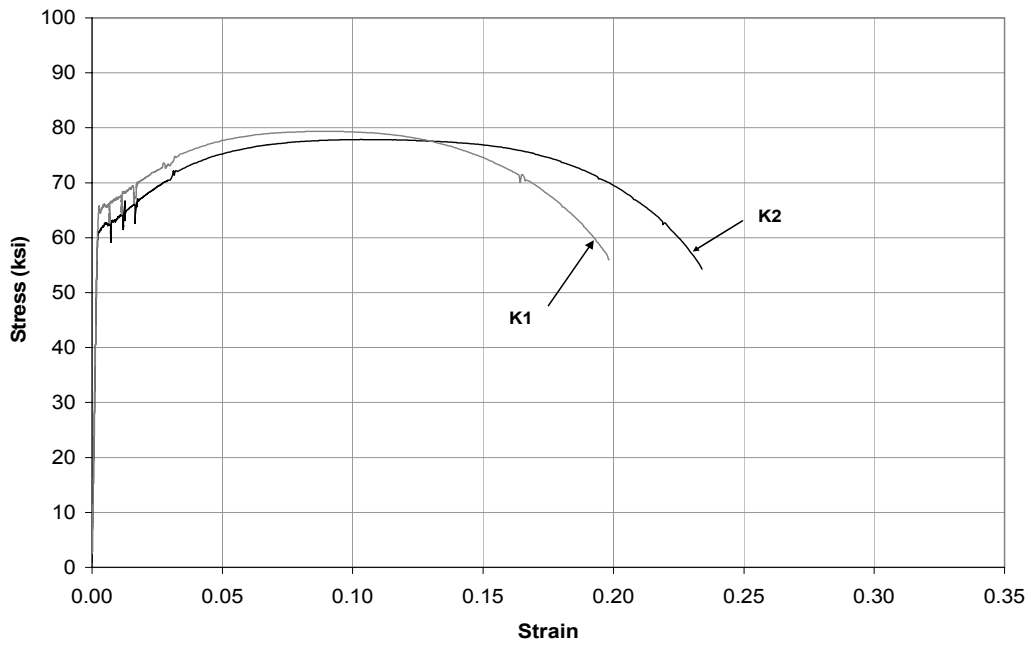
Figure 2.24 Tensile test results for coupons K1 and K2 from steel B
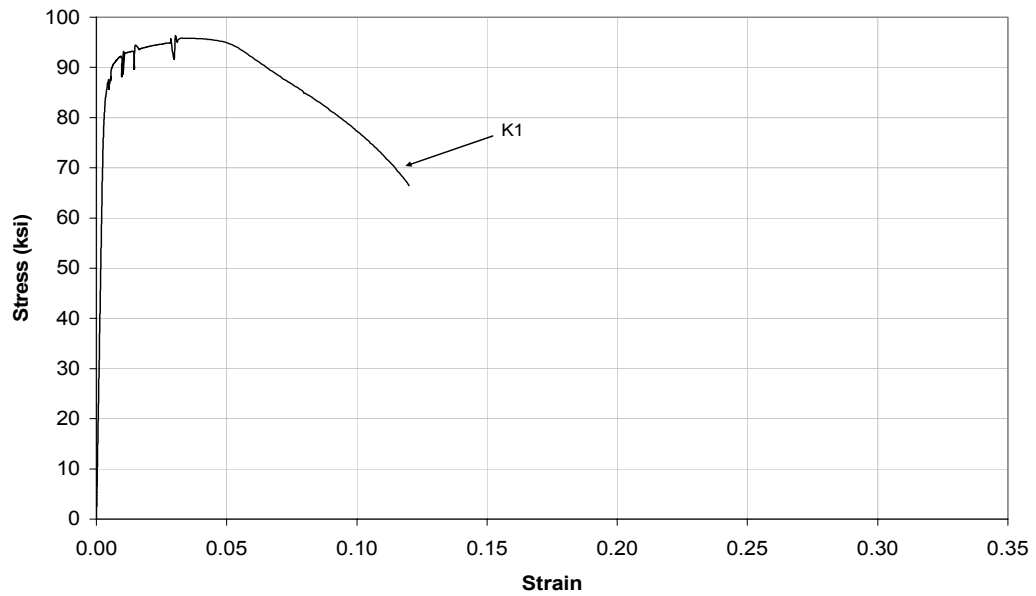
Figure 2.25 Tensile test results for coupons K1 from steel C

57

2.5   LOADING PROTOCOLS

Two different loading protocols were used to test the 10 shear links for this research. A loading protocol previously used by Ryu (2004), referred to by Ryu as the Severe Loading Protocol (SLP) was used for specimens in test series 1 and 2 (Specimens 1 to 7). The severe loading protocol, which is listed in Table 2.10, applies a large number of inelastic loading cycles to the specimen. It is a significantly more severe protocol, in terms of the number of cycles per deformation increment and the size of the deformation increments, as compared to the standard link loading protocol specified in the 2002 *AISC Seismic Provisions*. The severe loading protocol was chosen for specimens in the first two test series to promote the development of web fractures, and to therefore more clearly define the factors contributing to the web fractures.

As discussed earlier, specimens in the final test series (Specimens 8 to 10), were tested using a Revised Loading Protocol (RLP) developed by Richards and Uang (2005) and proposed for adoption in the 2005 AISC *Seismic Provisions*. Details of the revised loading protocol are listed in Table 2.11.

Table 2.10 Severe Loading Protocol (SLP) Used
in Specimens 1 through 7

Load Step	Cycles	Total link Rotation γ
1	3	±0.0025 rad.
2	3	±0.005 rad.
3	4	±0.01 rad.
4	4	±0.02 rad.
5	4	±0.03 rad.
6	4	±0.04 rad.
7	4	±0.05 rad.
8	4	±0.06 rad.
9	4	±0.07 rad.
10	4	±0.08 rad.
11	4	±0.09 rad.
Continue loading at increments of $\gamma = ±0.01$ rad. with four cycles of loading at each step		

Table 2.11 Revised Loading Protocol (RLP)
Used in Specimens 8 through 10
(per Richards and Uang,2003)

Load Step	Cycles	Total link Rotation γ
1	6	±0.00375 rad.
2	6	±0.005 rad.
3	6	±0.0075 rad.
4	6	±0.01 rad.
5	4	±0.015 rad.
6	2	±0.02 rad.
7	2	±0.03 rad.
8	1	±0.04 rad.
9	1	±0.05 rad.
10	1	±0.07 rad.
11	1	±0.09 rad.
Continue loading at increments of $\gamma = 0.02$ rad. with one cycle of loading at each step		

CHAPTER 3

Test Results

3.1   GENERAL

The experimental performance of each of the 10 shear links tested in this experimental program is summarized in this chapter. First, a description of key parameters used to characterize the response of the specimens is described. Then, key events of the response of each specimen, such as, yielding, buckling and fracture are described and accompanied by photographs. In addition, plots of the link shear versus total link rotation angle, γ, and link shear versus plastic link rotation angle, γ_p, are presented. Finally, a general discussion of the test results is presented at the end of the chapter.

3.2   LINK RESPONSE PARAMETERS

The total link rotation angle, γ, of the specimen is defined as the relative vertical displacement of the ends of the link divided by the link length, e. The link length, e, for all specimens in this program was 23-inches and it was measured as the clear distance between the end plates. The total link rotation angle, γ, includes

61

both the elastic and inelastic deformations of the link. In addition, elastic rotations of the link ends are also included.

The plastic link rotation angle, γ_p, is defined as:

$$\gamma_p = \gamma - \frac{V}{K},$$

Where, γ is the total link rotation, V is the link shear, and K is the elastic stiffness of the link specimens. K is computed as the ratio of the link shear, V, divided by the link rotation angle, γ, evaluated from elastic cycles of the specimen. In this test program, no yielding occurred in the test setup outside of the link specimens. Consequently, the plastic link rotation angle γ_p can be attributed solely to inelastic deformation of the links.

3.3   SPECIMEN 1

This specimen was the first one in a series of three specimens where the primary variable was the mill where the wide-flange sections used for the test specimens were produced. Specimen 1 was built using steel from Mill A. Whitewash was used for this specimen and for Specimen 2 to observe yielding of the link. However, the use of whitewash was suspended for the rest of the program because it interfered with the visibility of small cracks at early stages of the test. Figure 3.1 and 3.2 show the load deformation- response for Specimen 1

Figure 3.21 presents an overall view of the specimen before testing and before application of whitewash. During testing, the first signs of yielding were observed after the third cycle of load step 2 (γ = - 0.005 radian). However, the flaking of the whitewash in the web due to yielding was not visible until the end of the fourth cycle during load step 5 (γ = - 0.03 radian). At this point no cracks were visible, and no web buckling was observed. Even though there was no web buckling, the first cracks were observed during the first half of the fourth cycle of load step 8 (γ = - 0.06 radian). Three cracks were located at the termination of the welds of the stiffeners: one at the bottom of the north stiffener, one at the top of south stiffener and another small crack was detected at the bottom of the center stiffener. Figure 3.22 shows the crack observed at the toe of the weld of the north stiffener during load step 8 (γ = -0.06 radian). All cracks observed were found at the toe of the termination of the fillet welds of the stiffeners to the link web. The crack observed at the south stiffener was vertical and did not propagate throughout the specimen. The horizontal crack observed at the north stiffener propagated during the next cycle. Figure 3.23 shows the horizontal crack running parallel to the flange at the north center panel of the link during load step 9 (γ = + 0.07 radian). During the cycle corresponding to load step 9 (γ = + 0.07 radian) the horizontal crack observed at the north stiffener became very large, joining the crack observed at the center stiffener. However, the specimen successfully

completed the first half of the third cycle of load step 9 (γ = - 0.07 radian). Then, during the second half of this cycle the crack observed at the center stiffener propagated vertically, running parallel to the weld joining the stiffener to the web, as seen in Figure 3.24. It should be noted that no signs of web buckling were observed at this stage. During the upward portion of the fourth cycle of load step 9 (γ = + 0.07 radian), the center stiffener separated from the web and the upper flange of the link. As a result, the link strength decayed rapidly and the test was stopped at this point due to severe degradation in the link strength. Figure 3.25 shows the specimen after testing. This specimen achieved a plastic rotation, γ_p = ±0.06 radian.

3.4   SPECIMEN 2

The second specimen of the program was a replica of the first specimen, with the exception that the material used to build this specimen came from Mill B. Figures 3.3 and 3.4 show the load deformation- response for this specimen.

During testing, yielding was first observed at the center of the web during the first cycle of load step 3 (γ = +0.01 radian). Figure 3.26 shows the flaking of the whitewash as a result of web yielding. The first two cracks were observed at the end of the fourth cycle during load step 6 (γ = -0.04 radian). One crack was located at the termination of the weld at the bottom of the center stiffener, and an even smaller crack was observed at the termination of the weld at the bottom of

the south stiffener. Figure 3.27 shows the crack observed at the bottom of the center stiffener at the end of the fourth cycle of load step 6 (γ= -0.04 radian). During the end of the second cycle of load step 8 (γ = -0.06 radian), a new crack was observed at the termination of the weld at the top of the north stiffener. Then, an additional crack was observed at the termination of the weld at the top of the stiffener at the end of the fourth cycle of load step 8 (γ= -0.06 radian). As in the previous specimen, during this stage of the test web buckling was not observed. However, the cracks continued to appear and by the end of the second cycle of load step 9 (γ = -0.07 radian) cracks were observed at the termination of the welds at the top and bottom of all stiffeners. Figure 3.28 shows the cracks observed in all stiffeners at the end of the second cycle of load step 9 (γ = -0.07 radian).

Finally, during the third cycle of load step 9 (γ = +0.07 radian) the crack at the bottom of the center stiffener grew vertically and eventually joined the crack at the top, but no strength loss was observed at the end of this cycle. However, during the next cycle the specimen lost strength rapidly due to the horizontal propagation of the cracks at the top and bottom of the center stiffener. As a result, the intermediate stiffener separated from the bottom of the flange of the link and the test came to an end during the third cycle of load step 9 (γ = -0.07 radian) due the severe loss of load carrying capacity by the link. Figure 3.29

65

shows the specimen after testing. This specimen achieved a plastic rotation angle $\gamma_p = \pm 0.06$ radian.

3.5   SPECIMEN 3

The third specimen of the program was built as a replicate of the first two. However, the steel used to build this shear link came from Mill C. Figures 3.5 and 3.6 show the load deformation- response for this specimen

The first signs of yielding were observed at the web during the first cycle of load step 3 ($\gamma = +0.01$ radian). Unlike the preceding specimen, no cracks were observed at the end of load step 6 ($\gamma = \pm 0.04$ radian). During load step 8 ($\gamma = +0.06$ radian), small cracks were detected at the top and bottom of the north stiffener at the termination of the weld. Also, another small crack was observed at the termination of the weld on the top of the center stiffener. The cracks observed in this specimen were identical to the cracks observed in the first two specimens. Figure 3.30 shows one of the cracks observed at an early stage during the cycle at $\gamma = -0.06$ radian. However, no more cracks were detected at the end of the cycle. Then, during the second cycle of load step 9 ($\gamma = +0.07$ radian) two more cracks were detected. One small crack was observed at the toe of the weld at the top of the center stiffener, and the other located at the termination of the weld of the south stiffener. This specimen showed no web buckling, just like the first two. Although cracks were observed at the termination of the welds in all stiffeners,

66

the specimen successfully achieved a total angle rotation, $\gamma = \pm 0.07$ radian. Figure 3.31 shows an overall picture of the link during load step 9 ($\gamma = \pm 0.07$ radian), and no large cracks are visible. Note that the other two specimens failed before reaching the end of this load step.

The link completed the first half of the first cycle of load step 10 ($\gamma = \pm 0.08$ radian). However, the crack at the center stiffener grew along the weld, and the link lost strength during the second half of that cycle. Figure 3.32 shows the crack following the path of the weld of the center stiffener after the first cycle of load step 10. Finally, the center stiffener separated from the web and the upper flange of the link resulting in severe strength degradation of the specimen and termination of testing. Figure 3.33 shows the specimen after testing.

This specimen performed better than the first two, completing two more cycles than Specimen 1 (Mill A) and Specimen 2 (Mill B. This specimen reached a plastic rotation $\gamma_p = \pm 0.06$ radian.

3.6   SPECIMEN 4

The first specimen of the second series was built from steel from Mill B. This steel was chosen because Specimen 2 (Mill B) performed slightly worse than the specimens constructed of sections from the other two mills. This shear link specimen was constructed in a similar fashion to the first 3, except that it had

67

stiffeners on both sides of the web. Figures 3.7 and 3.8 show the load deformation- response for this specimen

During testing, the first signs of yielding were observed at the end of the fourth cycle of load step 2 ($\gamma = \pm0.005$ radian). Figure 3.34 shows the yielding in the panels of the link at an early stage during load step 2 ($\gamma = \pm0.005$ radian). Essentially all of the mill scale on the web of the specimen fell off by the end of load step 5 ($\gamma = -0.03$ radian). The first cracks were observed during the second cycle of load step 8 ($\gamma= +0.06$ radian). One crack was located at the termination of the weld at the bottom of the north stiffener and the other crack was observed at the termination of the weld at the top of the same stiffener. Figure 3.35 shows the crack observed at the end of the fourth cycle of load step 8 ($\gamma = -0.06$ radian). During load step 9 ($\gamma = \pm0.07$ radian), the crack at the bottom of the north stiffener propagated horizontally, parallel to the flange in the north direction. Also, another crack appeared at the top of the center stiffener and grew horizontally in the south direction parallel to the flange. Figure 3.36 shows both cracks during the second cycle of load step 9 ($\gamma = +0.07$ radian). Even though the cracks propagated rapidly during this cycle the link did not suffer a severe loss of strength, as shown in the load-deformation plot in Figure 3.7. The link lost more strength as the cracks at the top and bottom of the web propagated vertically during the first cycle of load step 10 ($\gamma = +0.08$ radian). The test came to an end

after severe degradation of the strength of the link at the end of the second cycle of load step 10 ($\gamma=+0.08$ radian). Figure 3.37 shows the bending of the stiffeners and the cracks at the top and bottom in the link after testing. This specimen performed similarly to the preceding specimens, reaching a plastic rotation, $\gamma_p = \pm0.06$ radian.

3.7   SPECIMEN 5

This specimen was constructed in manner similar to Specimen 4, with the exception that the stiffeners were not welded to the web. Figure 3.38 shows Specimen 5 before testing. Note that stiffeners were welded only to the flanges, as detailed in Figure 2.10. Figures 3.9 and 3.10 show the load deformation-response for this specimen.

In this specimen, web yielding was observed at the end of the second cycle of load step 2 ($\gamma = -0.005$ radian). Previous specimens with stiffeners welded to the web showed diagonal and then horizontal and vertical yield lines at early stages when the web was yielding. Specimen 5, on the other hand, showed only horizontal and vertical yield lines in the web. Figure 3.39 illustrates the horizontal yield lines observed after completing the first cycle of load step 3 ($\gamma =0.01$ radian). Unlike the earlier specimens with stiffeners welded to the web, signs of web buckling appeared in Specimen 5 during load step 6 ($\gamma = -0.04$ radian). Web yielding increased during the following cycles. However, no cracks

were observed anywhere within the specimen. Figure 3.40 shows the web buckling in the link after completion of the first cycle of load step 9 ($\gamma = +0.07$ radian). The web buckles initially appeared to occur primarily within each panel of the link, rather than extending over the full length of the link. This suggests that the stiffeners were effectively restraining web buckling, even though they were not welded to the web.

A small crack was observed at approximately mid-depth of the web, behind the center stiffener. It appeared that this crack was created by the rubbing of the stiffener against the web. As the test continued, this crack continued to grow. During the second cycle of load step 10 ($\gamma = +0.08$ radian) the load carrying capacity of the link started to decrease. Finally, the link suffered substantial strength degradation due to growth of the cracks behind the center stiffener. Figure 3.41 shows the crack behind the center stiffener at the end of the test and Figure 3.42 presents an overall view of the link after testing. This specimen performed better than Specimen 4 by reaching a plastic rotation angle $\gamma_p = \pm 0.07$ radian.

3.8   SPECIMEN 6

This specimen was replicate of Specimen 4, with the exception that the stiffeners were welded to the web and flanges of the link using the FCAW process with an E70T-6 electrode. In Specimen 4, as in all previous specimens, the

stiffeners were welded using the SMAW process with E7018 electrodes. Figures 3.11 and 3.12 show the load deformation- response for Specimen 6.

The first signs of yielding were observed after completing load step 2 ($\gamma = \pm 0.005$ radian). The first cracks were observed during the second cycle of load step 6 ($\gamma = -0.04$ radian). One crack was found at the termination of the weld at the bottom of the south stiffener and another at the termination of the weld at the top of the center stiffener. An additional crack was observed at the termination of the weld at the bottom of the north stiffener during the second cycle of load step 7 ($\gamma = +0.05$ radian). By the end of the fourth cycle of load step 7 ($\gamma = -0.05$ radian) cracks were observed at the termination of the welds at all the stiffeners. However, the web did not exhibit buckling and the specimen completed load step 7 ($\gamma = \pm 0.05$ radian) without loss of strength. Figure 3.43 shows the cracks at the termination of the fillet welds of the stiffeners during load step 8 ($\gamma = +0.06$ radian). During the subsequent cycles the cracks at the center stiffener grew horizontally, parallel to the flanges as seen in the previous specimens. Figure 3.44 shows the horizontal crack at the end of the fillet weld at the top of the center stiffener during load step 8 ($\gamma = -0.06$ radian). Even though the cracks observed at the end of the fillet welds of the center stiffener propagated, the specimen did not suffer loss of strength and completed two cycles of load step 8 ($\gamma = \pm 0.06$ radian). Figure 3.45 shows the horizontal cracks observed at the top and bottom of the

stiffener after completing two cycles in load step 8 ($\gamma = \pm0.06$ radian). During the third cycle of load step 8 ($\gamma = -0.06$ radian) the horizontal cracks propagated further and the specimen suffered severed strength degradation during the following cycle. Finally, the test was terminated at the end of the fourth cycle of load step 6, ($\gamma = -0.06$ radian). Figure 3.46 shows the specimen after testing. Note that these cracks are similar to those observed in previous specimens. This specimen reached a plastic rotation of $\gamma_p = \pm0.05$ radian.

3.9   SPECIMEN 7

The last specimen of the second series was a replicate of Specimen 2, with the exception that the stiffeners were welded to the web only. Figures 3.13 and 3.14 show the load deformation- response for Specimen 7. Figure 3.47 shows the specimen before testing.

The first signs of web yielding were observed during the first cycle of load step 3 ($\gamma = +0.01$ radian). This specimen exhibited diagonal and then horizontal and vertical yield lines in the web during early stages of yielding in the web as observed in the previous specimens where the stiffeners were welded to the web. Mill scale fell off completely from the web by the end of the fourth cycle of load step 5 ($\gamma = -0.03$ radian). Figure 3.48 shows the specimen after completion of the fourth cycle of load step 6 ($\gamma = -0.04$ radian) and no cracks were observed at this point .However, after the first half of the fourth cycle in load step 7 ($\gamma = +0.05$

radian) the first cracks became visible. The cracks were similar to the ones seen in the preceding specimens. One crack was located at the top of the north stiffener, and another crack was observed at the bottom of the same stiffener. Figure 3.49 shows the crack observed at the termination of the weld at the bottom of the north stiffener during load step 7 (γ = -0.05 radian). After completing load step 7 (γ = -0.05 radian), signs of web buckling were observed in the two center panels. Even though the web buckling was not severe during the first cycle of load step 8 (γ = +0.06 radian), cracks were observed at the bottom of the south stiffener. Then, after completing the first half of the third cycle of load step 8 (γ = +0.06 radian) the cracks propagated horizontally, and the specimen started to lose strength. Figure 3.50 shows the cracks observed at the top and bottom of the center stiffener. The north stiffener and the center stiffener appeared to be separating in a horizontal direction due to web buckling. During the second half of this cycle the crack at the bottom of the center stiffener joined the crack at the bottom of the south stiffener, and the specimen started to rapidly lose strength. Figure 3.51 shows the horizontal crack observed in the south center panel, after the completion of load step 8 (γ = +0.06 radian). Finally, the test was stopped due to severe strength degradation in the link due to the vertical propagation of the bottom crack in the south and north center panel. Figure 3.52 shows the specimen after testing. This specimen achieved a plastic rotation γ_p = ±0.05 radian.

73

3.10 SPECIMEN 8

This specimen was a replicate of the original Specimen 5 in which stiffeners were not welded to the web of the link. However the loading protocol used to test this specimen was the revised loading protocol presented in Table 2.7. Figures 3.15 and 3.16 show the load deformation- response for this specimen.

During the test, horizontal yield lines were observed at the center of the web during the first cycle of load step 3 (γ = +0.0075 radian). Figure 3.53 shows the horizontal yield lines during the third cycle of load step 3 (γ = +0.0075 radian). The mill scale on the center of the web came off completely by the end of the first cycle of load step 9 (γ= -0.05 radian), as shown in Figure 3.54. Note the difference in color of the center of the web and the k-area regions. The first signs of web buckling were observed after completing the first half of the first cycle of load step 10 (γ = ±0.07 radian). During the following cycles, web buckling concentrated in the two center panels, as shown in Figure 3.55. However, no cracks were observed in the specimen. During the first cycle of load step 12 (γ = ±0.11 radian) the damage suffered by the web due to the rubbing of the center stiffener became visible. Figure 3.56 shows the damage caused by the center stiffener to the web after the first half of the first cycle of load step 13 (γ = ±0.13 radian). The first crack was observed in the region damaged by the rubbing of the center stiffener with the center of the web after completing the second cycle of

74

load step 13(γ = ±0.13 radian), as shown in Figure 3.57. Even though web buckling was more severe at this stage, the specimen completed load step 13(γ = ±0.13 radian) without lost of strength. Finally, two cracks appeared behind the center stiffener, growing horizontally and causing the specimen to lose strength. Figure 3.58 shows the specimen after testing. This specimen reached a maximum plastic rotation γ_p= ±0.012 radian.

3.11   SPECIMEN 9

This specimen was fabricated as a replicate of Specimen 6, in which stiffeners were welded using the FCAW process. However, it was tested following the revised loading protocol presented in Table 2.7. Figures 3.17 and 3.18 show the load deformation- response for this specimen.

Web yielding was noted first after completing the sixth cycle of load step 2 (γ = -0.005 radian). Figure 3.59 shows the flaking of the mill scale after the sixth cycle of load step 4 (γ = -0.01 radian). Cracks were not visible in the specimen until the first cycle of load step 9 (γ = -0.05 radian) when a small crack was detected at the termination of the weld at the top of the south stiffener. During the following cycle another crack appeared at the termination of the fillet weld joining the web to the top part of the center stiffener. After completing the first cycle of load step 10 (γ = -0.07 radian), a crack was observed at the bottom of the north stiffener. Figure 3.60 shows the cracks at the ends of all stiffeners

after the first cycle of load step 11 (γ = -0.09 radian). At this point, the specimen exhibited no web buckling. One load step later, the crack observed at the top stiffener grew horizontally, parallel to the flange, as shown in Figure 3.61. As the cracks at the top and bottom of the center stiffener grew horizontally (Figure 3.62), the specimen started to unload during the first half of the first cycle of load step 13 (γ = +0.13 radian). These cracks were also observed in Specimen 6. Next, a vertical crack propagated along the center stiffener, of the specimen exhibited significant loss of strength, and the test was ended. Figure 3.63 shows the specimen after testing. This specimen achieved a plastic rotation γ_p = ±0.10 radian.

3.12   SPECIMEN 10

This specimen was similar to Specimen 2, with the exception that only two stiffeners were welded to the flanges and the web. Also, this specimen was tested using the revised loading protocol shown in Table 2.7. Figure 3.64 shows the specimen before testing, and Figures 3.19 and 3.20 show the load-deformation response for this specimen.

During testing, web yielding was first observed after completing load step 2 (γ = ± 0.005 radian). During the following cycles the mill scale of the web came off due to progressive web yielding. Figure 3.65 shows web yielding during load step 3 (γ = ±0.0075 radian). During the first half of the first cycle of load step 11

76

(γ = +0.09 radian), the first crack was observed at the termination of the fillet weld at the bottom of the north stiffener, as shown in Figure 3.66. This crack was similar to the cracks previously observed in the links where three stiffeners and sixth stiffeners were welded to the web. During the second half of the same cycle, web buckling was noted in the center panel. Figure 3.67 shows the web buckling seen in the center panel after completing the first cycle of load step 11 (γ = ±0.09 radian). As the test progressed, another crack appeared at the termination of the fillet weld at the bottom of the south stiffener. Then, during the first cycle of load step 13 (γ = -0.13 radian) the crack observed in the south stiffener grew horizontally, parallel to the flange in the south panel. Figure 3.68 shows the horizontal crack observed at the termination of the fillet weld of the south stiffener during load step 13 (γ = - 0.13 radian). Also, during this cycle buckling was more severe and concentrated in the center panel. After completing the first cycle of load step 14 (γ = -0.15 radian), a crack was also observed in the center panel, as shown in Figure 3.69. As the crack in the center panel propagated vertically during the beginning of the first cycle of load step 14(γ = -0.15 radian), the specimen lost strength rapidly. The test was stopped due to severe loss of strength caused by the extensive fracture of the web. Figure 3.70 shows the specimen after testing. This specimen reached a plastic rotation γ_p = ±0.12 radian.

3.13   DISCUSSION OF RESULTS

Ten specimens were tested and divided into three series. The first series was constructed to study the effects of k-area material properties on the development of web fractures. The second series was constructed to evaluate the effects of different arrangements of stiffeners and stiffener welding details and procedures on the development of web fractures. For this second series, links were tested with stiffeners on one side and on two sides. In addition, two different stiffener welding procedures were investigated: SMAW with E7018 electrodes and FCAW with E70T-6 electrodes. Also, the effects of not welding the stiffener to the web or the flanges were studied. Finally, in the third series, selected links were tested using the revised loading protocol (Richards & Uang, 2002) to investigate if they would meet the required plastic rotation in the *2002 AISC Seismic Provisions*.

Table 3.1 provides a summary of results. Included in Table 3.1 is the loading protocol used to test each specimen, along with the load step and load cycle at which link failure occurred for that protocol. Failure is defined to have occurred when the link shear resistance drops below the nominal shear strength of the link, based on a yield stress of 50 ksi. Table 3.1 also lists the maximum shear force developed by each link specimen as well as the maximum end moment. Also listed is the plastic rotation developed by each specimen. This is defined as

the maximum plastic rotation sustained by a link specimen for at least one full load cycle. Finally, Table 3.1 also provides a brief description of the failure mode for each link specimen.

In Table 3.1 the differences in load step and cycle at failure are larger between similar links tested under the severe loading protocol (Table 2.9) than between those links tested under the revised loading protocol (Table 2.10). For example, Specimens 5 and 6 showed a larger difference in the number of load steps to failure when tested with the severe loading protocol than when tested with the revised loading protocol. The severe loading protocol applies four loading cycles at each deformation increment in the inelastic range, whereas the revised loading protocol applies only one or two cycles of loading at each deformation increment in the inelastic range. As described in Chapter 2, the severe loading protocol was chosen to promote fracture of the link web by applying a large number of cycles, and to thereby permit better evaluation of the factors affecting fracture. The results in Table 3.1, as noted above, suggest that the severe loading protocol was successful in this regard.

3.13.1 Effects of Material properties

The first three specimens exhibited different plastic rotations, different plastic shear strengths, and different ultimate shear strengths, although these specimens were nominally identical and all constructed using a W10x33 section

of ASTM A992 steel. However, these three specimens were fabricated using three different heats of W10X33 sections. In this section, the possible factors that may have influenced the variations in plastic rotation, plastic shear strength and ultimate shear strength for the specimens are discussed.

Specimens 1, 2 and 3 were nominally identical, except for their material properties. Each heat of steel had somewhat different mechanical properties in the web, in the flanges, and in the k-areas. Initially, it was theorized that poor material properties in the k-area may be correlated to the development of web fractures in shear links. From k-area coupons, Figures 2.24, 2.25 and 2.26, Specimen 2 was expected to develop a higher plastic rotation than Specimens 1 and 3, since it had better ductility (i.e. higher elongation). Also, hardness results in the location where fillet welds joining the web to the stiffeners were terminated in the test specimens had a value 11% lower for Specimen 2 than Specimen 1 (Figure 2.17). However, both specimens reached the same plastic rotation $\gamma_p = \pm 0.06$ radian. In addition, the results from Specimen 3 contradicted the initial theory since the specimen reached a plastic rotation $\gamma_p = \pm 0.07$ radian although it exhibited similar properties to Specimen 1. In addition, these three specimens presented the same failure mode regardless their k-area properties. In each specimen, web fractures initiated at the termination of the fillet welds that joined the stiffeners to the web. These results would suggest that mechanical properties of steel in the k-area are

not entirely responsible for the overall cyclic deformation capacity of shear links as controlled by web fracture. However, as discussed below, the data from this test program suggest that the potential for web fracture may be more related to the material properties of the k-area after it has been welded since heat input due to welding might modify the mechanical properties of the steel.

In addition to evaluating the effects of material properties on the deformation capacity of the links, the first thee specimens also allow the opportunity to evaluate the effect of material properties on link shear strength. There are two link shear strength values of interest in EBF design. The first is the plastic shear strength of the link, V_p. This is the link shear at first significant yield of the link and is the basis for sizing links in EBFs. The second strength level of interest is the ultimate shear strength of the link. This is the maximum shear force that is developed by the link under cyclic loads, and is the basis for sizing the braces, beam segments outside of the links, and the columns in EBFs.

Based on the shear force versus link rotation plot for Specimen 2 (Figure 3.4), the link shear at first significant yield is approximately 90 kips. However, the computed plastic shear capacity listed in Table 2.4 was 99.7 kips based on measured dynamic yield stress. Meanwhile, Table 2.5 reports a plastic shear capacity of 93.3 kips based on measured static yield stress. Note that all links were quasi-statically tested. During the loading process of the shear links in the

inelastic range, there was typically a pause of approximately 5 seconds after loading was stopped and before data was read with the data acquisition system. During this pause, the load on the link usually dropped a small amount, reflecting the differences between static and dynamic yield. Due to practical time constraints, it was not possible to pause several minutes before reading to obtain a more accurate static yield strength value (as was done with the tension coupons). Therefore, the plastic shear strength values exhibited by the test specimens reflect a strain rate intermediate between a dynamic value and a static value. Nonetheless, the strength values of the link specimens are likely closer to a static value, since most of the load drop from dynamic to static levels occurs within a few seconds after loading is stopped. . Therefore, due to the nature of the testing procedure, the use of static yield stress to calculate the plastic shear strength would result in a better approximation to the actual plastic shear values obtained from testing. Overall, considering variations and uncertainties in strain rates, the plastic shear strength observed in the test specimens match reasonably well with the values computed in Table 2.5 using the measured static yield stress values.

Specimens where whitewash was not used exhibited what appeared to be difference in yielding stages between the web and the k-area. For instance, in Figure 3.54 there is a difference in the center of the web and the regions near the k-area. It is possible that the center of the web yielded first, and then the regions

around the k-area. On the other hand, this difference in colors of the center of the web and the "k" region might be due to the roller straightening process causing the mill scale in the k-area to fall off, therefore during testing only the center of the web appears to be yielding while k-area regions do not show any signs of yielding.

It was observed that the maximum link shear reached by Specimens 1 and 3 was higher than the link shear reached by Specimen 2. Specimen 1 reached a maximum link shear of 135 kips and Specimen 3 reached 141 kips. Meanwhile, Specimen 2 only reached a maximum link shear of 120 kips. This is somewhat contrary to expectations based on the measured yield and tensile strength of the web material. That is, the web coupons for Specimen 2 (Steel B) had a higher yield and tensile strength than the web coupons for Specimens 1 and 3 (Steel A and C), but Specimen 2 developed a significantly lower ultimate shear strength than Specimens 1 and 3. This apparent contradiction may potentially be explained by the k-area material properties. From Table 2.17, it is observed that coupons from the k-area of Specimens 1 and 3 exhibited substantially higher yield strength and higher ultimate strength than the k-area coupons from Specimen 2. If it is assumed that the k-area properties occur over a depth of web equal to approximately one-inch at both the top and bottom of the web, and the maximum strength that the link can achieve is calculated including the k-area, then the

maximum strength that the link can achieve can be estimated as:

$$V_{max} = 0.6(d - 2t_f - 2'')t_w F_{u_{web}} + 0.6(2'')t_w F_{uk-area}$$

Using this equation, the calculated V_{max} would be: 137 Kips for Specimen 1, 121 Kips for Specimen 2, and 135 Kips for Specimen 3. The links showed a tendency for higher ultimate strength when the k-area had higher ultimate strength Therefore, based on these results it appears that the strength of the k-area and the overall strength of the links are correlated. However, in deeper sections the effects of the strength of the k-area might not be as critical when calculating the ultimate strength in a shear link, since the portion of the web with elevated tensile strength will be a smaller fraction of the total web area.

3.13.2 Effect of one sided vs. two-sided stiffeners and welding procedures

In this section two issues are addressed. First, it was postulated that links with two-sided stiffeners might fail at lower rotation levels than links with one-sided stiffeners because of the additional welding in the k-area. That is, it was postulated that the web fracture problem might be more severe in links where stiffeners are welded on both sides. Therefore, Specimen 4 was provided with stiffeners on both sides of the web. Specimen 2 was nominally identical to Specimen 4, expect that Specimen 2 has stiffeners on only one side of the web. Consequently, Specimens 2 and 4 provide a direct comparison of links with stiffeners on one side versus on both sides.

84

Secondly, Specimen 6 was constructed as a replicate of Specimen 4 but the stiffeners were welded using a different welding procedure. It was theorized that welding procedures that generate higher heat input might have more adverse effects on the material properties at the termination of the stiffener weld in the k-area. Therefore, these procedures might affect the occurrence of web fracture. The stiffeners for Specimen 4 were welded by SMAW process with E7018 electrodes, whereas the stiffeners for Specimen 6 were welded with FCAW process using E70T-6 electrode.

The test results indicate that the Specimen 4 (stiffeners on both sides) performed no worse than Specimen 2 (stiffeners on one side only). Consequently, welding stiffeners on both sides of the web is not necessarily more detrimental with respect to web fracture than welding stiffeners on one side only. Interestingly, Specimen 4 actually performed slightly better than Specimen 2, sustaining one additional load cycle prior to failure. This difference in performance might be explained by the additional support given by the additional stiffeners provided at the back of the link, which help prevent a severe drop in the load sustained by the link once web fracture occurred. In addition, web fractures in Specimen 4 were not observed in earlier cycles than in Specimen 2. Fractures were observed at a later stage, but they initiated at the same location where fractures in Specimen 2 initiated. Although Specimen 4 was constructed with

85

additional welding in the k-area, both specimens achieved the same plastic rotation $\gamma = \pm0.06$ radian. It appears that the additional welding in the web does not have a negative impact in the properties of the k-area. It is probable that the thickness of the web was adequate to prevent welding from one side affecting the properties of the k-area of the other side. Therefore, it is expected that links with thicker webs will also not be likely experience detrimental effects due to the additional welding on the opposite side of the web. Thus, two-sided stiffeners can likely be used in links with thicker webs than the W10x33 sections, without increasing the possibility of web fractures.

As described above, Specimens 4 and 6 were nominally identical, except for the welding process used to connect the stiffeners to the link. Even though the welding procedures used in both links are different, the failure mode remained unchanged. Both specimens failed by web fracture initiating at the termination of the fillet welds. However, Specimen 6 where stiffeners were welded with FCAW showed cracks substantially earlier than Specimen 4 where stiffeners were welded with SMAW. The first cracks were observed in Specimen 4 during the second cycle at $\gamma = \pm0.06$ radian. Meanwhile, in Specimen 6 cracks were observed first during the first cycle at $\gamma = \pm0.04$ radian. Cracks not only showed up at an earlier stage for Specimen 6, but also caused failure at an earlier stage. Specimen 4 reached a plastic rotation $\gamma_p = \pm0.06$ radian while Specimen 6 reached a plastic

86

rotation of only $\gamma_p = \pm 0.05$ radian. These results indicate that the use of the FCAW process prompted web fracture at an early stage resulting in a lower plastic rotation. Consequently, the welding process used for the stiffeners can have a significant impact on the development of web fractures. However, the failure mode is identical in both specimens.

3.13.3 Effects of other stiffener details on web fractures

This section presents the analysis of the results of two specimens where the stiffeners were either not welded to the web of the link, or were not welded to the flanges of the link. Data gathered in the earlier specimens demonstrates that links where stiffeners are welded to the flanges and the web experience web fractures. Therefore, one specimen was constructed where the stiffeners were not welded to the web, but only to the flanges. A second specimen was constructed where the stiffeners were not welded to the flanges, but only to the web. This attempt was made to delay or possibly eliminate web fractures, as discussed in Chapter 2. In addition to potentially mitigating the fracture problem, eliminating some of the stiffener welds would also reduce fabrication cost.

Specimen 5 was provided with stiffeners front and back but not welded to the web. It was theorized that by avoiding the fillet weld of the stiffener to the web, the stress concentration at the k-area would be eliminated, resulting in the elimination of web fractures. Also, the reinforcement provided by the stiffeners

87

was thought to be adequate to avoid severe web buckling at an early stage during the test. Specimen 5 not only reached higher plastic rotation than Specimens 2 and 4, but it did not experience web fractures in the k-area. The fractures observed in this specimen appeared at the center of the web. There is a possibility that the web fracture shown in Figure 3.41 might have been initiated by a cut produced by the center stiffeners due to the rubbing of the stiffeners and the center of the web. These results suggest that web fractures in the k-area were prevented by not welding stiffeners to the web. Overall, the results of Specimen 5 are very promising.

Specimen 7 was constructed by welding the stiffeners only to the web, and not to the flanges. As described in Chapter 2, bending of the stiffeners caused by warping deformations of the link may increase the stress concentration at the termination of the stiffener to link web weld. Therefore, it was postulated that by not welding the stiffener to the flanges of the link, the stiffeners no longer resist warping and bending of the stiffener is reduced. As a result, stress concentrations at the termination of the weld may be reduced and web fracture may be prevented or delayed.

During testing of Specimen 7, web buckling was observed. However, fractures appeared at the termination of the fillet welds before web buckling appeared. When web buckling was observed the fractures propagated more

rapidly. It appears that the combined effect of the fractures and the web buckling resulted in a lower plastic rotation.

This specimen achieved a total plastic rotation $\gamma_p = \pm 0.05$ radian. The data suggest that by eliminating the fillet weld joining the stiffeners to the flanges, the web is allowed to buckle as shown in Figure 3.71, resulting in a less desirable type of failure. As illustrated in this figure, the link flanges appeared to rotate in this specimen, likely causing significantly larger stress concentrations the stiffener to web weld terminations. It is not clear why the link flanges had a tendency to rotate, but such rotation was observed in the specimen. Welding the stiffeners to the flanges apparently restrains link flange rotation. Overall, Specimen 7 with stiffeners welded to the web only showed poor performance.

Zones affected by removing welding in the flanges
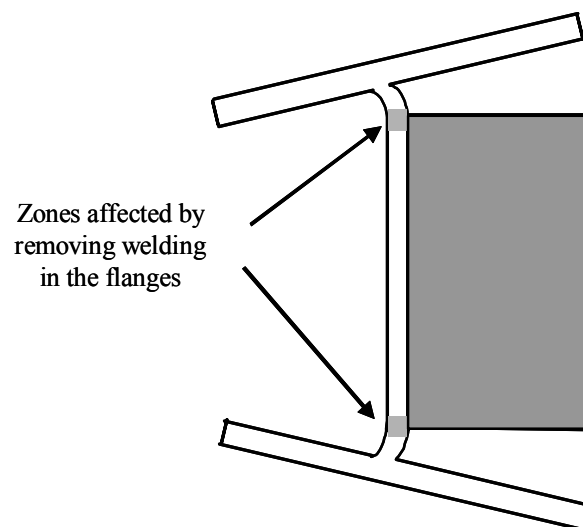
Figure 3.71 Failure mode experienced by Specimen 7

3.13.4 Evaluation of the required plastic rotation in selected links

In this section, the results of selected links tested under the revised loading protocol are examined. These links were tested under this loading protocol to determine if they could meet the plastic rotation requirements set by the *2002 AISC Seismic Provisions*. Replicates of Specimens 5 and 6 were constructed, were designated as Specimens 8 and 9, and were tested using the revised loading protocol.

Two specimens were selected from the preceding series to be tested using the revised loading protocol (Richards & Uang, 2002). Specimen 5 (stiffeners welded to flanges only) was selected, since it did not show web fractures under the severe loading protocol Since Specimen 5 demonstrated such promising performance, it was retested (as Specimen 8) to determine if a link constructed with stiffeners welded only to the flanges can achieve the plastic rotation required in the *2002 AISC Seismic Provisions*. In addition, Specimen 6 was selected. The FCAW procedure used in Specimen 6 appeared to affect the specimen is a more manner than the SMAW procedure used in Specimen 4. Therefore, there was some concern that links with stiffeners welded using this procedure would not meet the plastic rotation required by the *2002 AISC Seismic Provisions*.

After the promising results in Specimen 5, a replicate was tested using the revised loading protocol (Richards & Uang, 2002) and denominated Specimen 8. Also, in this specimen an attempt was made to smooth the surfaces of the

stiffeners, so they would not cut the web of the link. Even though some benefit was obtained by smoothing the surface of the stiffeners, a similar cut was observed in the web as in Specimen 5, as seen in Figure 3.56. It appears that the stiffeners used in these specimens were not thick enough. Therefore, they buckled and damaged the web. A better approach to solve this problem could be to provide thicker stiffeners. Even though the crack might have been initiated by the cut produced by the stiffeners, the plastic rotation of 0.12 radian achieved by this specimen significantly exceeded the 0.08 radian required by the *2002 AISC Seismic Provisions*. This result suggests that links constructed by welding stiffeners to the flanges only can provide excellent cyclic loading performance and can exceed the performance requirements of the *2002 AISC Seismic Provisions*

Specimen 9, which was a replicate of Specimen 6, was tested using the revised loading protocol (Table 2.7) to investigate if it would meet the plastic rotation requirement of 0.08 radian set by the *2002 AISC seismic provisions*. Even though the loading procedure was changed, web cracks initiated at the ends of fillet welds connecting the stiffeners to the web. Also, the fractures propagated similarly to the fractures seen in Specimen 6. The mode of failure was the same in Specimens 6 and 9. However, Specimen 9 reached a plastic rotation $\gamma_p = \pm 0.10$ radian. Consequently, even though the use of FCAW for welding stiffeners is

detrimental to link rotation capacity, the specimen still achieved the 0.08 radian required by the *2002 AISC Seismic Provisions.*

3.13.5 Sparse stiffening and web fractures

In this section the results of Specimen 10 are analyzed. Specimen 10 was constructed with two stiffeners welded to the web and flanges, as an attempt to replicate specimens tested in the 1980's where web fracture was not observed. The majority of links tested in the 80's would not meet current requirements for spacing between stiffeners. Therefore, as discussed in Chapter 1, it was theorized that the smaller stiffener spacing required by the *2002 AISC Seismic Provisions* changes the controlling failure mode from web buckling to web fracture.

Even though the spacing between stiffeners in this specimen was increased from 5.75" to 7.66", cracks were still observed before web buckling was noticed. Therefore, it appears that small spacing between stiffeners required in the *2002 AISC Seismic Provisions* is not likely responsible for the initiation of cracks at the termination of the fillet welds that connect the stiffeners to the web of the link. This observation combined with the results obtained from coupons of the K-area of steel B suggest the possibility that web fracture is the product of other factors, such as the welding procedure. The effect of the welding in the properties of steel appears to play a more important role in the occurrence of web fracture than the spacing between stiffeners or k-area properties before welding. Even though web

fractures were not prevented in Specimen 10, the plastic rotation requirements were met. This specimen exceeded the code requirements by 25% although spacing between stiffeners was increased 33%. The results suggest that current stiffener spacing criteria should be reviewed. Stiffener spacing in Specimen 10 violated current requirements but the specimen still easily achieved the required plastic rotation.

Table 3.1 Summary of Results

Specimen	Loading Protocol	Test Results				
		V_{max}(kips)	M_{max}(kip-in) at either the column or the beam end of the link	γ_p (radian)	Load Step and load cycle at failure*	Failure Mode
1	SLP	135	1650	±0.06	9, ±3	Fracture of the web initiating at the termination of the fillet welds joining the stiffeners to the web
2	SLP	120	1469	±0.06	9, +3	Fracture of the web initiating at the termination of the fillet welds joining the stiffeners to the web
3	SLP	141	1753	±0.07	10, ±1	Fracture of the web initiating at the termination of the fillet welds joining the stiffeners to the web
4	SLP	128	1545	±0.06	9, +4	Fracture of the web initiating at the termination of the fillet welds joining the stiffeners to the web
5	SLP	117	1544	±0.07	10, +2	Severe web buckling followed by a fracture initiated by the rubbing of the center stiffener at the center of the link's web
6	SLP	123	1507	±0.05	8, ±3	Fracture of the web initiating at the termination of the fillet welds joining the stiffeners to the web
7	SLP	120	1395	±0.05	8, +3	Fracture of the web initiating at the termination of the fillet welds joining the stiffeners to the web, followed by web buckling
8	RLP	118	1381	±0.12	13, ±1	Severe web buckling followed by fracture initiated by the rubbing of the center stiffener at the center of the link's web
9	RLP	133	1589	±0.10	13, +1	Fracture of the web initiating at the termination of the fillet welds joining the stiffeners to the web
10	RLP	127	1538	±0.12	13, ±1	Fracture of the web initiating at the termination of the fillet welds joining the stiffeners to the web, followed by web buckling

* The symbol (±) denotes total completion of a cycle. Meanwhile, the symbol (+) denotes completion of only the positive excursion of that cycle. For instance Specimen 4 completed three cycles and failed after completing the positive portion of the fourth cycle during load step 9.
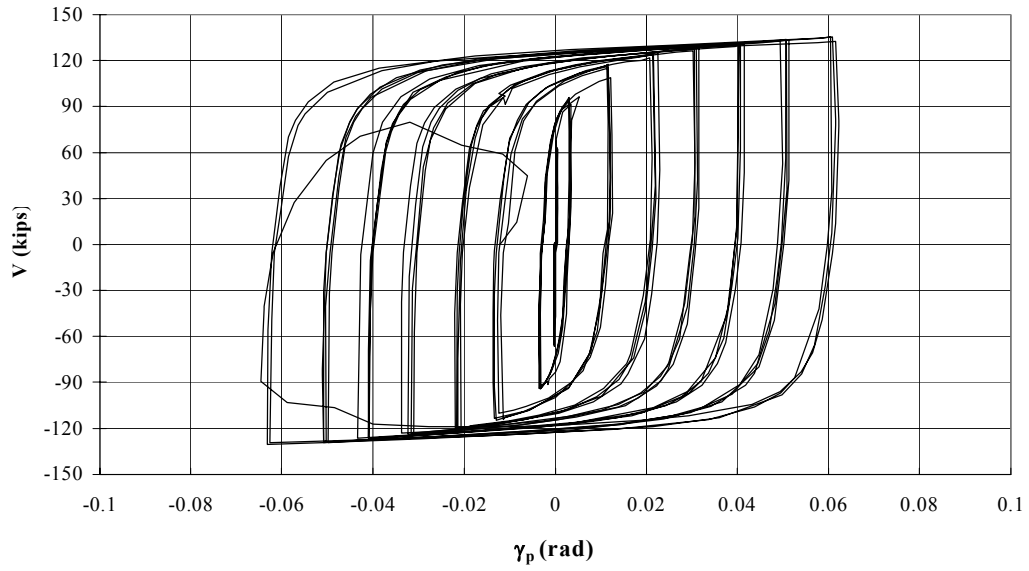
Figure 3.1 Link shear vs. plastic rotation angle for Specimen 1
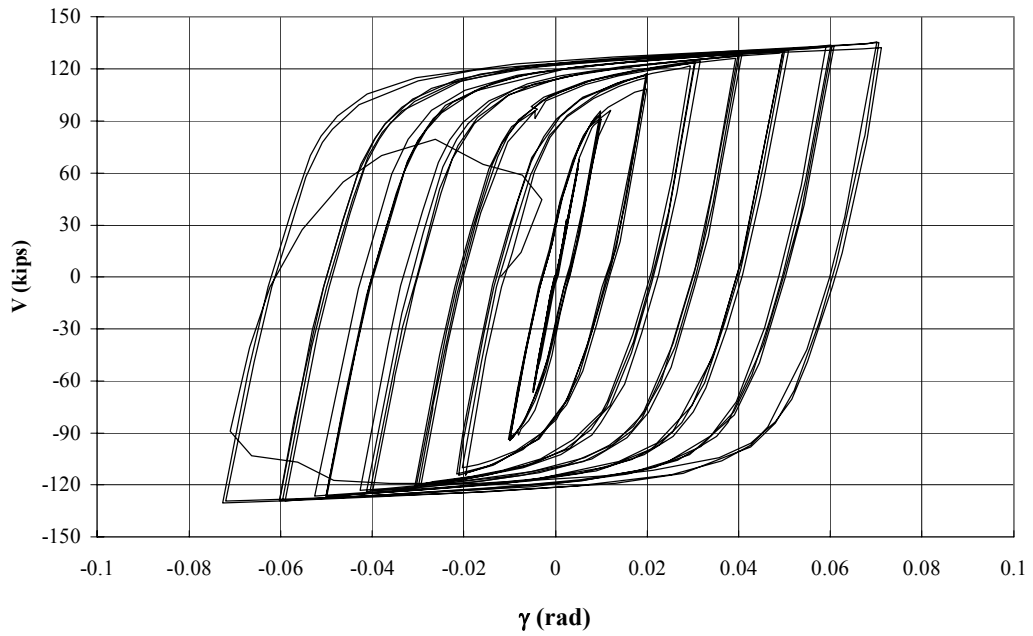
Figure 3.2 Link shear vs. total rotation angle for Specimen 1

95
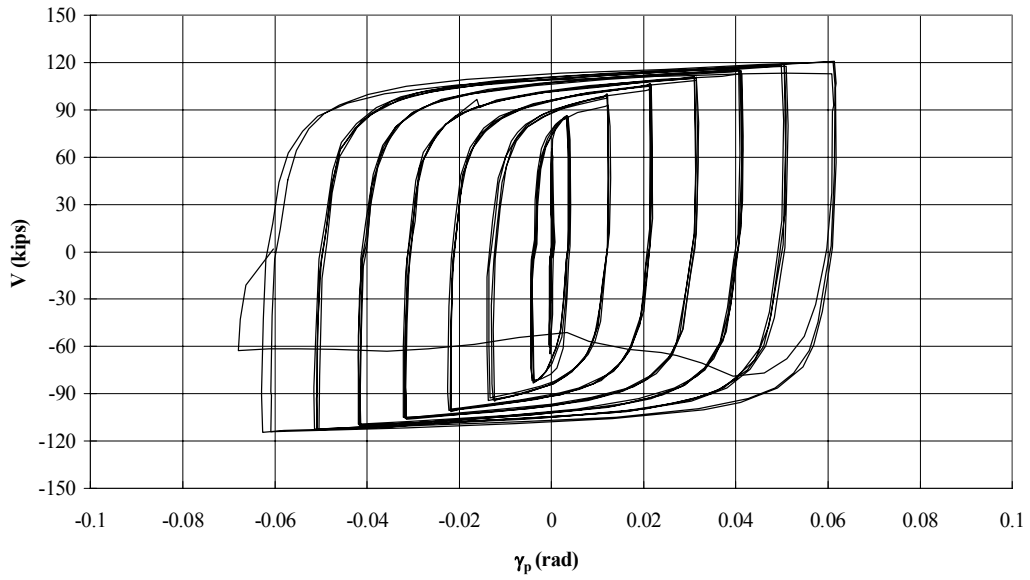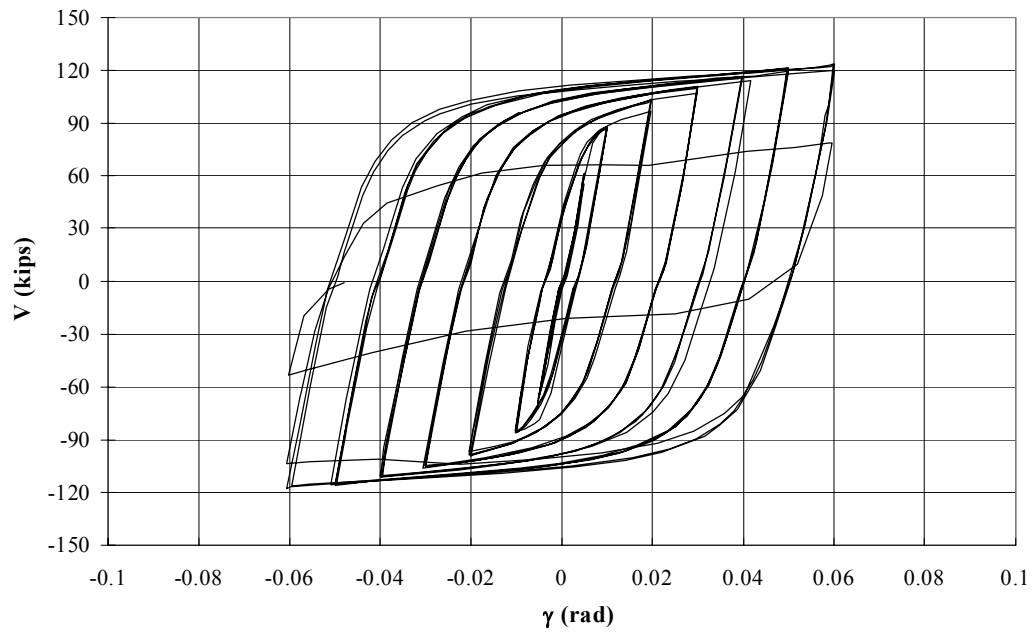
Figure 3.3 Link shear vs. plastic rotation angle for Specimen 2
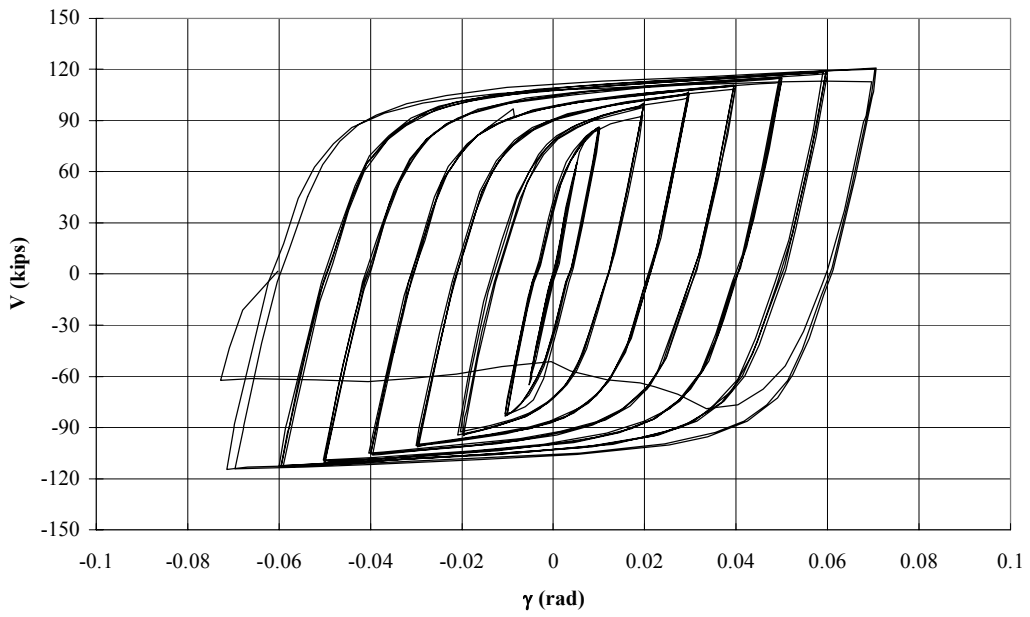
Figure 3.4 Link shear vs. total rotation angle for Specimen 2

96
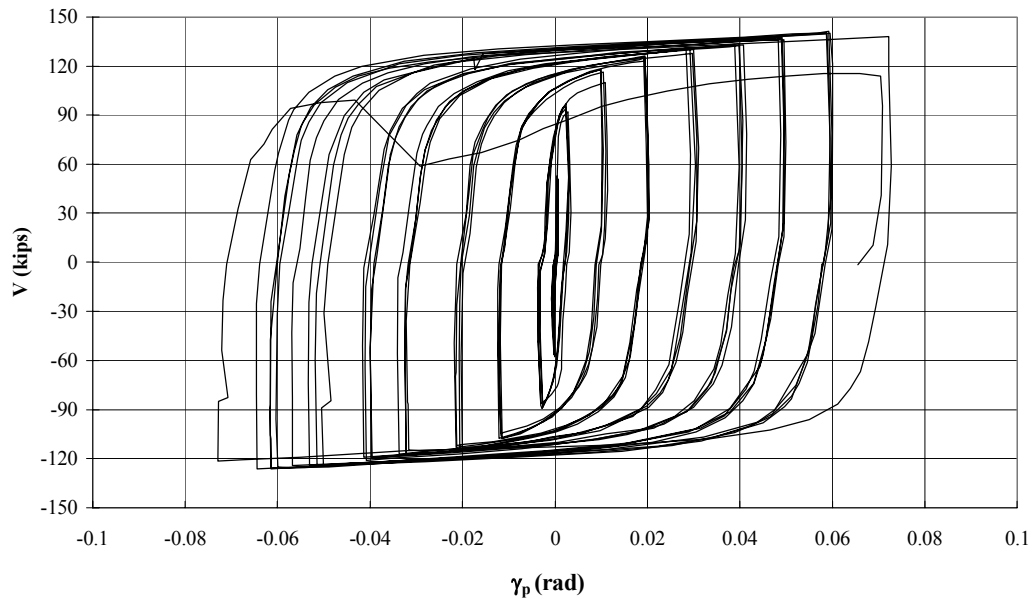
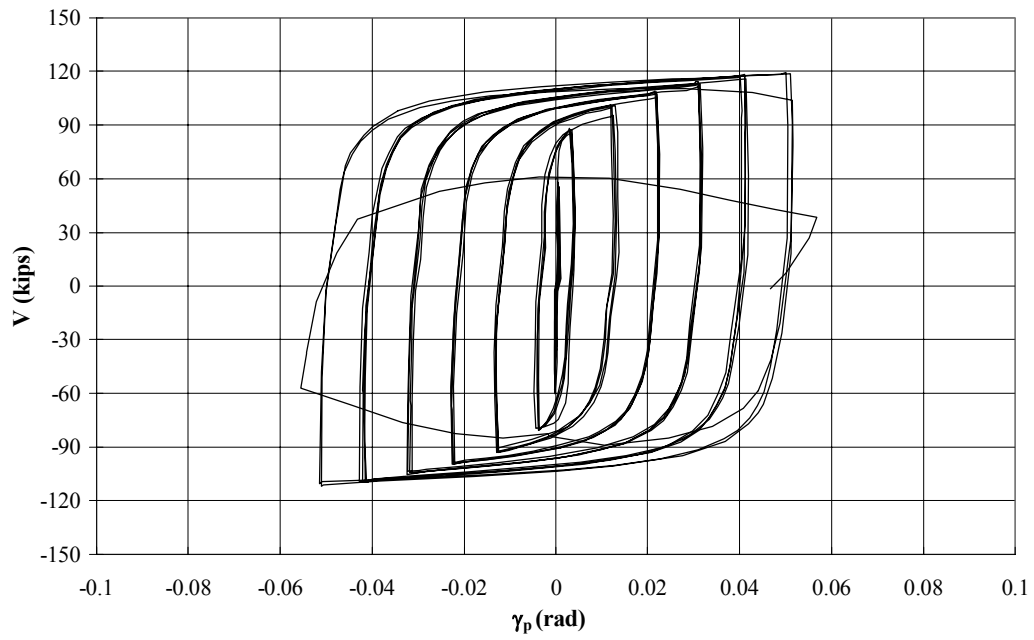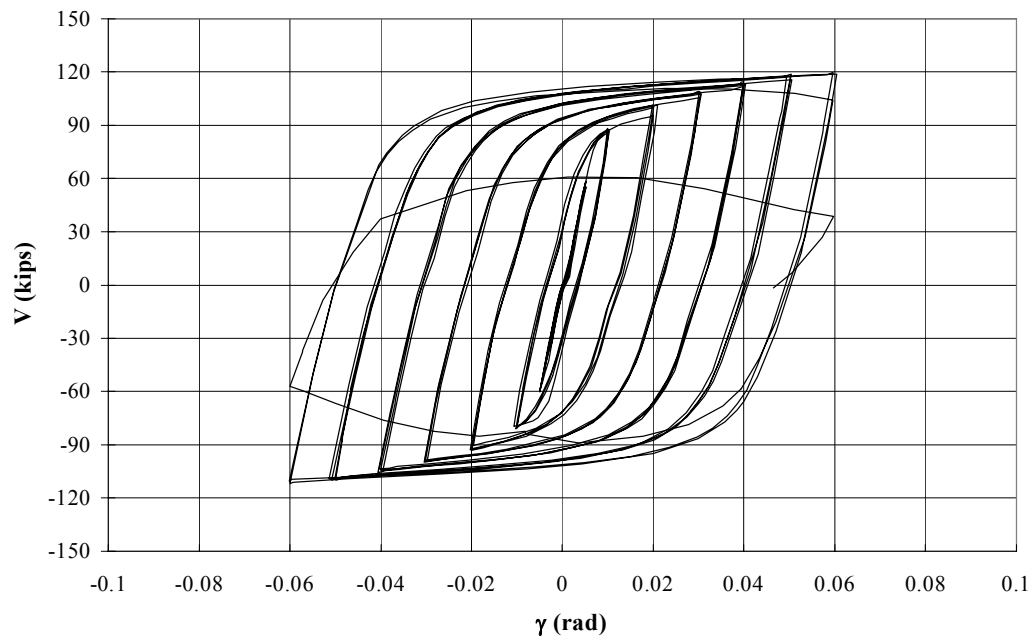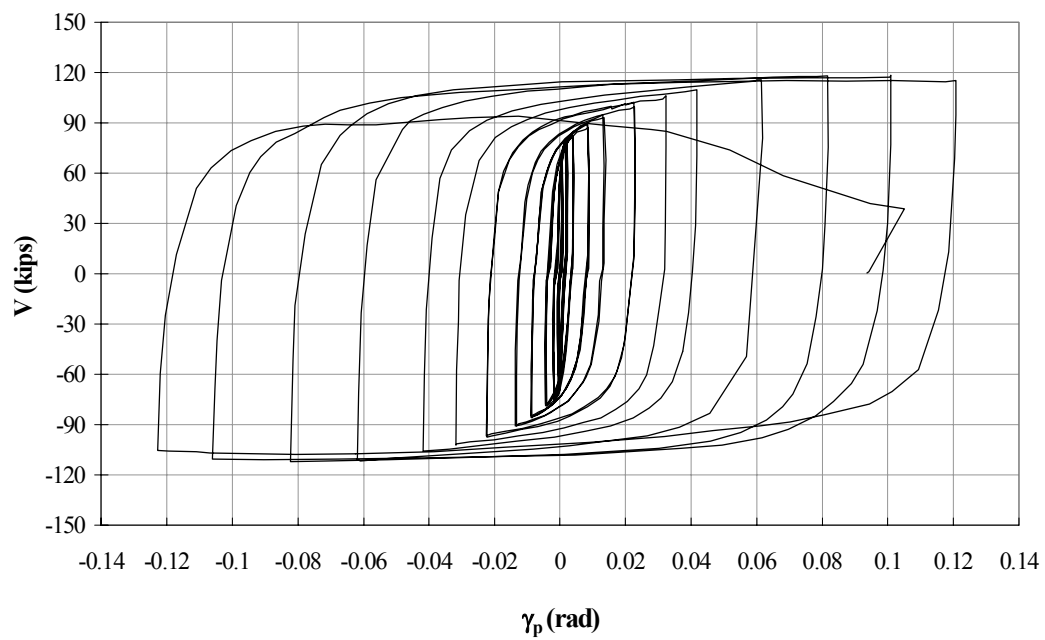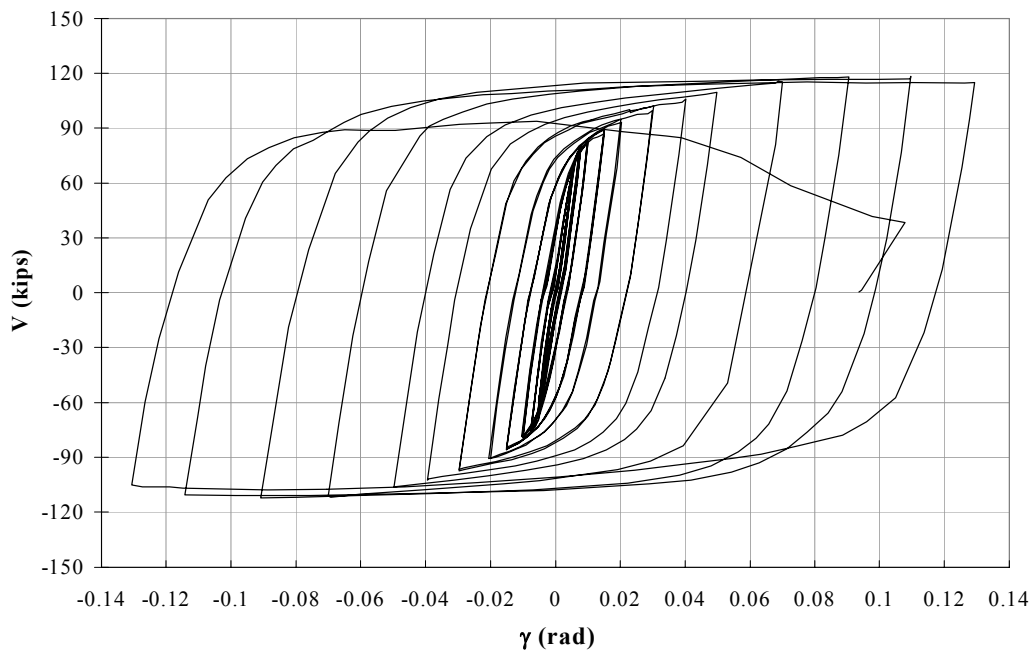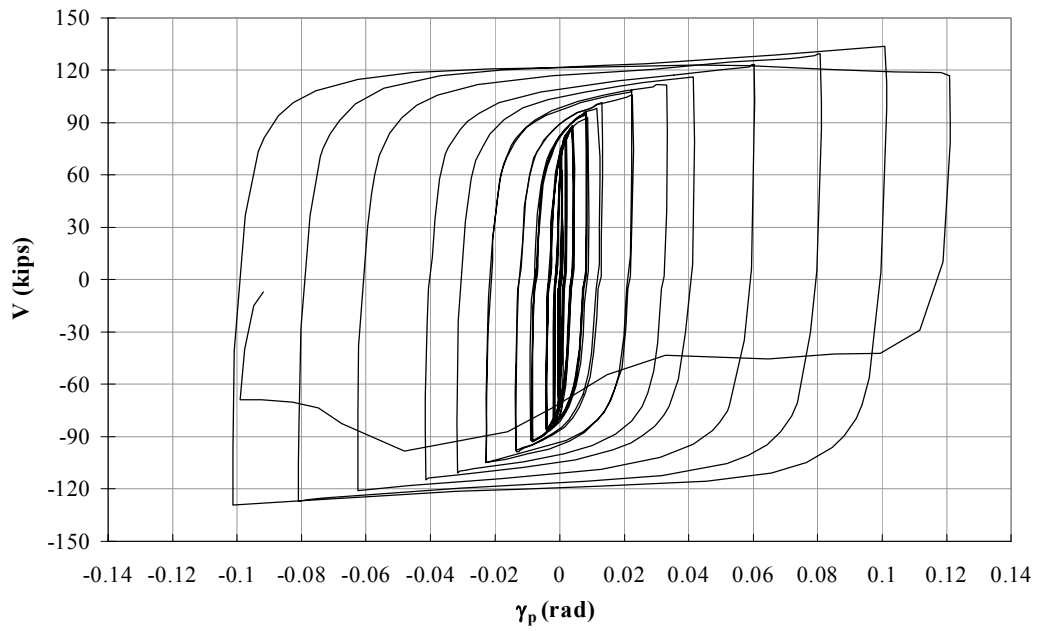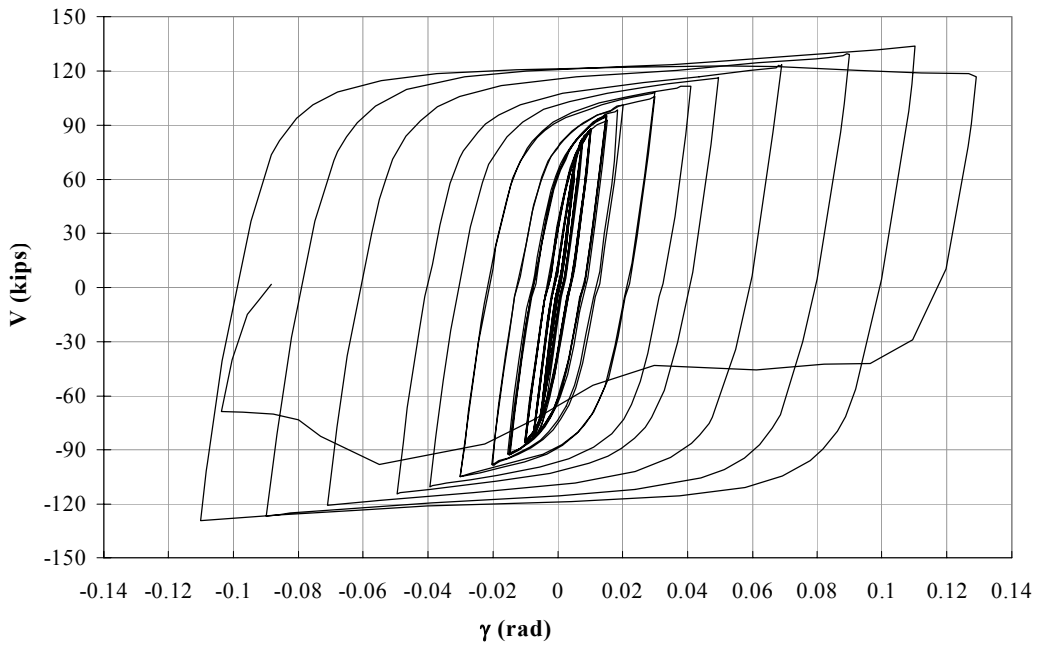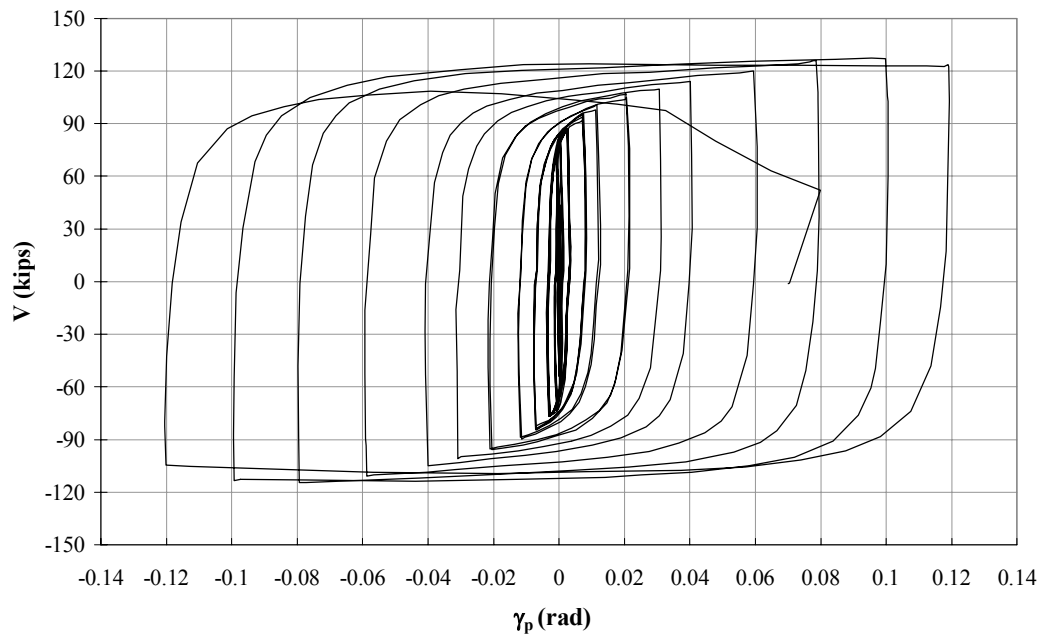*Figure 3.5 Link shear vs. plastic rotation angle for Specimen 3*
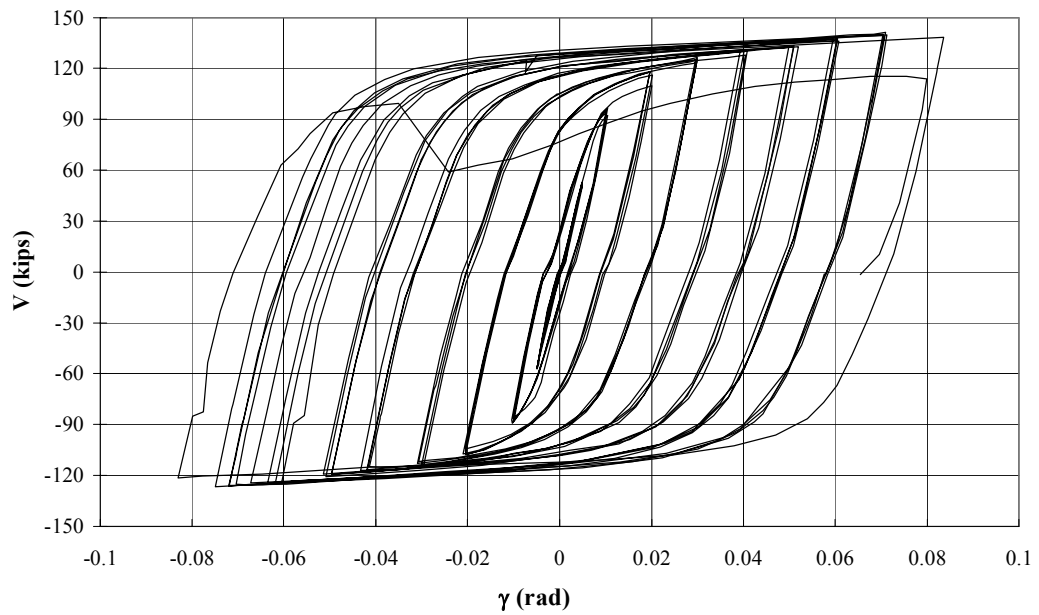
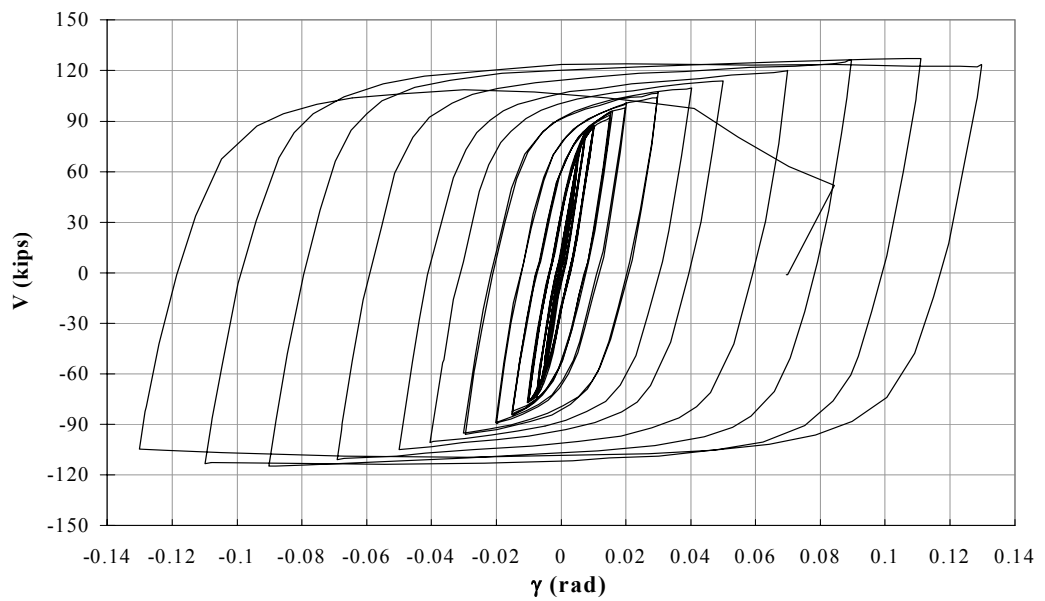*Figure 3.6 Link shear vs. total rotation angle for Specimen 3*

97
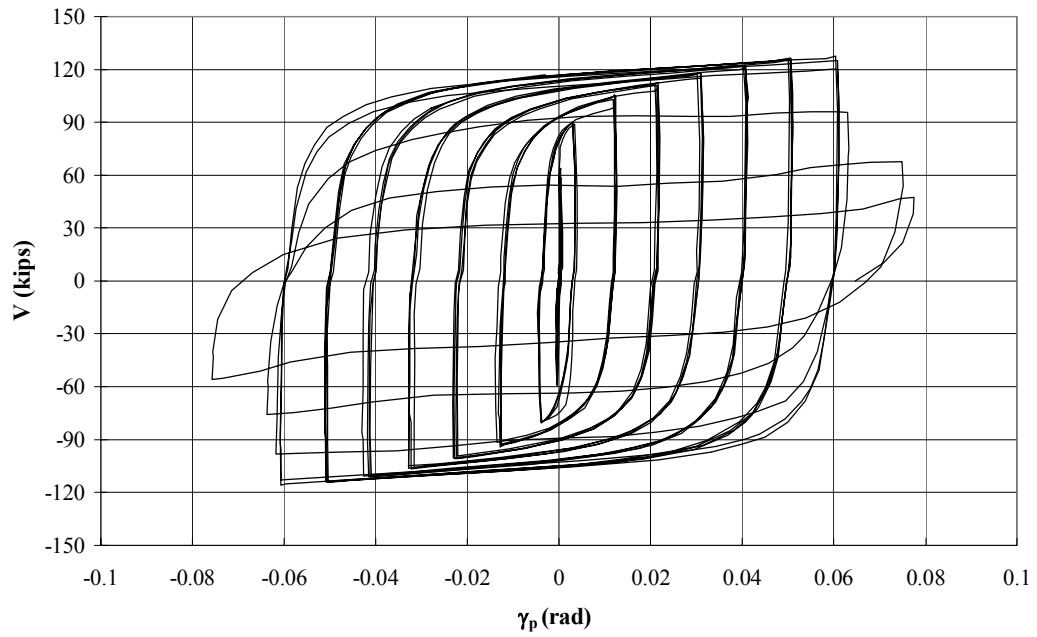
Figure 3.7 Link shear vs. plastic rotation angle for Specimen 4
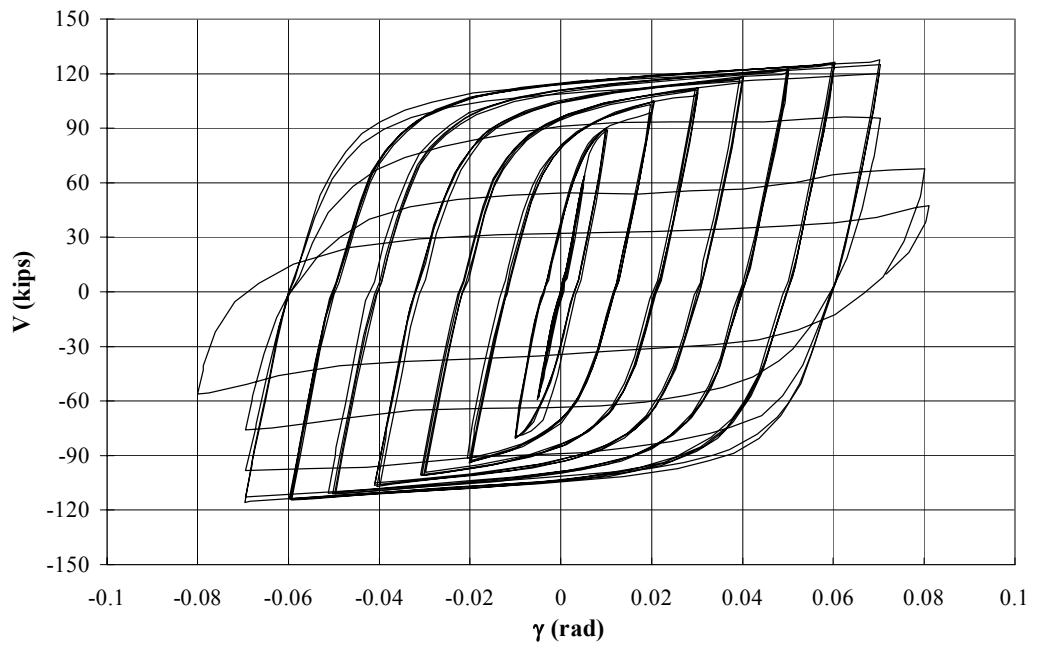
Figure 3.8 Link shear vs. total rotation angle for Specimen 4

98
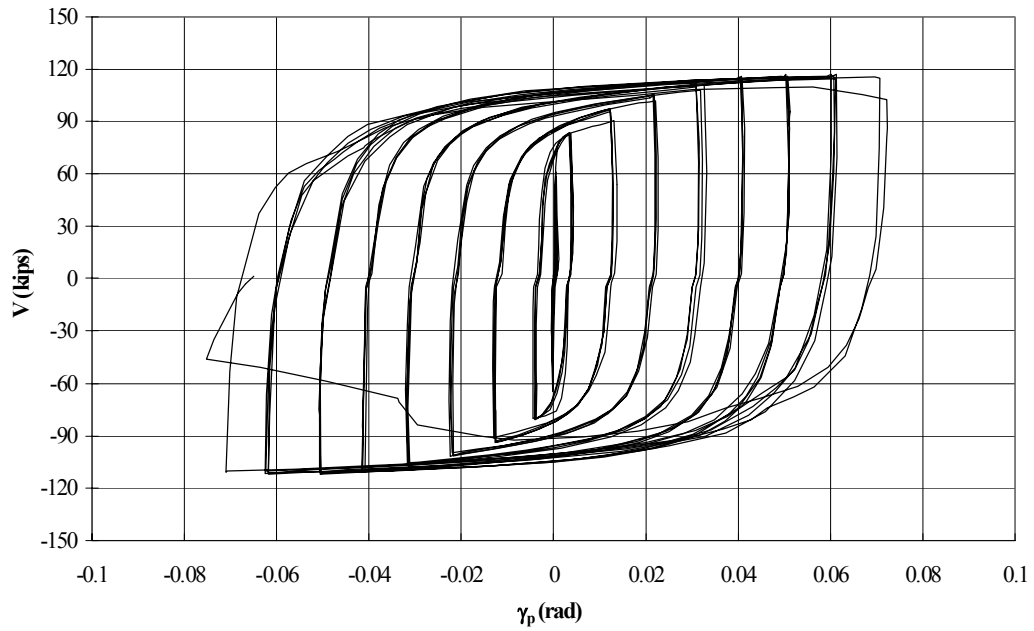
Figure 3.09 Link shear vs. plastic rotation angle for Specimen 5
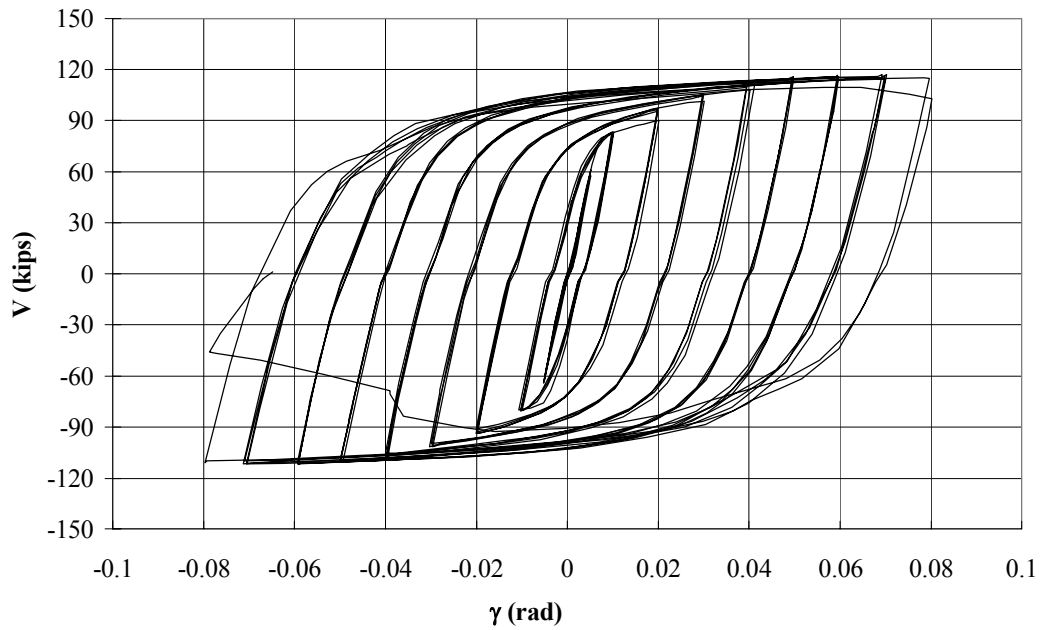
Figure 3.10 Link shear vs. total rotation angle for Specimen 5

99
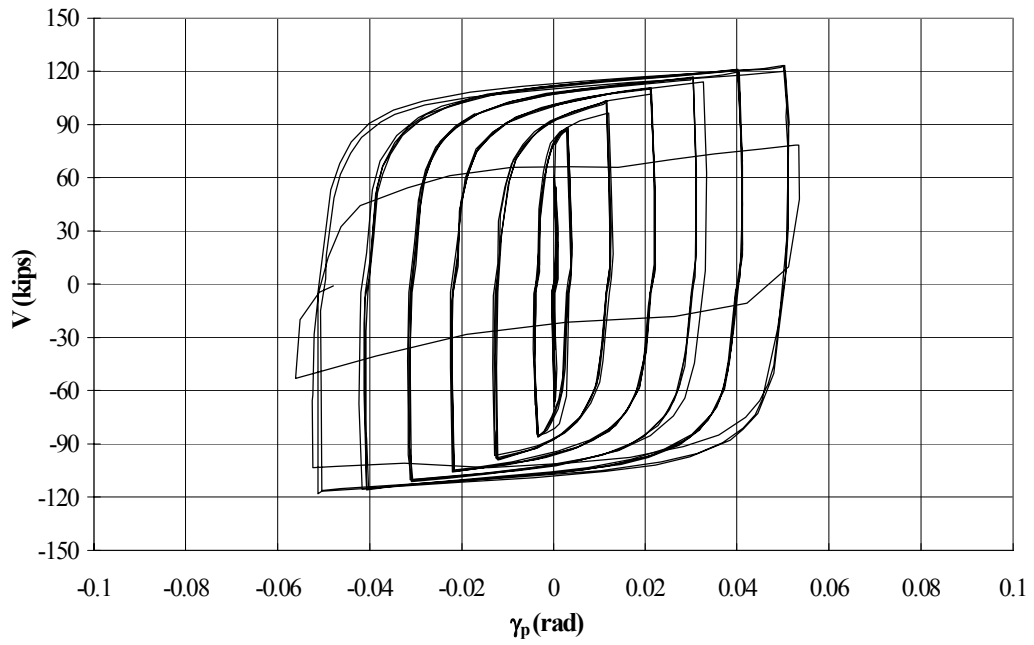
Figure 3.11 Link shear vs. plastic rotation angle for Specimen 6

Figure 3.12 Link shear vs. total rotation angle for Specimen 6

Figure 3.13 Link shear vs. plastic rotation angle for Specimen 7

Figure 3.14 Link shear vs. total rotation angle for Specimen 7

101

Figure 3.15 Link shear vs. plastic rotation angle for Specimen 8

Figure 3.16 Link shear vs. total rotation angle for Specimen 8

102

Figure 3.17 Link shear vs. plastic rotation angle for Specimen 9

Figure 3.18 Link shear vs. total rotation angle for Specimen 9

103

Figure 3.19 Link shear vs. plastic rotation angle for Specimen 10

Figure 3.20 Link shear vs. total rotation angle for Specimen 10

104
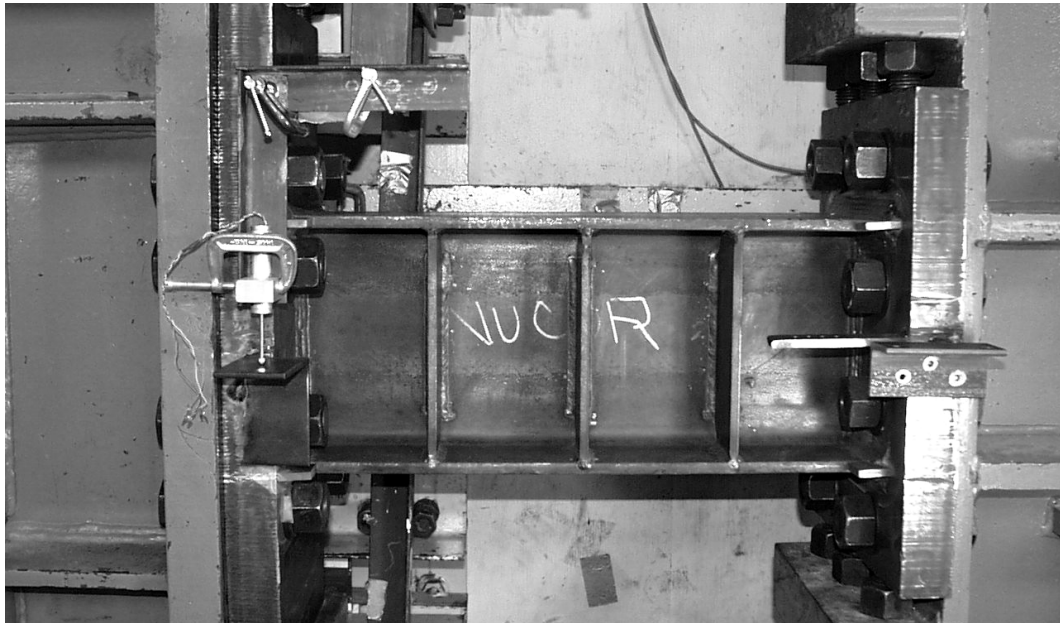
Figure 3.21 Specimen 1: Before testing

Figure 3.22 Specimen 1: Crack observed at the toe of the welding of the far
north stiffener during the fourth cycle of load step 8 (γ = -0.06 radian)
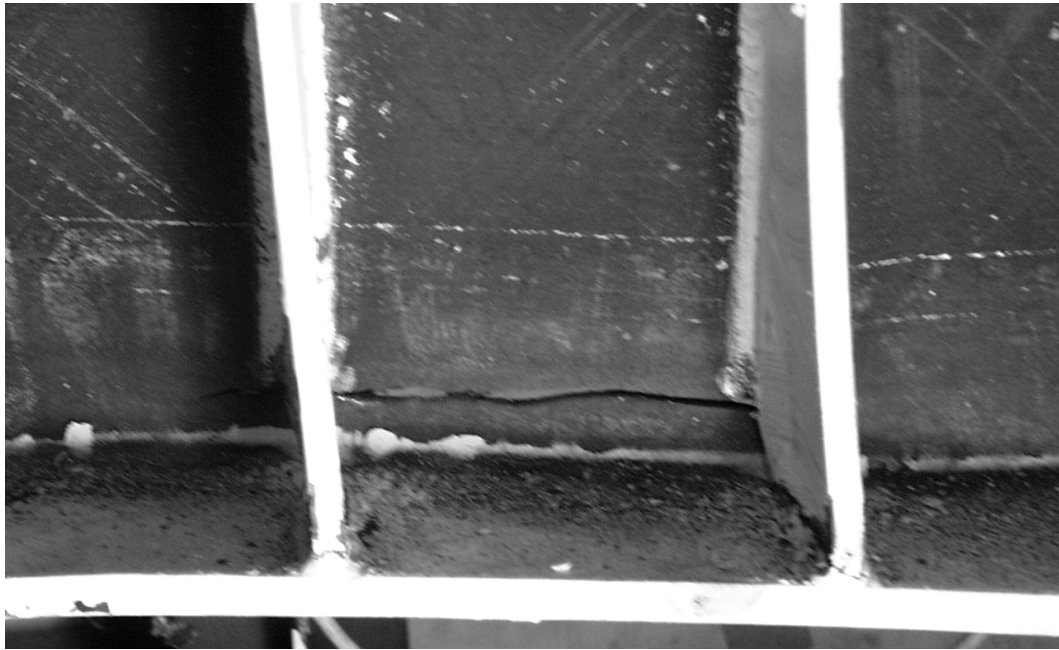
***Figure 3.23 Specimen 1: Horizontal crack after completing the second cycle of
load step 9 (γ = +0.07 radian)***
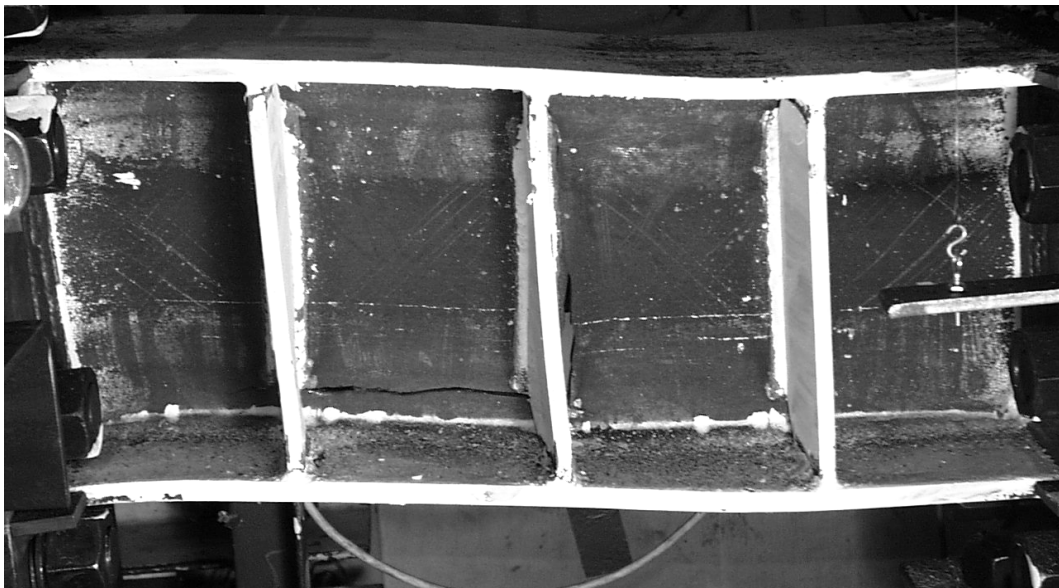
***Figure 3.24 Specimen 1: Horizontal and vertical crack observed after the third
cycle of load step 9(γ = +0.07 radian)***
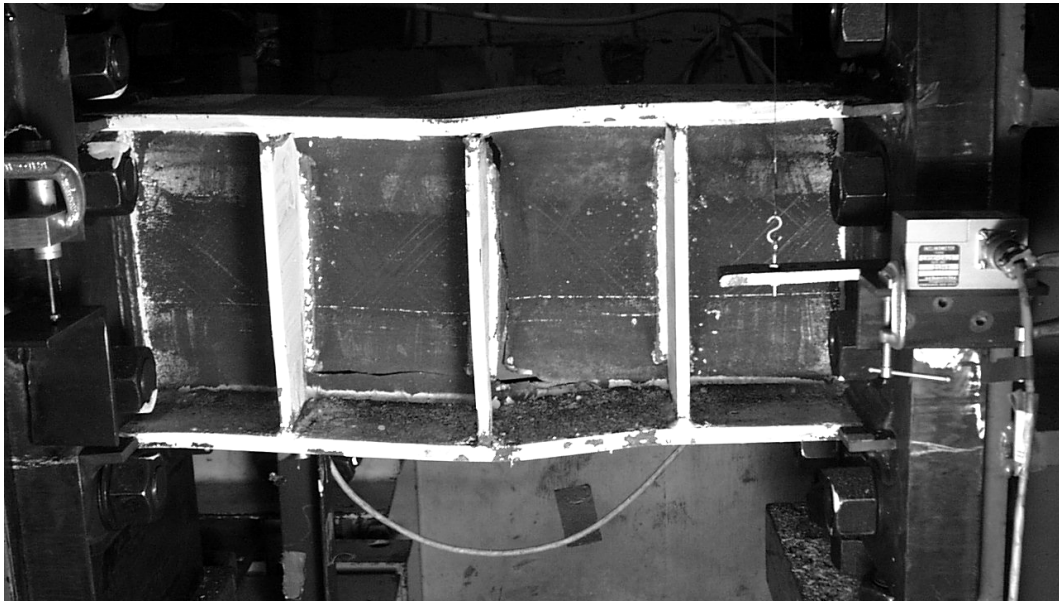
Figure 3.25 Specimen 1: After testing

Figure 3.26 Specimen 2: Web yielding after the first cycle of load step 3
(γ = +0.01 radian)

*Figure 3.27 Specimen2: First crack observed at the bottom of the center
stiffener after the fourth cycle of load step 6 (γ = +0.04 radian)*
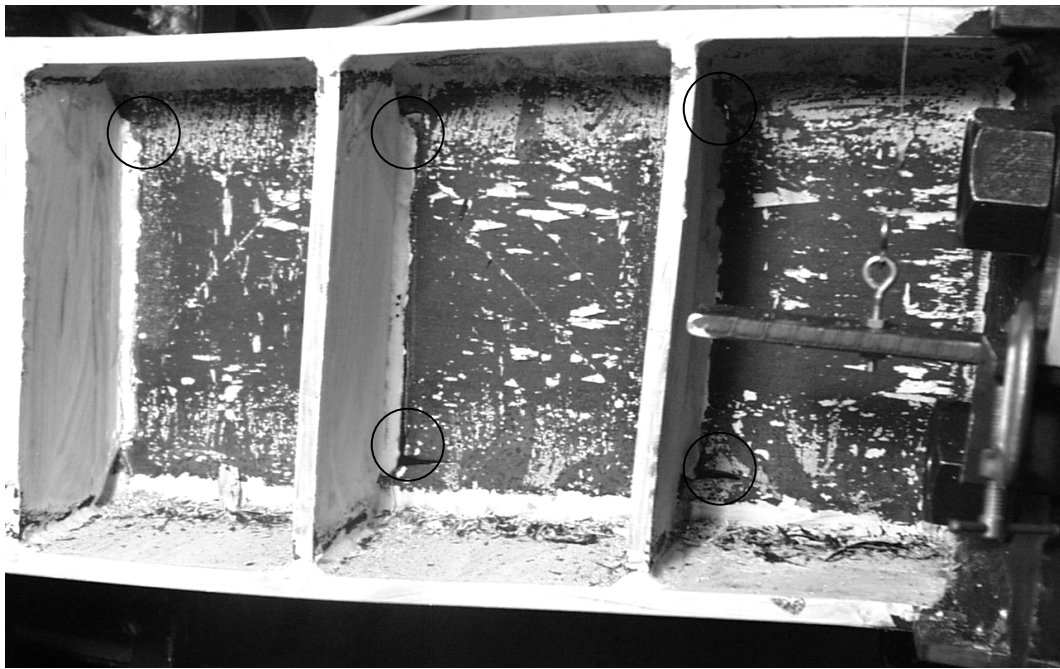
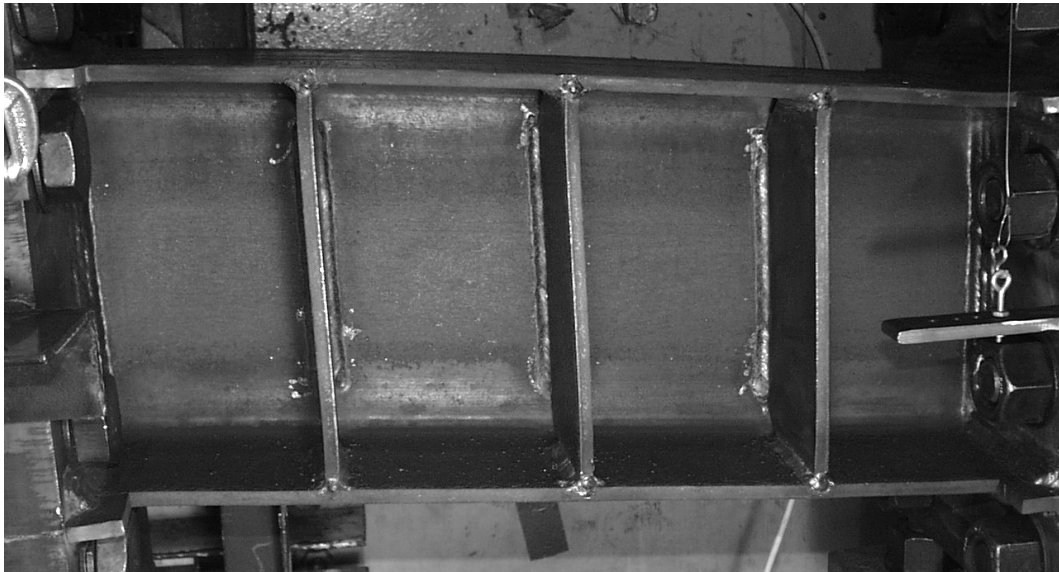*Figure 3.28 Specimen 2: Cracks at the termination of the welds of the stiffeners
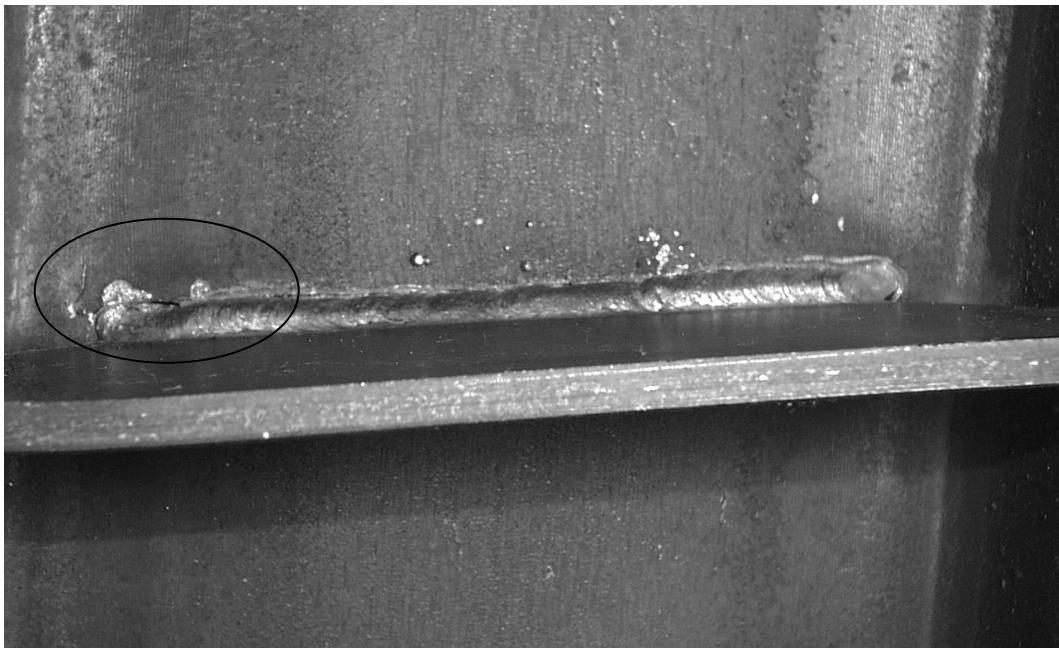after the second cycle of load step 9 (γ = -0.0 7 radian)*
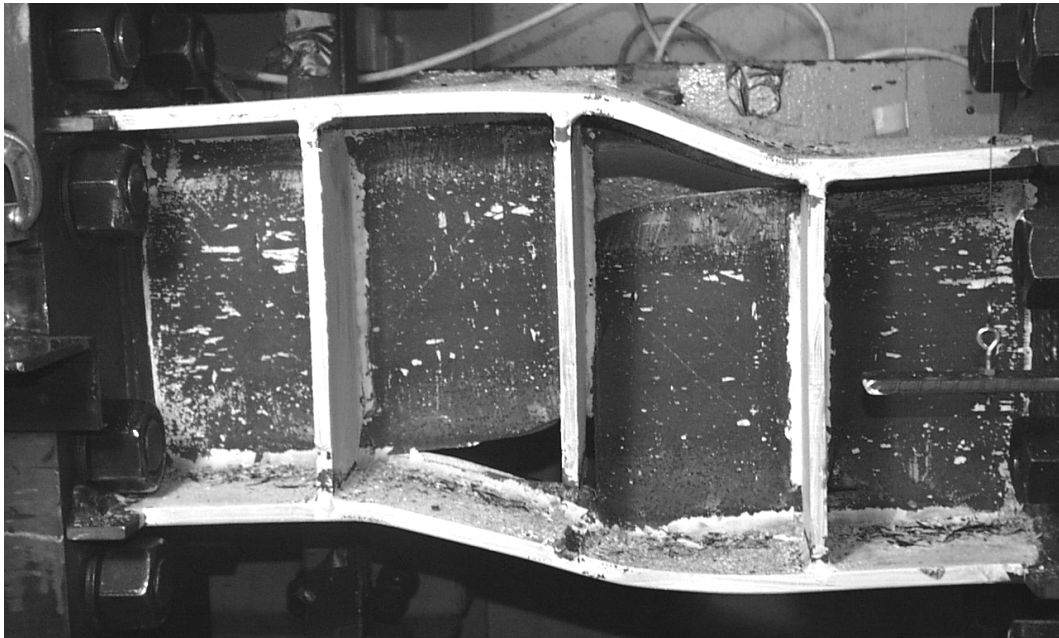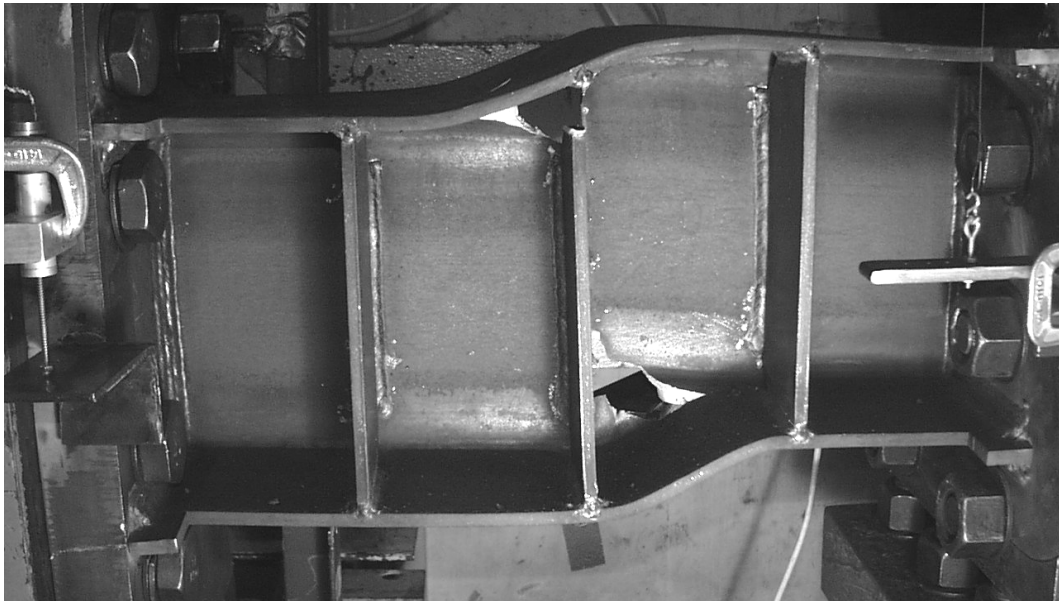
Figure 3.29 Specimen 2: After testing
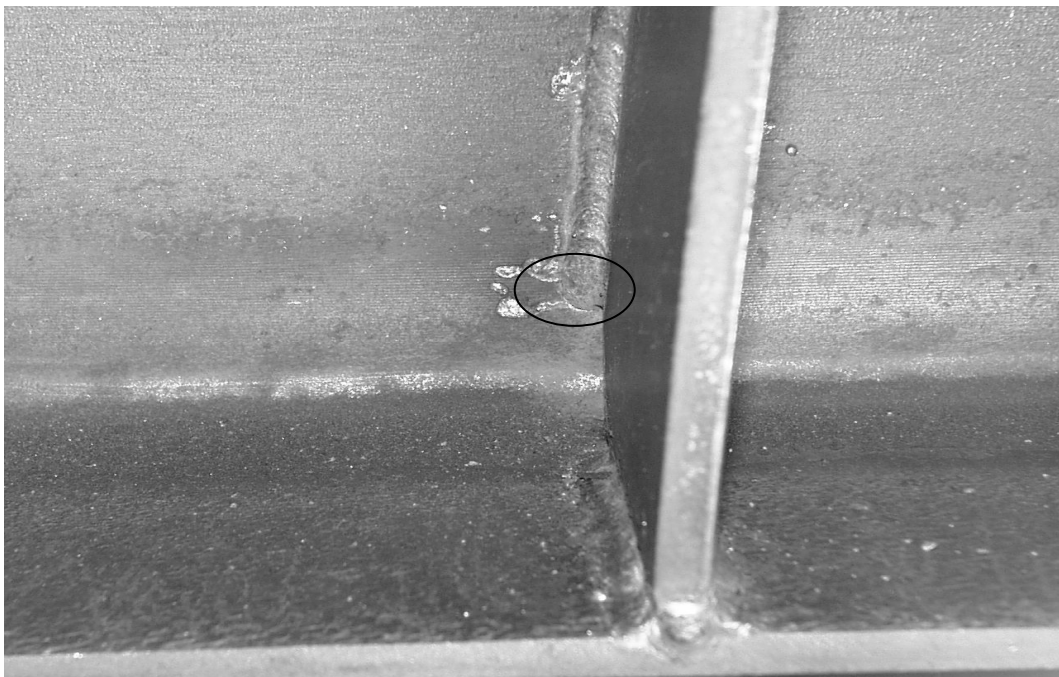
Figure 3.30 Specimen 3: Crack at the termination of the welding at the north stiffener after the fourth cycle of load step 8 (γ = -0.06 radian)

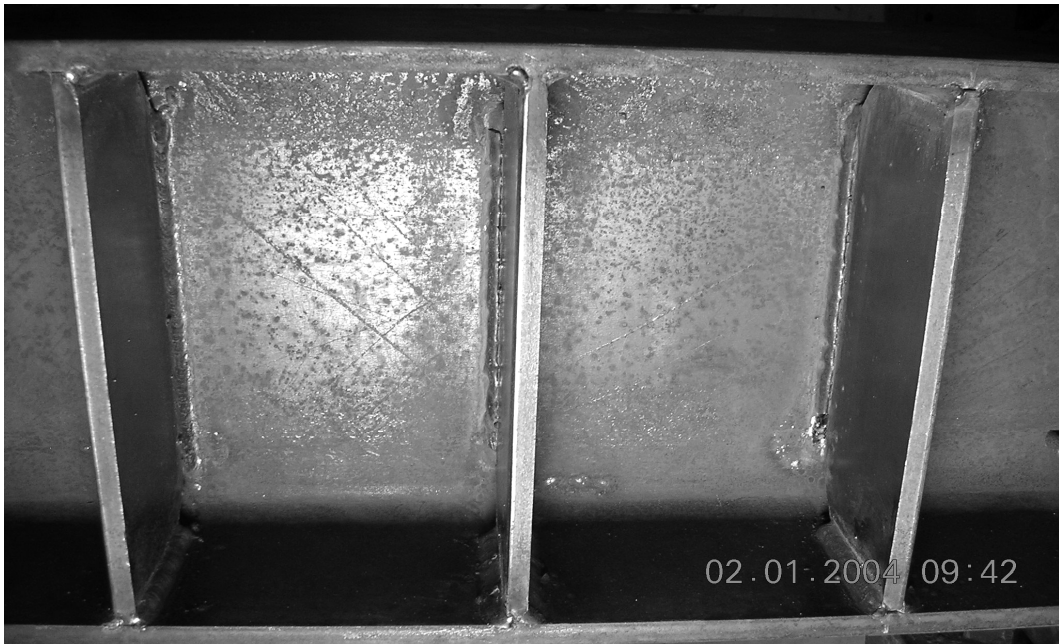*Figure 3.31 Specimen 3: Overall view after completing the fourth cycle of Load step 9 (γ = ± 0.07 radian)*

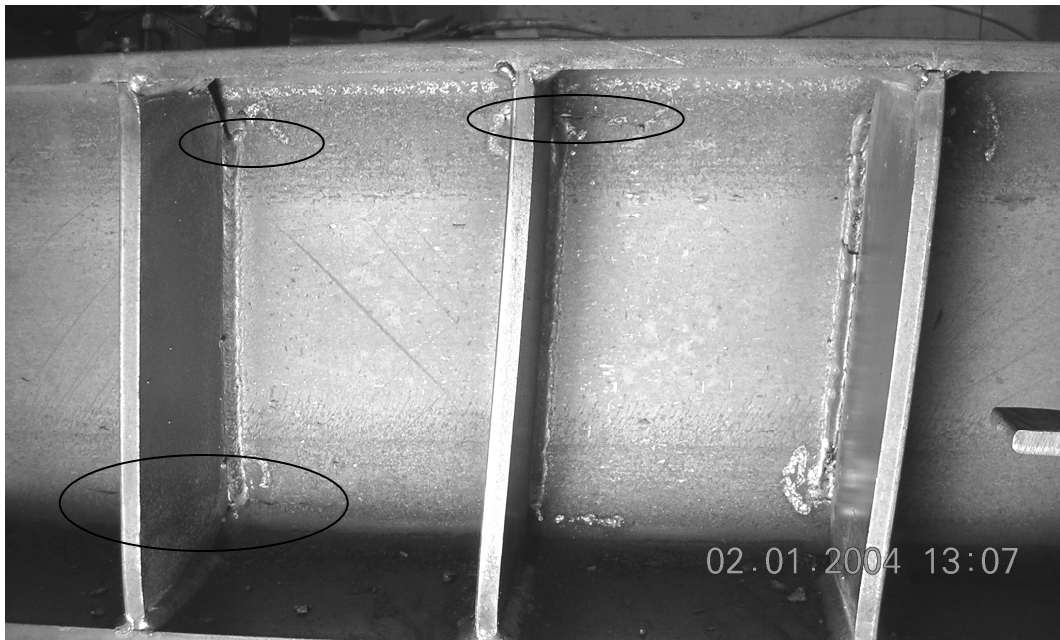*Figure 3.32 Specimen 3: Crack at the center stiffener during the first cycle of load step 10 (γ = + 0.08 radian)*
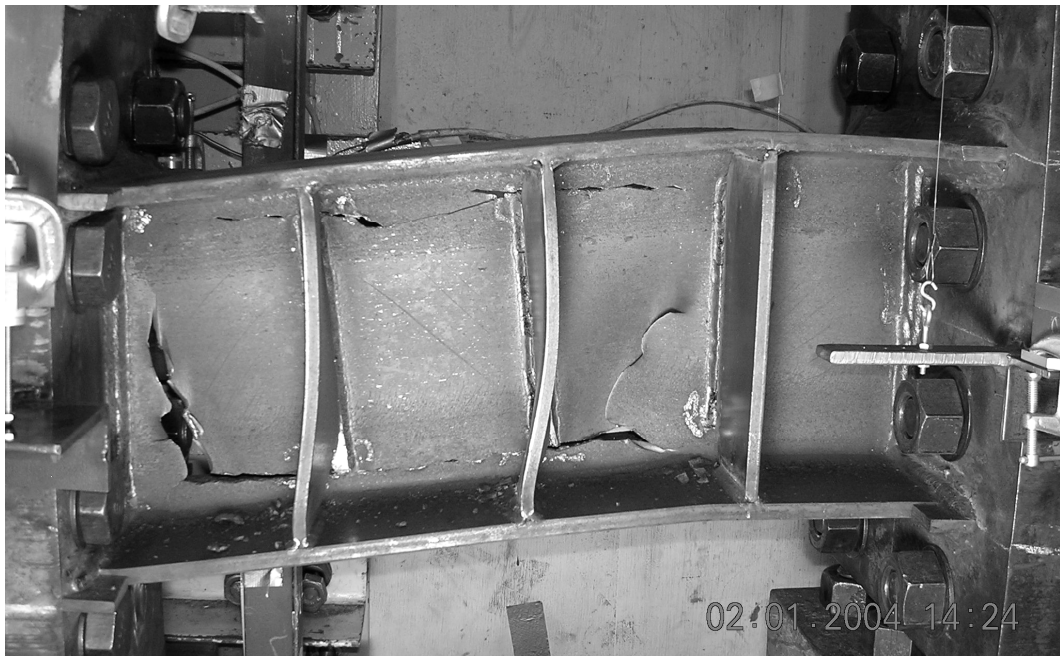
Figure 3.33 Specimen 3: After testing

Figure 3.34 Specimen 4: Web yielding observed at an early stage after the third cycle of load step 2 (γ = ±0.005 radian)

111

Figure 3.35 Specimen 4: Crack observed after the fourth cycle of load step 8 (γ= -0.06 radian)

Figure 3.36 Specimen 4: Cracks observed after the second cycle of Load step 9 (γ= + 0.07 radian)
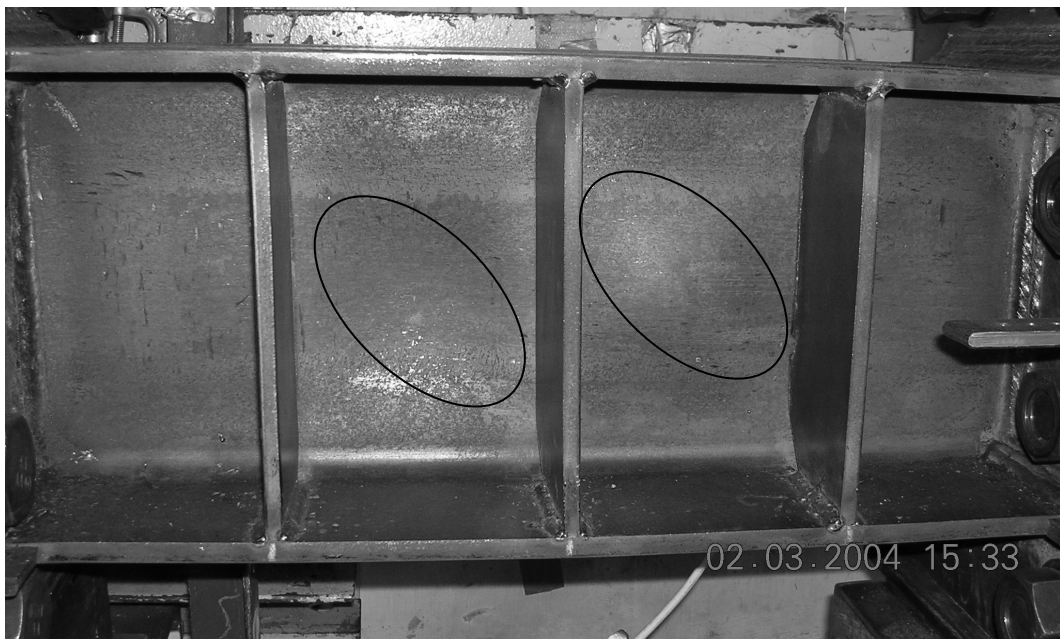
Figure 3.37 Specimen 4: After testing

Figure 3.38 Specimen 5: Before testing

113

Figure 3.39 Specimen 5: Web yielding after completion of the first cycle of load step 3 (γ= ±0.01 radian)
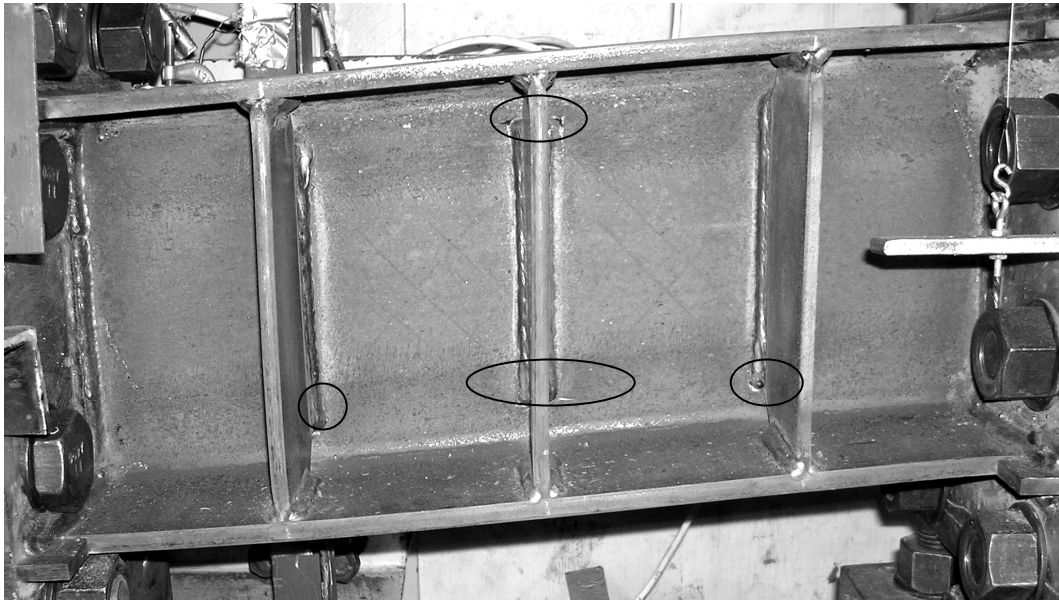

Figure 3.40 Specimen 5: Web buckling observed during the first cycle of load step 9 (γ= +0.07 radian)

Figure 3.41 Specimen 5: Closer look at the crack formed behind the center stiffener after testing

Figure 3.42 Specimen 5: After testing

Figure 3.43 Specimen 6: Cracks observed at the termination of the fillet welds after the first half of the third cycle of load step 8 (γ = +0.06 radian)

Figure 3.44 Specimen 6: Crack at the top of the center stiffener during the first Half of the third cycle of load step 8 (γ = -0.06 radian)

116
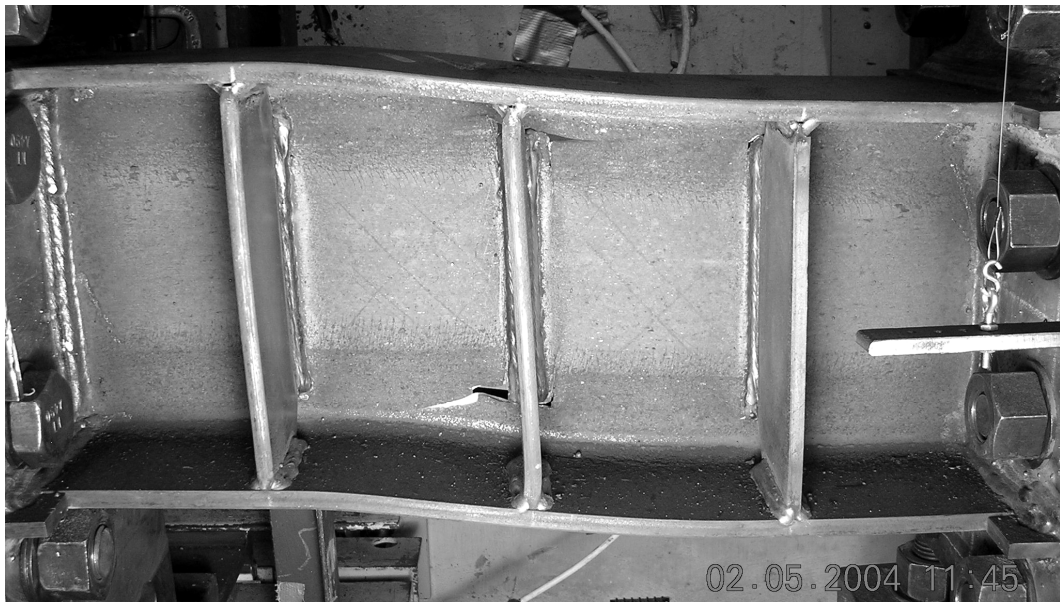
Figure 3.45 Specimen 6: Cracks running parallel to the flanges during the second half of the third cycle of load step 8 (γ= -0.06 radian)

Figure 3.46 Specimen 6: After testing

117
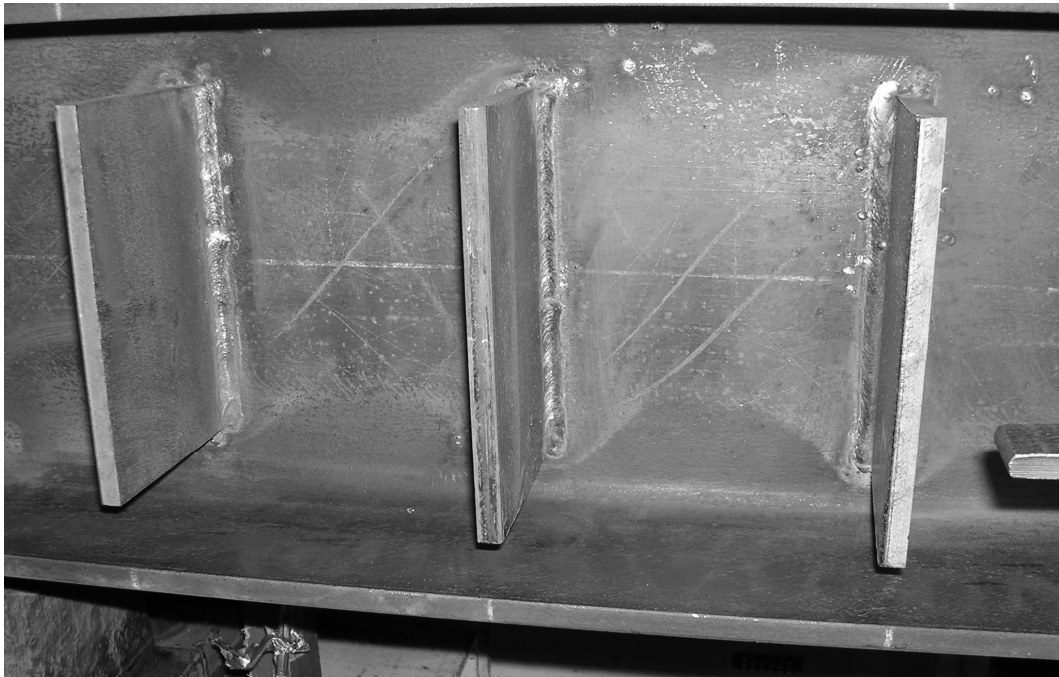
Figure 3.47 Specimen 7: Before testing
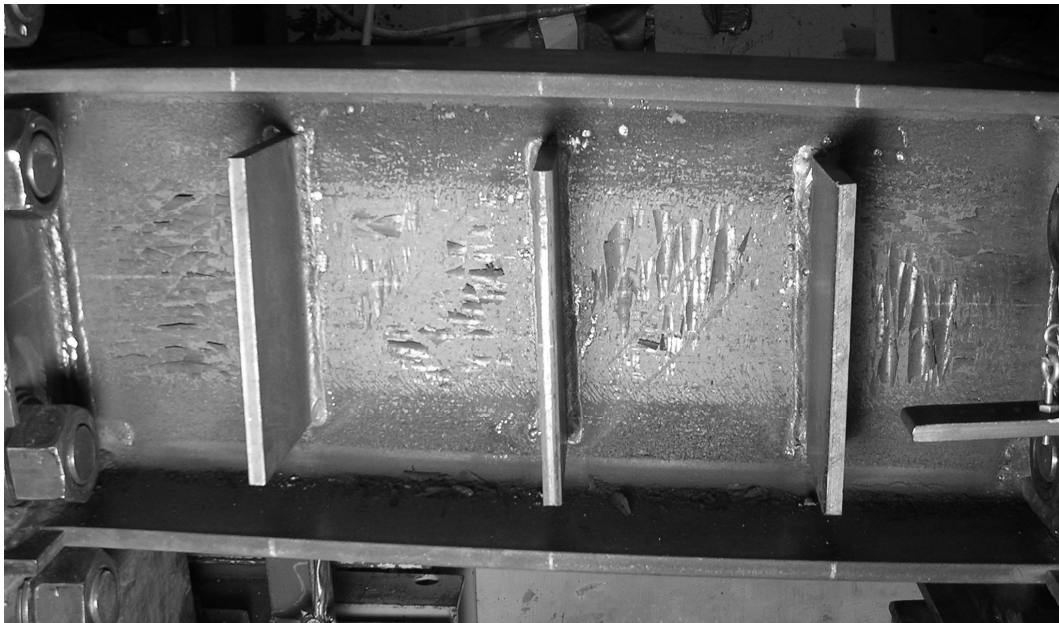
Figure 3.48 Specimen 7: Web yielding observed during the fourth cycle of load step 6 (γ = -0.04 radian)

Figure 3.49 Specimen 7: Crack observed at the bottom of the north stiffener after the fourth cycle of load step7 (γ =-0.05 radian)
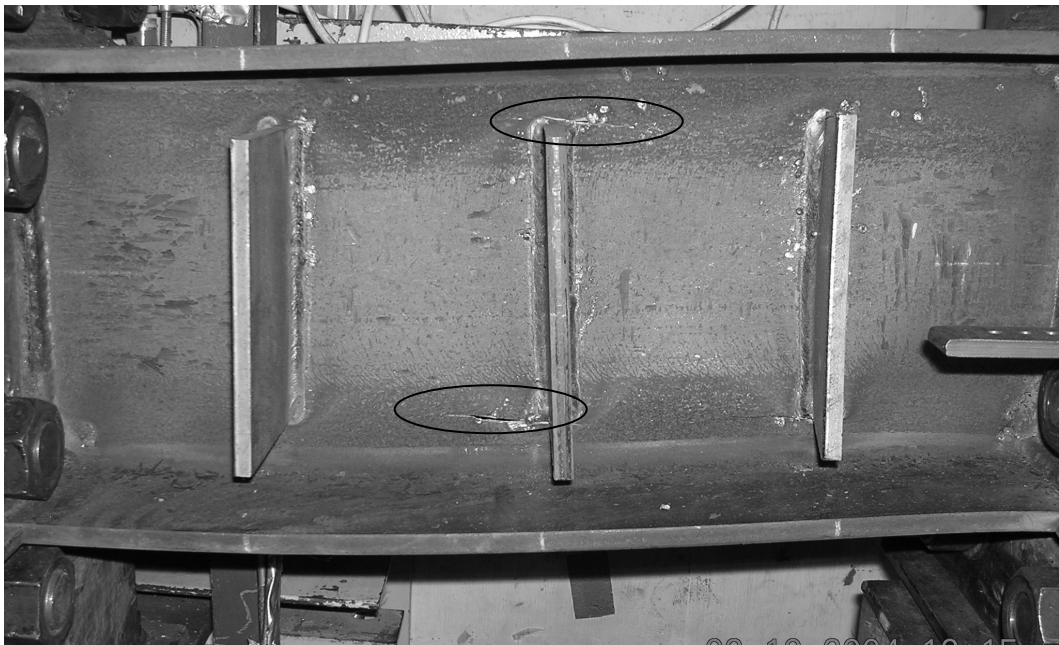
Figure 3.50 Specimen 7: Horizontal cracks observed during the first half of the third cycle of load step 8 (γ= +0.06 radian)

119
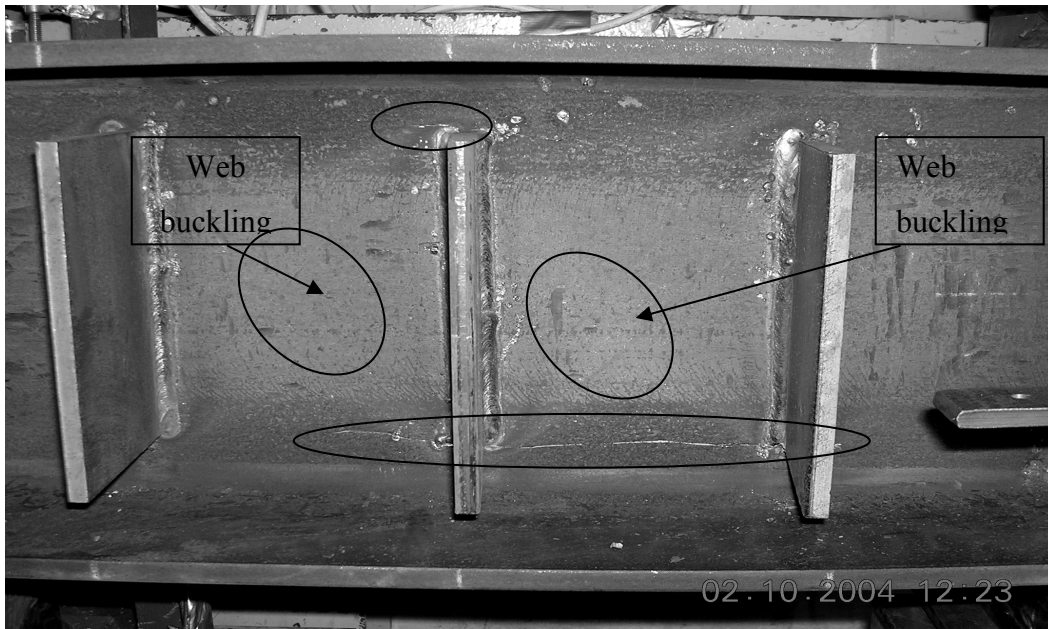
Figure 3.51 Specimen 7: Horizontal crack observed during the second half of the third cycle of load step 8 (γ= -0.06 radian)
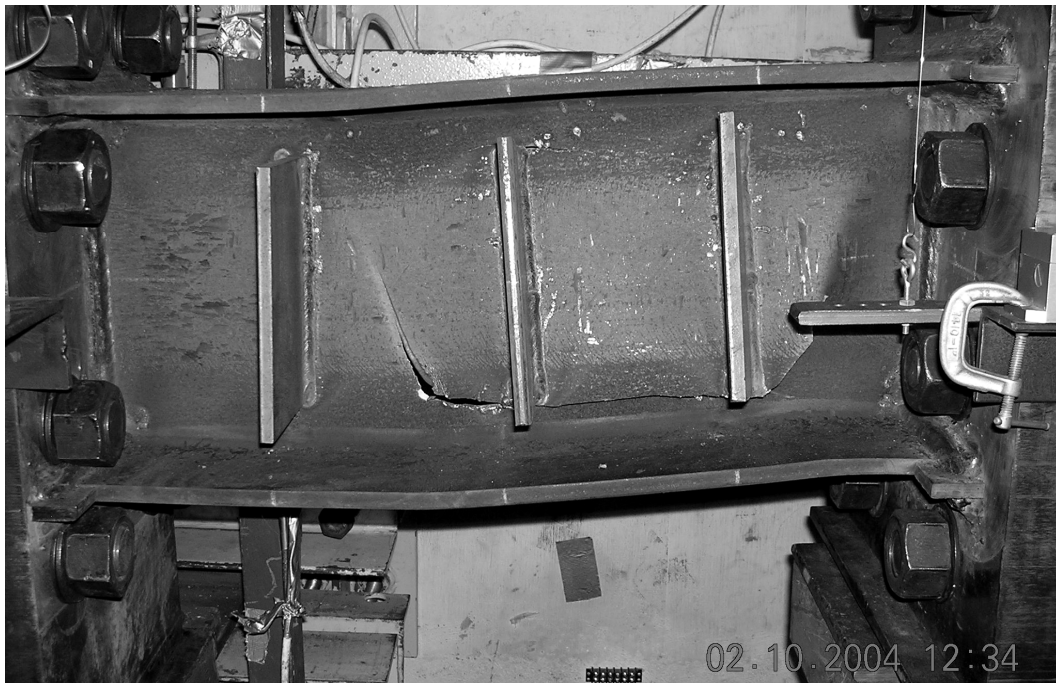
Figure 3.52 Specimen 7: After testing
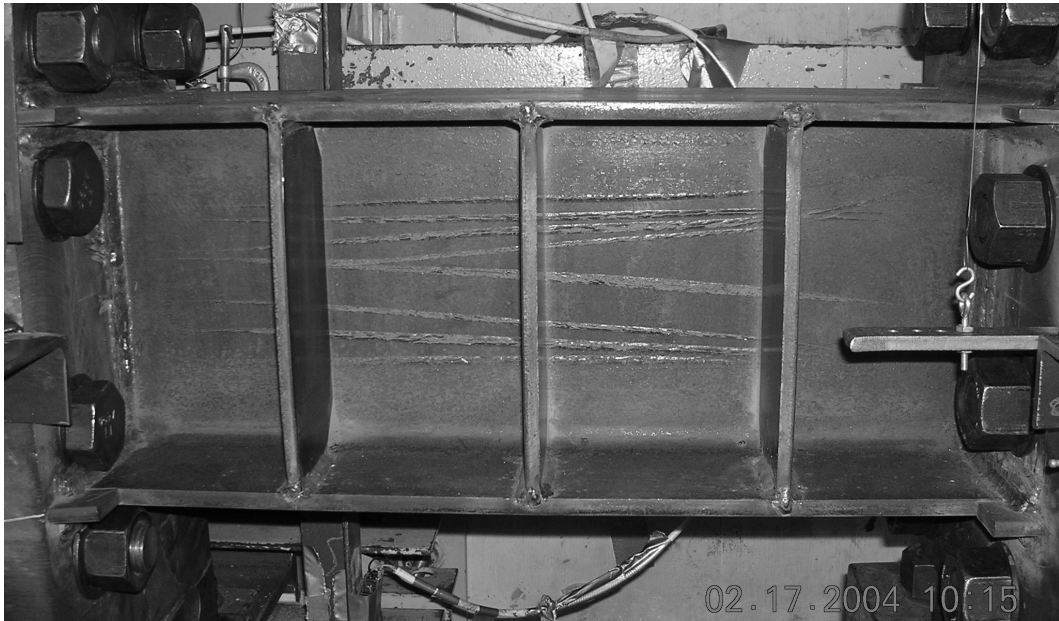
Figure 3.53 Specimen 8: Web yielding at an early stage during the third cycle of load step 3(γ = -0.0075 radian)
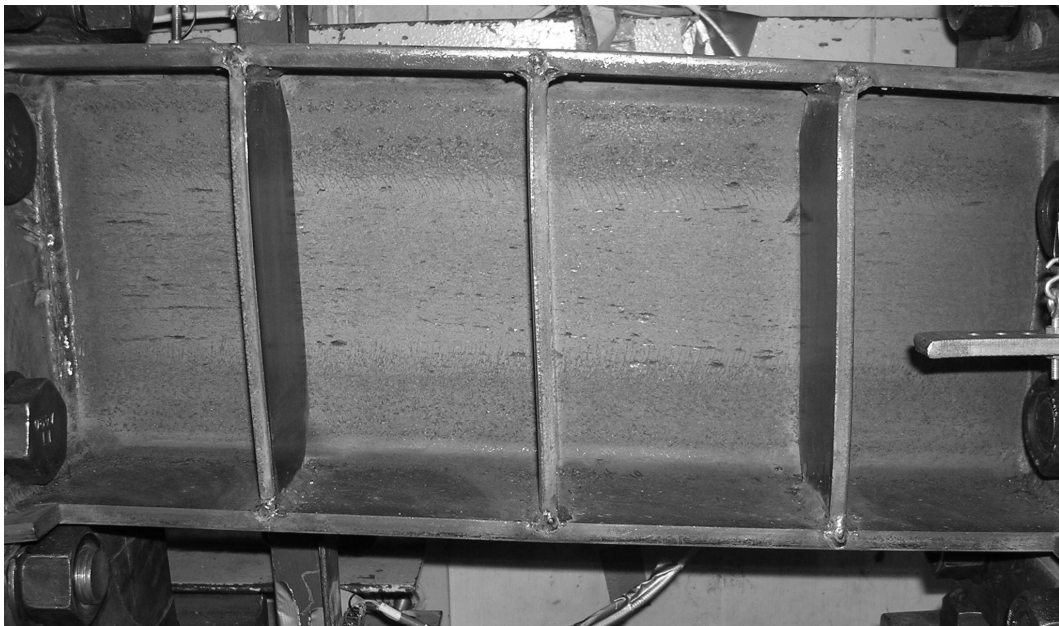
Figure 3.54 Specimen 8: No mill scale observed at the center of the web after the second cycle of load step 7(γ =0.003 radian)

121
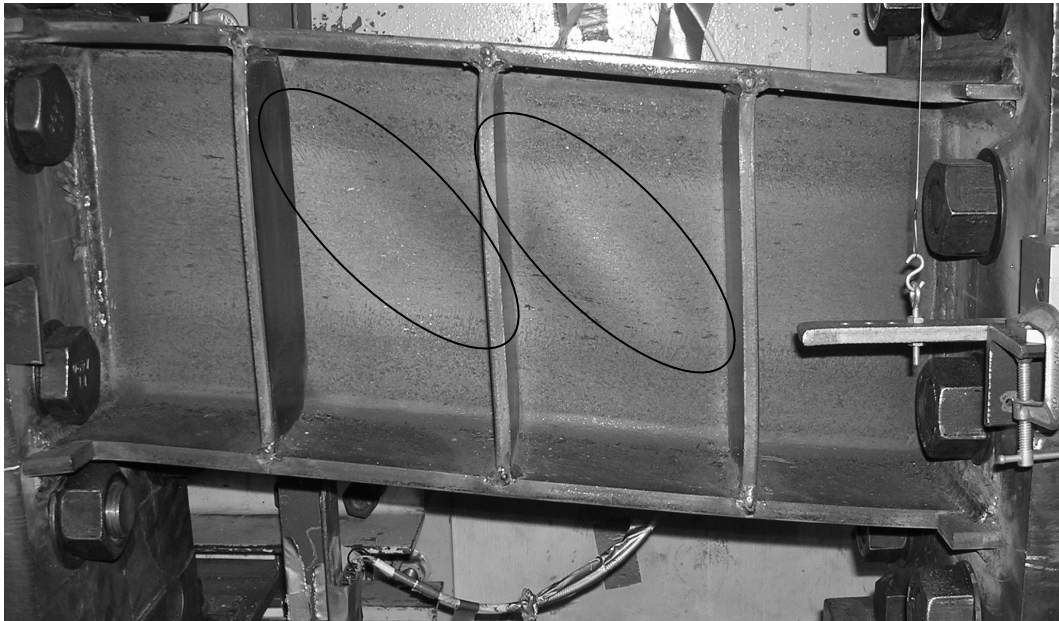
Figure 3.55 Specimen 8: Web buckling during the first cycle of load step 11
(γ = -0.09 radian)
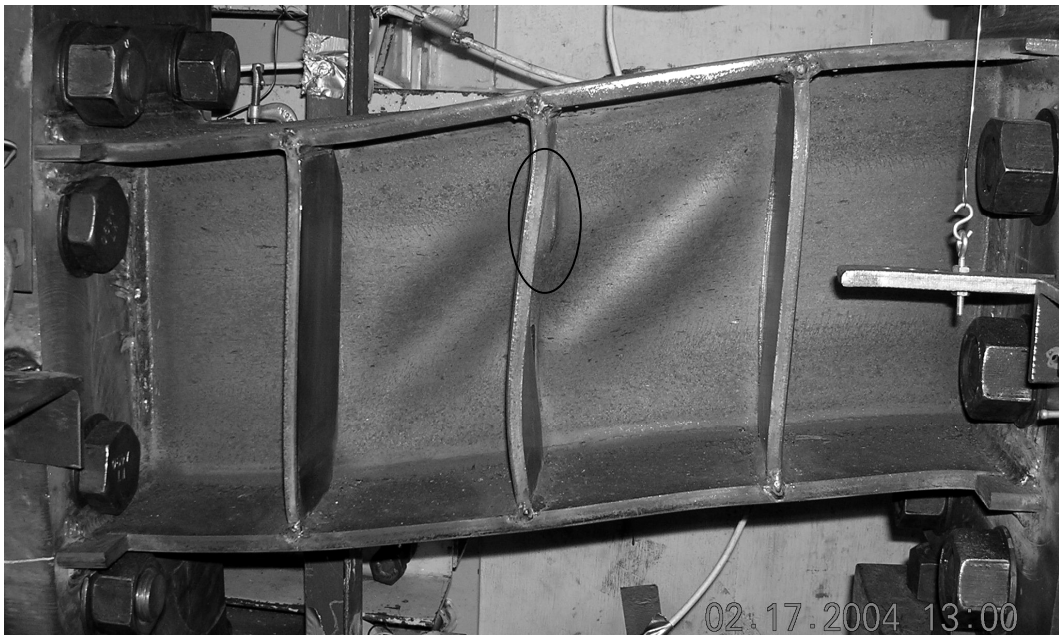
Figure 3.56 Specimen 8: Web damage due to the rubbing of the center stiffener
during the first cycle of load step 13
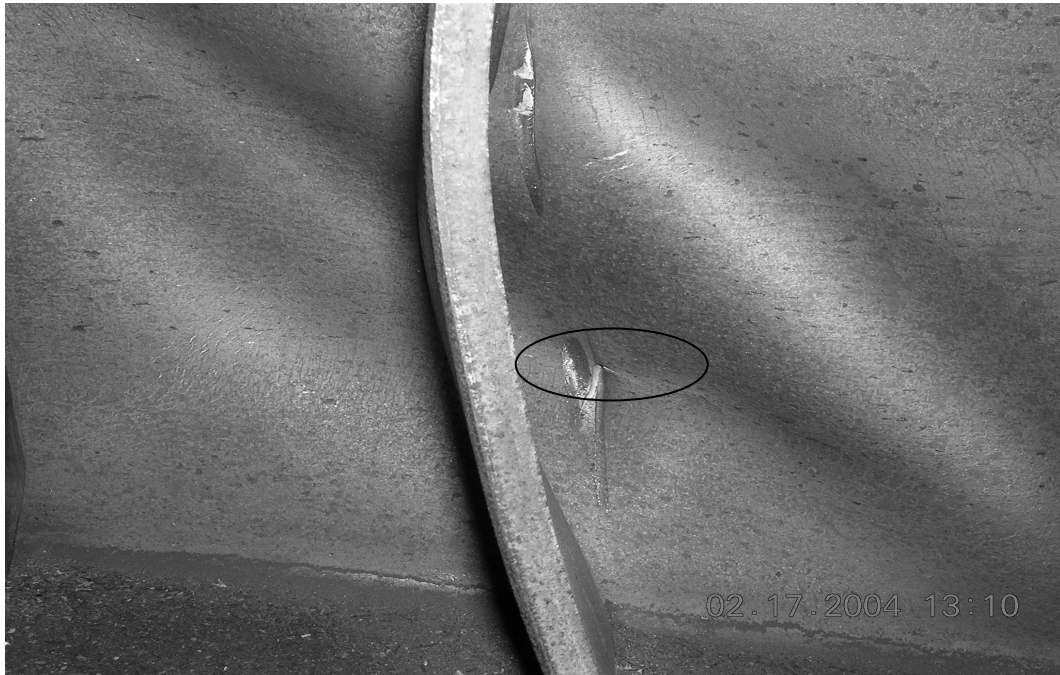
Figure 3.57 Specimen 8: Crack initiated in the damaged region of the web during the first half of the first cycle of load step 13(γ = +0.13 radian)
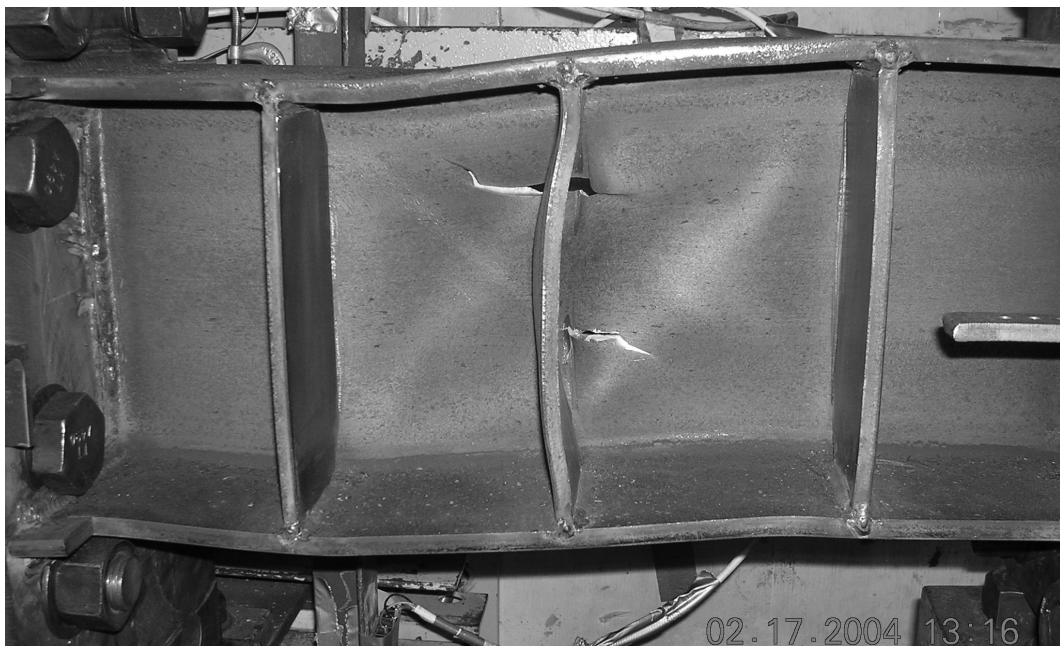
Figure 3.58 Specimen 8: After testing

123

Figure 3.59 Specimen 9: Web yielding during the sixth cycle of load step 4
(γ = -0.01 radian)

Figure 3.60 Specimen 9: Cracks observed after the first cycle of load step 11
(γ= -0.09 radian)

124

Figure 3.61 Specimen 9: Cracks observed during the first cycle of load step 12
(γ= 0.11 radian)
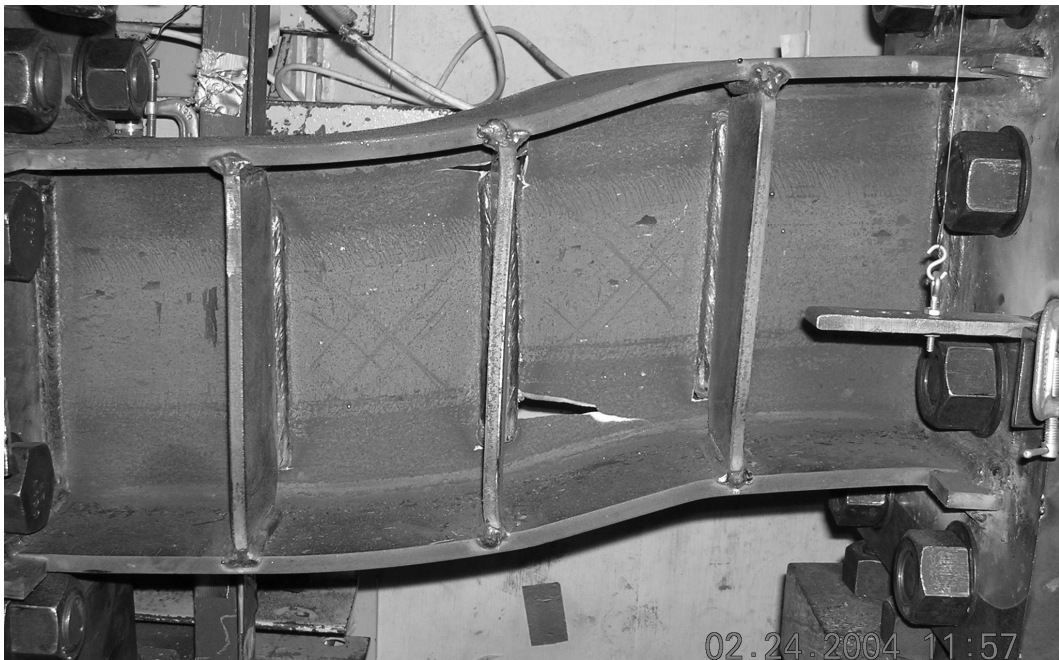
Figure 3.62 Specimen 9: Cracks during the first cycle of load step 13
(γ= -0.13 radian)
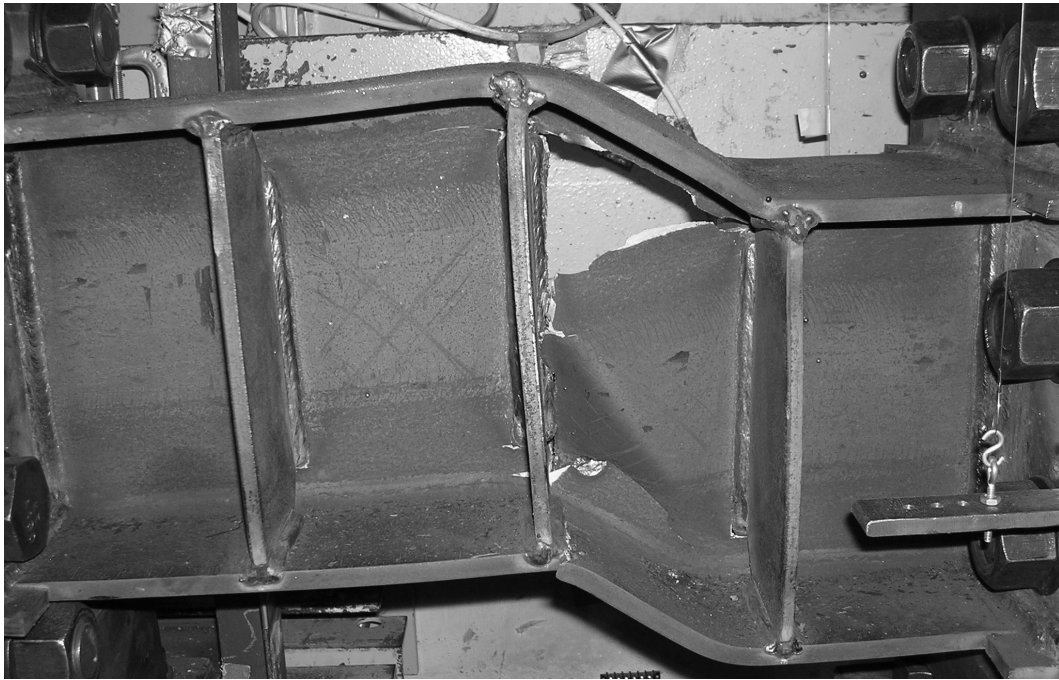
Figure 3.63 Specimen 9: After testing
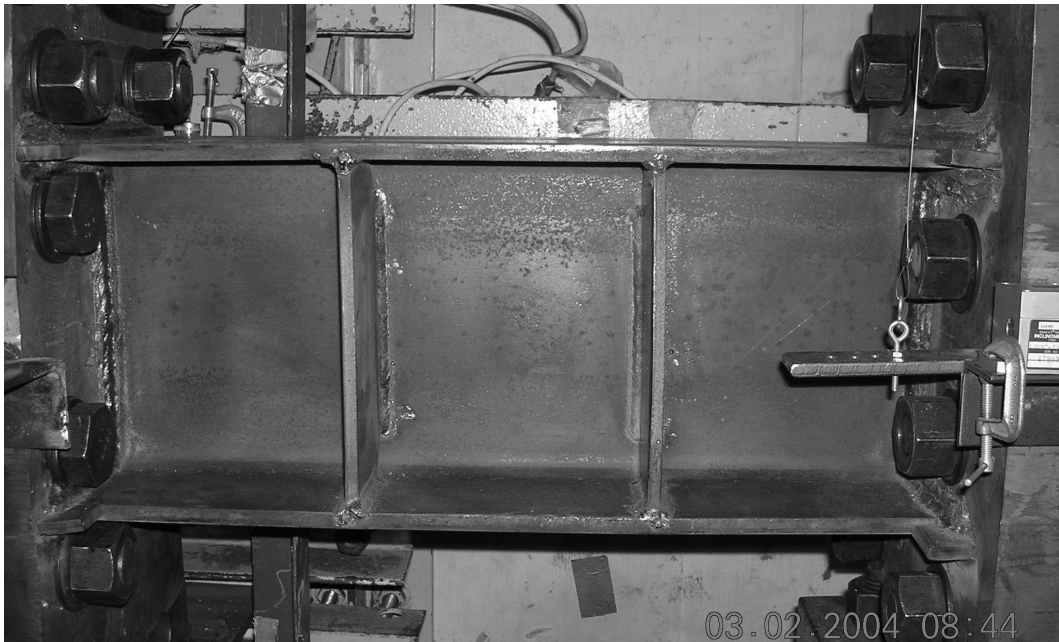
Figure 3.64 Specimen 10: Before testing

Figure 3.65 Specimen 10: Web yielding observed after the fourth cycle of load step 3 (γ = 0.0075 radian)

*Figure 3.66 Specimen 10: Crack observed at the bottom of the north stiffener after the first cycle of load step 11 (γ = +0.09 radian)*

127

Figure 3.67 Specimen 10: Web buckling observed after the first cycle of load step 11 (γ = -0.09 radian)

Figure 3.68 Specimen 10: Web buckling and cracks observed after the first cycle of load step 13 (γ = -0.13 radian)
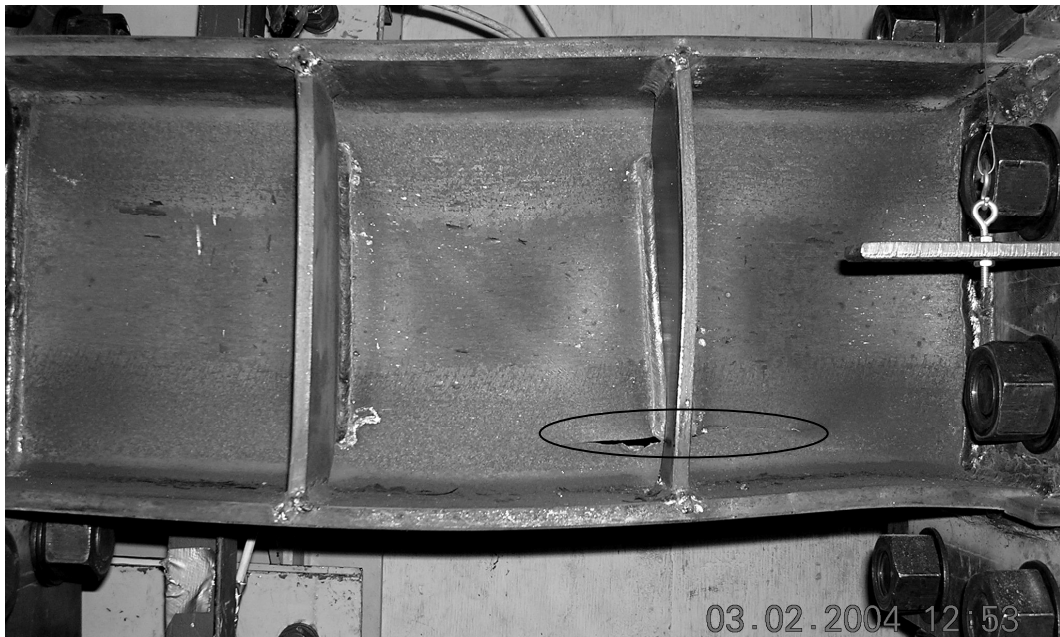
Figure 3.69 Horizontal crack observed at the web during the first cycle of load step 14 (γ = -0.15 radian)
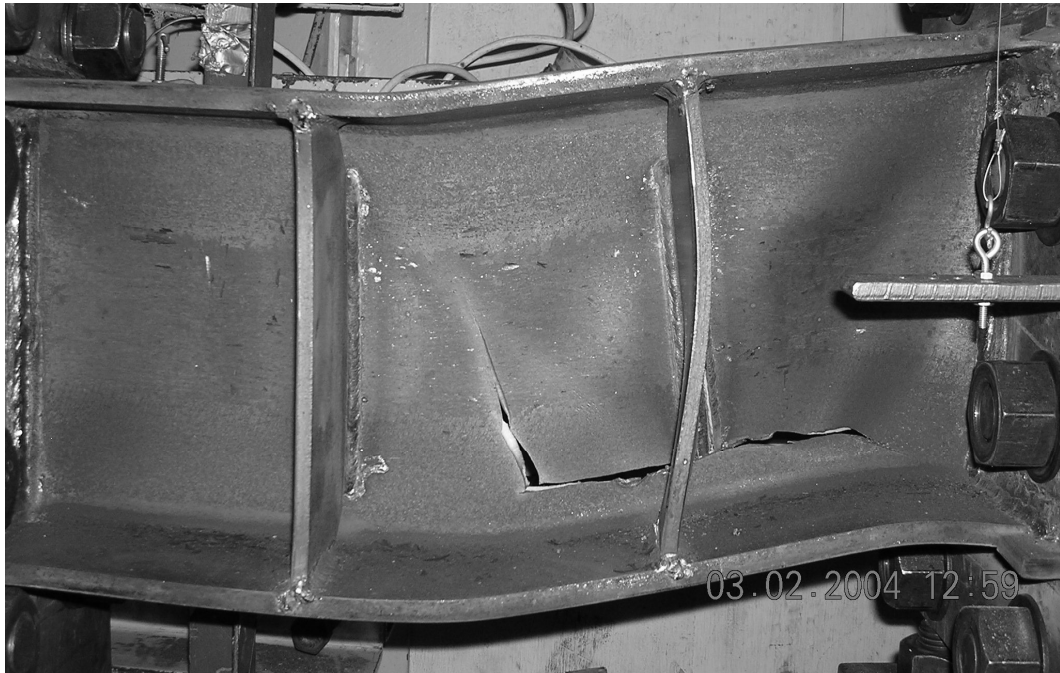
Figure 3.70 Specimen 10: After testing

CHAPTER 4
Additional Experimental Data

4.1   GENERAL

This chapter provides additional data gathered in this test program. Link overstrength data is presented for each specimen. In addition, the end moments on the column side and beam side of the link are compared for each specimen.

4.2   LINK OVERSTRENGTH DATA

Link overstrength is defined as the maximum shear force developed by a link divided by the plastic shear capacity of the link V_n, defined as the lesser of V_p or $(2M_p)/e$, as defined by the 2002 AISC Seismic Provisions. Link overstrength, i.e., the development of shear forces in the link that exceed the plastic shear capacity, is believed to be caused primarily by material strain hardening. Other factors, such as the development of shear resistance by link flanges, has also been cited as a possible contributor to overstrength (Arce 2002). Link overstrength is of particular interest in EBF design, since the braces, beam segments outside of the links, and the columns are all designed to remain essentially elastic under the maximum forces generated by a fully yielded and strain hardened link. The maximum forces that can be generated by a link are estimated by taking the link

130

plastic shear capacity and multiplying by an overstrength factor. Consequently, a realistic but not overly conservative estimate of link overstrength is needed for safe and economical EBF design.

Link overstrength varies depending on the length of the link. For example, Arce (2002) reports link overstrength ranging from1.19 to 1.29 for flexural and intermediate links ($e>1.6M_p/V_p$), with an average of 1.24. Meanwhile, shear links ($1.1M_p/V_p{\leq}e{\leq}1.6M_p/V_p$) exhibited an overstrength ranging from 1.28 to 1.45, with an average of 1.37. Arce's results are similar to overstrength factors reported by other researchers, such as, Ramadan and Ghobarah (1995) who reported link overstrength factors ranging from 1.25 to 1.35 in shear links. However, overstrength factors can be as high as 1.8 for built-up shear links (Itani et al, 1998).

In this study, link overstrength was computed with respect to V_n using actual measured static yield stress. All specimens tested in this program were shear yielding links, so the plastic shear capacity V_n is taken as V_p. The results obtained in all specimens are summarized in Table 4.1. The maximum shear, V_{max}, is the absolute value of the largest shear reached by the specimen during testing, and M_{max} is the absolute value of the greatest moment developed in the link at either the beam side or the column side. As indicated by the data in Table 4.1, link overstrength (V_{max}/V_n) for the test specimens ranges from 1.25 to 1.55,

131

with an average of 1.36. These results are fairly consistent with overstrength factors reported by Arce (2002) and other researchers.

4.2.1 Effect of material properties and stiffeners details on link overstrength

In the first series of the test program (Specimens 1 to 3) the specimens were nominally identical, except for the material properties of the W10x33 sections used to construct the specimens. All three specimens were A992 steel, but the steel used for the specimens came from three different mills, and therefore had somewhat different measured material properties (see Chapter 2). The material used for all three specimens had reasonably similar values of F_u and of F_u/F_y for coupons taken from mid-depth of the web. Consequently, reasonably similar link overstrength might be expected. However, as indicated by the data in Table 4.1, there is a significant difference between overstrength factors observed in Specimens 1 (V_{max}/V_n = 1.48) and 3 (V_{max}/V_n = 1.55 when compared with Specimen 2 (V_{max}/V_n = 1.29).

The differences in overstrength factors between the first three specimens may have resulted from differences in k-area properties. As shown in Figure 2.17, Specimens 1 and 3 exhibited higher hardness at the k-area than Specimen 2. Further, the measured tensile strength of material taken from the k-area is significantly higher for Specimens 1 and 3, as compared to Specimen 2 (see Table

2.6). It is possible that the high tensile strength exhibited in the k-areas of Specimens 1 and 3 contributed to the increase in the overstrength factor for these two specimens.

In the second test series (Specimens 4 to 7), all specimens were constructed using W10x33 sections from the same mill. These specimens used the same mill material as was used for Specimen 2 in the first test series. Consequently, Specimens 2, and 4 through 7 all used material from the same heat of steel. The differences in these specimens related to the arrangement and welding details of the stiffeners. Despite being made of the same material, these specimens exhibited somewhat different overstrength factors, ranging from 1.25 (Specimen 5) to 1.37 (Specimen 4). It appears that the arrangements of stiffeners played a role in the variation of overstrength in the specimens. For instance, Specimen 4 exhibited a higher overstrength factor than Specimen 2, although they were fabricated from the same material. It appears that the stiffeners provided in the back of the specimen helped increase the overstrength factor. The tendency for a higher overstrength factor in specimens with two-sided stiffeners is also exhibited by Specimens 6 and 9.

In Specimen 5 stiffeners were welded to the flanges only, and exhibited the smallest overstrength factor out of the 10 specimens. Also, Specimen 8, which was nominally identical to specimen 5, exhibited a similar overstrength factor

even though it was tested under a different loading protocol. It is possible that specimens with stiffeners not welded to their webs might exhibit lower overstrength factors than specimens with stiffeners welded to their webs. This lower link overstrength factor may be advantageous in EBFs, since less force is transferred to the remaining frame elements. In general, the arrangement and welding details of the stiffeners affect the degree of strain hardening that can develop before link strength is affected by instability or fracture within the link. In this manner, the stiffener details apparently influence link overstrength.

4.2.2   Effect of loading protocol on link overstrength

It appears that the loading protocol has some influence in the overstrength developed by the link. Nominally identical specimens exhibited different overstrength factors when tested with different loading protocols.

Specimens 8 and 9 were nominally identical to Specimens 5 and 6. However, Specimens 5 and 6 were tested using the severe loading protocol, whereas Specimens 8 and 9 were tested using the revised loading protocol, As indicated in Table 4.1, Specimens 8 and 9 exhibited higher overstrength factors. This phenomenon was observed by Ryu (2004) in nominally identical specimens when tested under different loading protocols. It appears that the loading protocol affects the overstrength factors in links.

134

Table 4.1 Overstrength factors

Specimen	V_p(Kips)	M_p (kip-in)	$2\dfrac{M_p}{e}$	V_n(Kips)	V_{max}(Kips)	M_{max}(kip-in)	$\dfrac{M_{max}}{M_p}$	$\dfrac{V_{max}}{V_n}$
1	91.0	2072	180	91.0	135	1650	0.80	1.48
2	93.3	2165	188	93.3	120	1469	0.68	1.29
3	90.4	2107	183	90.4	141	1753	0.83	1.55
4	93.3	2165	188	93.3	128	1545	0.71	1.37
5	93.3	2165	188	93.3	117	1544	0.71	1.25
6	93.3	2165	188	93.3	123	1507	0.70	1.32
7	93.3	2165	188	93.3	120	1395	0.64	1.29
8	93.3	2165	188	93.3	118	1381	0.60	1.26
9	93.3	2165	188	93.3	133	1589	0.69	1.42
10	93.3	2165	188	93.3	127	1538	0.66	1.36

Note: V_p, M_p, and V_n in this table are based on measured section dimensions and measured static yield stress values.

4.3   LINK END MOMENTS

The EBF test setup for this investigation was designed so that the initial elastic moment developed at the column end of the link would be greater than the initial elastic moment at the beam end of the link, as shown in Figure 2.2. This replicates the condition normally found in a single diagonal EBF where one end of the link is attached to a column. Because the elastic rotational stiffness at the column end of the link is typically larger than at the beam end of the link, the initial elastic link end moments are not equal. As the link yields, end moments tend to equalize. However, as indicated in the commentary of the *2002 AISC Seismic Provisions*, complete equalization of link end moments is not expected to occur for short shear yielding links.

In this section, data on the moment measured at both ends of the link are presented. The sign convention adopted for the calculation of resultants at the end of the links is shown in Figure 4.1. The moment on the column side is denoted as M_C and the moment on the beam side of the link is denoted as M_B. The dotted line shown on each of Figures 4.2 to 4.11 represents the condition where M_C equals M_B.

136
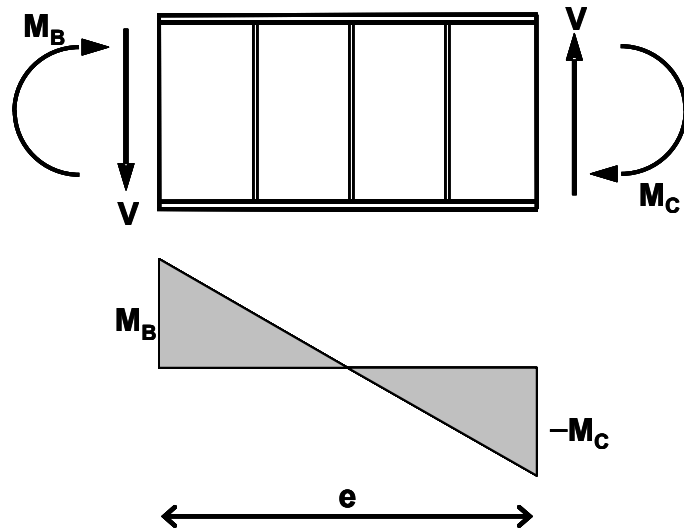
Figure 4.1 Sign convention used for link end force resultants

The plots indicate a higher initial moment at the column end of the link, as expected. Further, the plots show how moment redistributed from the column end of the link to the beam end of the link as the links yielded.

In Figure 4.11 for Specimen 10, the arrow points where the link started to exhibit irregular behavior. This coincides with the severe load degradation due to the propagation of the vertical crack at the welds of the center stiffener in the specimen. This behavior was also observed in the other specimens. Figures 4.2 to 4.11 also show an offset of the response with respect to the origin. This phenomenon was also observed by Arce (2002). It is believed that this phenomenon is the result of the movement of the clevises as the various reaction points of the test setup pass through zero force.
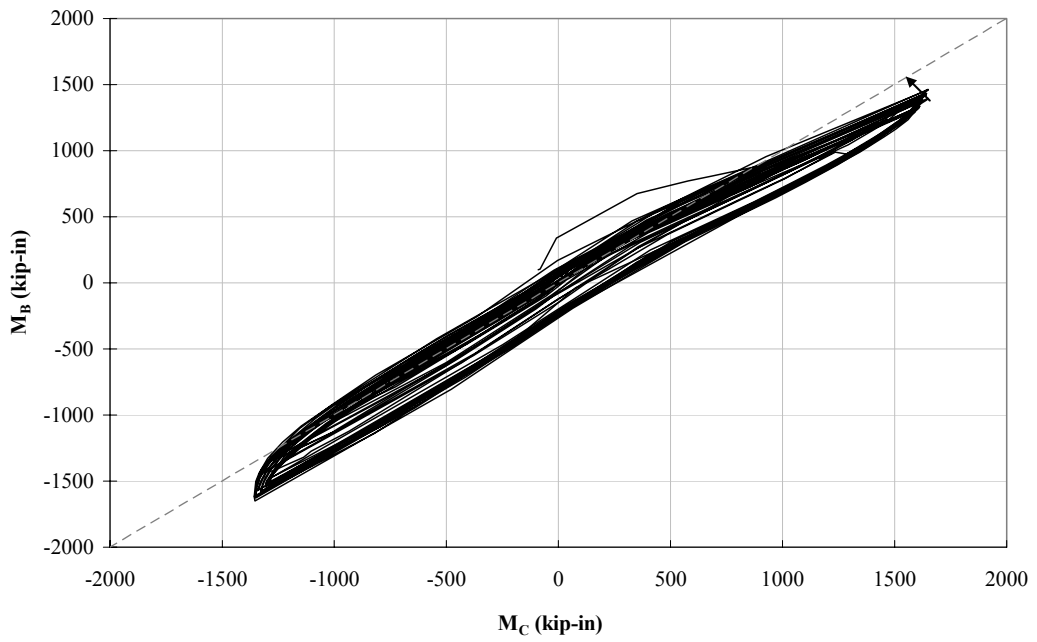
Figure 4.2 Link end moment relationship of Specimen 1
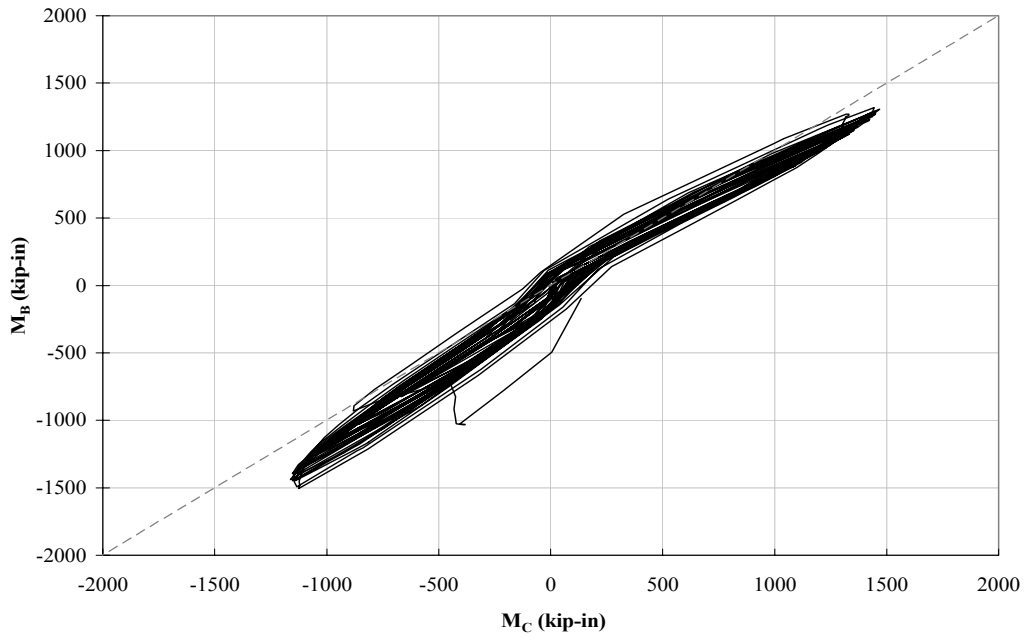
Figure 4.3 Link end moment relationship of Specimen 2

138

Figure 4.4 Link end moment relationship of Specimen 3

Figure 4.5 Link end moment relationship of Specimen 4

Figure 4.6 Link end moment relationship of Specimen 5

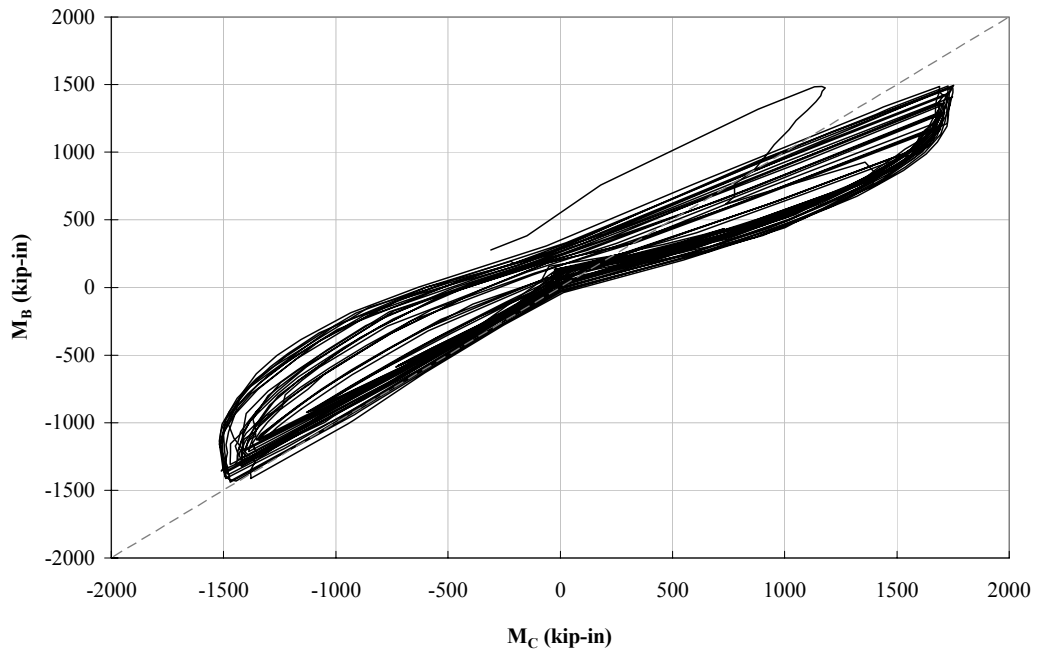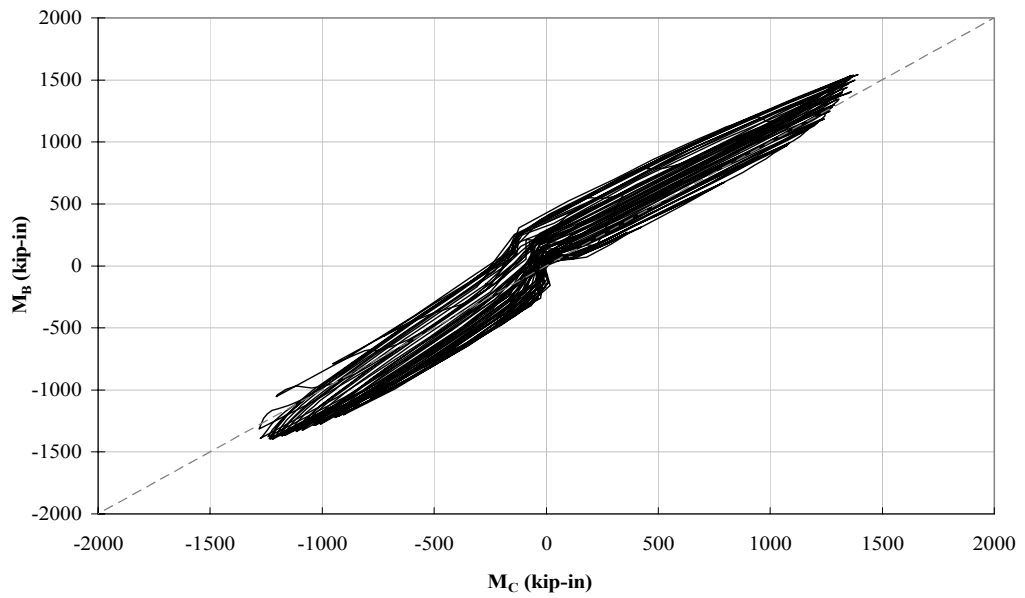*Figure 4.7 Link end moment relationship of Specimen 6*

140
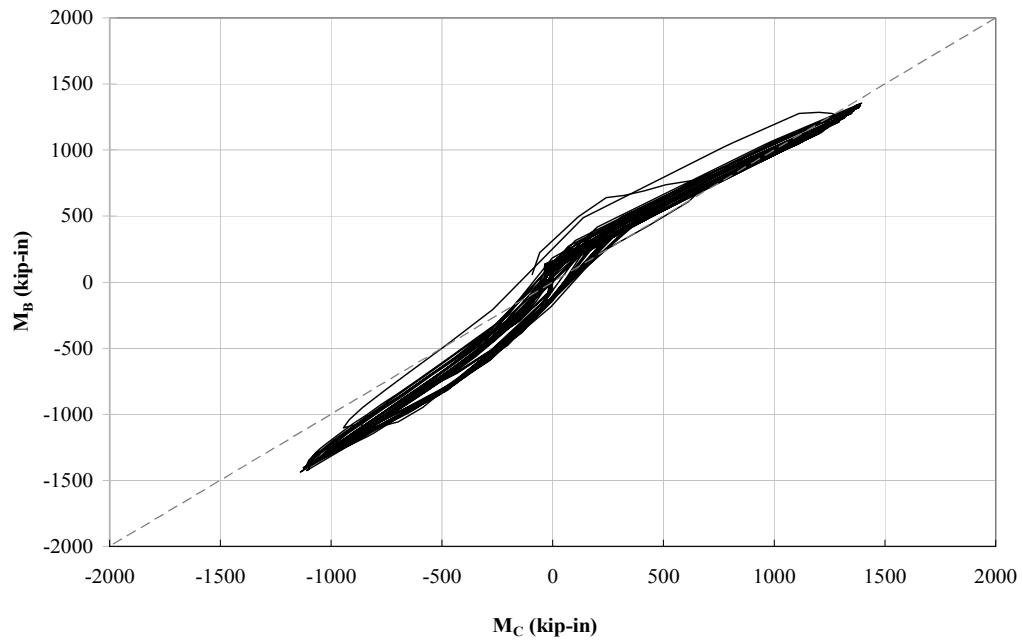
Figure 4.8 Link end moment relationship of Specimen 7
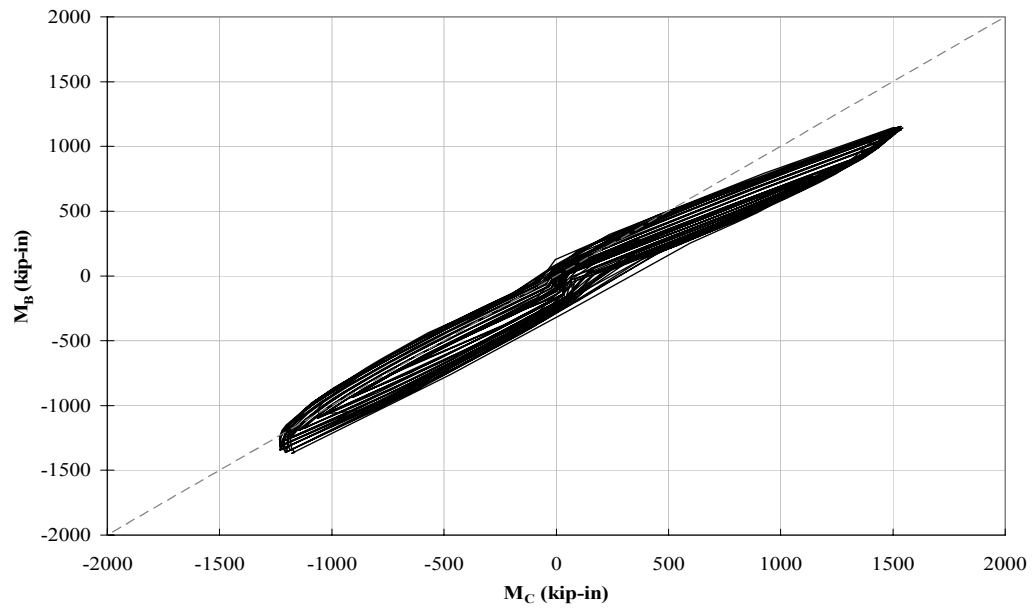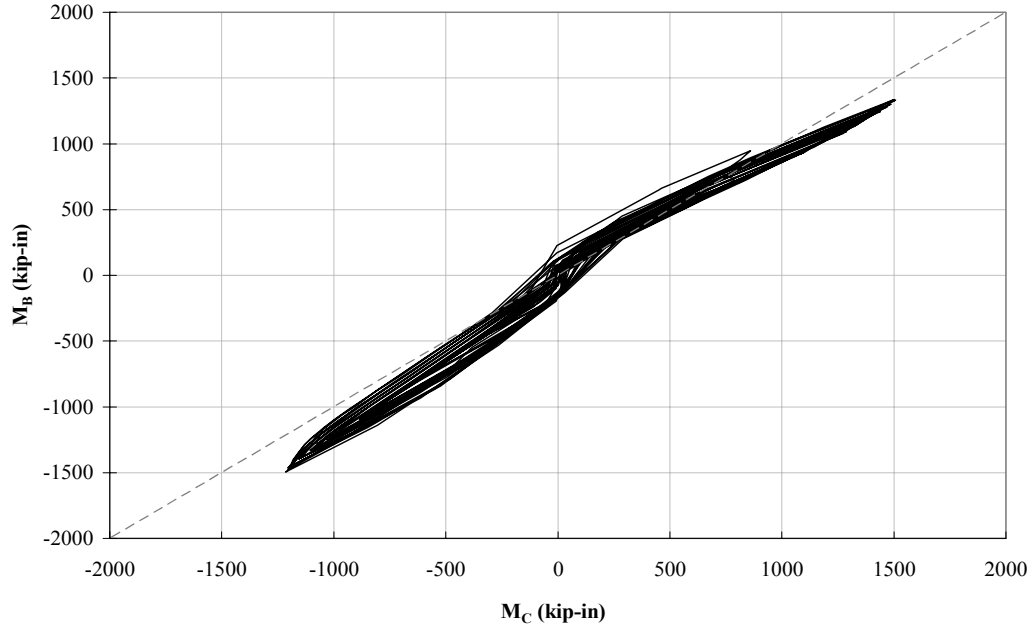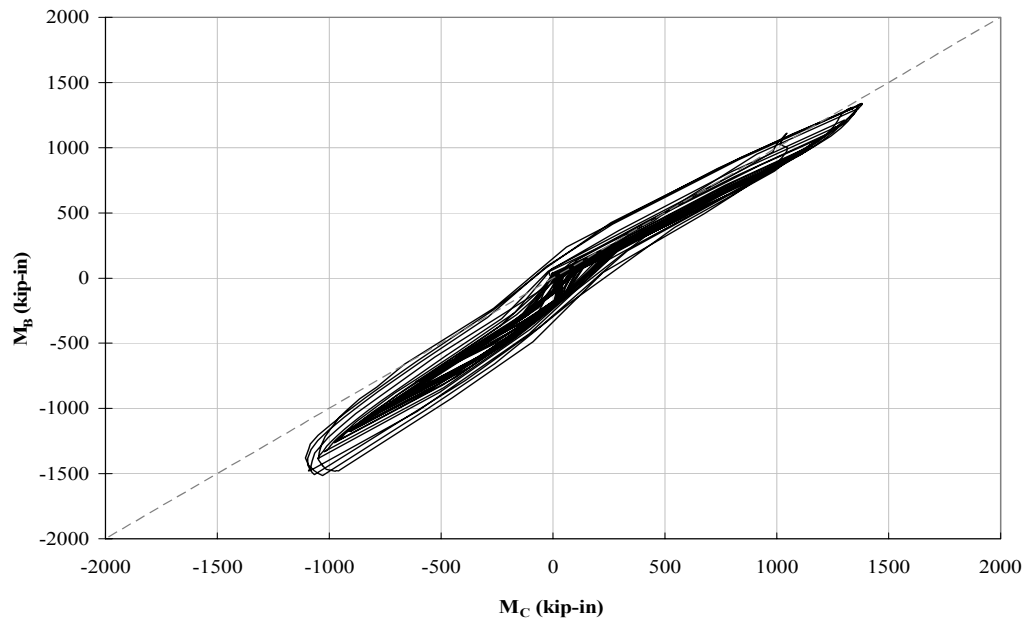

Figure 4.9 Link end moment relationship of specimen 8

141
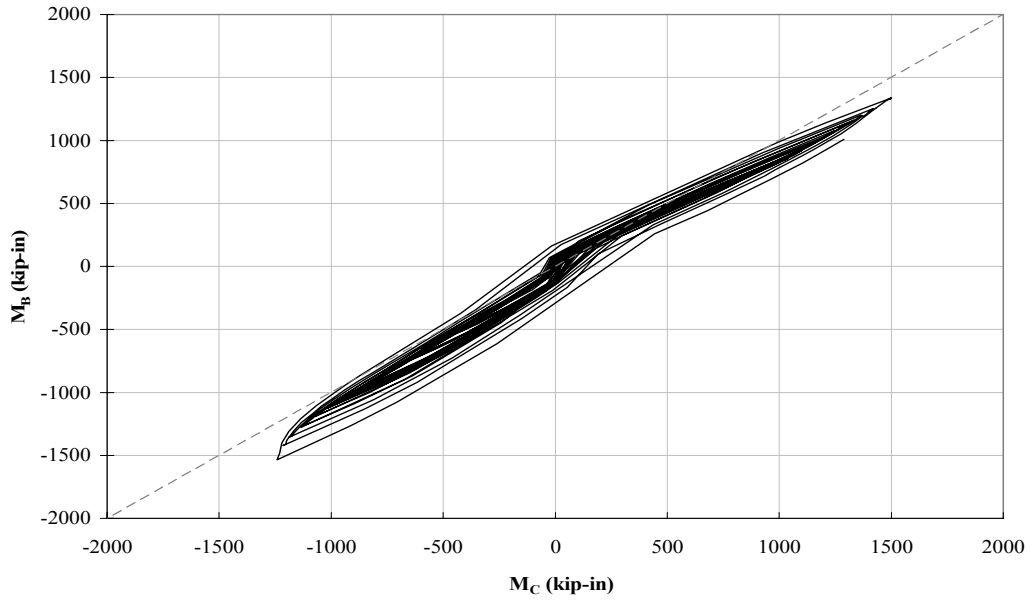
Figure 4.10 Link end moment relationship of specimen 9
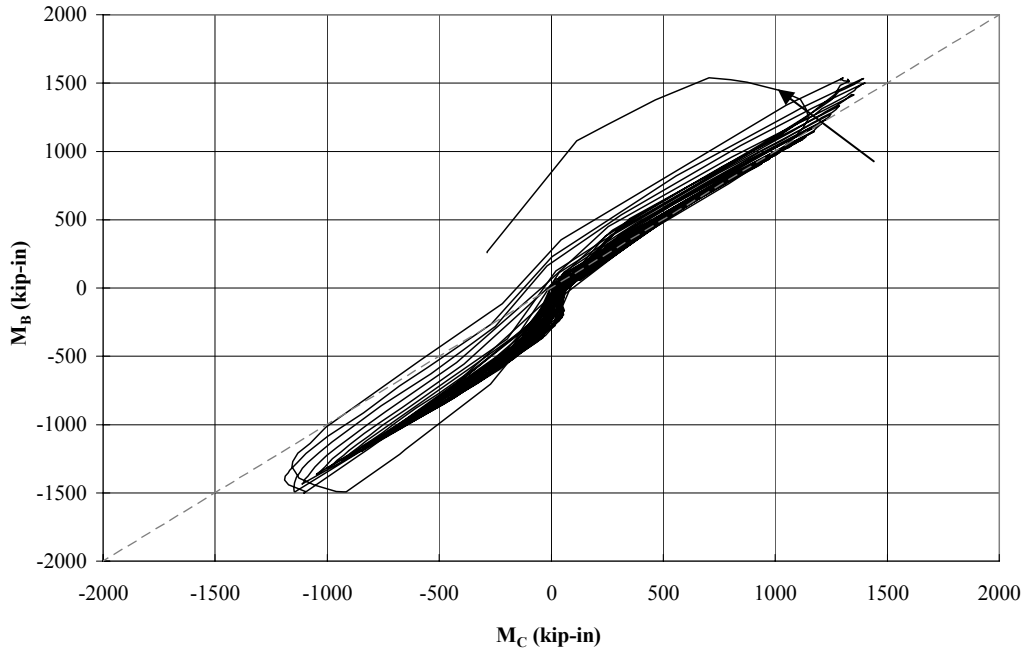
Figure 4.11 Link end moment relationship of specimen 10

142

CHAPTER 5
Summary and Conclusions

5.1   SUMMARY

This thesis has documented the results of a research program investigating the cause of web fractures in links of eccentrically braced frames (EBFs). In recent laboratory tests, EBF links have, in some cases, failed prematurely due to fracture of the link web (Arce 2002, Ryu 2004). The objective of this experimental program was to extend previous work by Arce (2002) and Ryu (2004) investigating the factors affecting the occurrence of web fractures in shear links.

All specimens tested in this program were built from A992 steel. The 10 shear links tested in this program were built from W10X33 sections. The first three specimens were built from steel from three different steel mills, designated in this report as Mills A, B and C. The rest of the specimens were built using steel from Mill B.

The test setup used to test the specimens was designed to reproduce forces and deformations that occur in a link in a single diagonal EBF. The first seven specimens were tested using a severe loading protocol to evaluate the effect of the different variables on the occurrence of web fracture. This severe loading protocol

was used to enhance the effect of different variables on the occurrence of web fracture. The plastic rotation developed by a specimen was the main parameter for comparison with other specimens. The final three specimens were tested using the revised loading protocol proposed by Richards and Uang (2004). The revised loading protocol was used to determine if selected links would meet acceptability requirements by developing the required plastic rotation of 0.08 radian set in the *AISC Seismic Provisions*.

In brief, this research program examined the following issues:

- Correlation of k-area material properties with link web fracture. Nominally identical specimens were built from W10X33 sections of A992 steel from Mills A, B and C. Hardness tests results of the k-area of each section of each Mill were different. It was postulated that poor material properties of the steel in the k-area were a factor responsible for the occurrence of web fracture.

- Effects of one-sided vs. two-sided stiffeners on link web fracture.

  It was postulated that links with two-sided stiffeners might fail at lower rotational levels than links with one-sided stiffeners. The additional welding in the k-area used to join the additional stiffeners may potentially cause web fracture at lower rotational levels.

- Effect of welding procedures on link web fracture.

It was postulated that the process used to weld stiffeners to the web of the link may influence the occurrence of web fracture. Two different welding procedures were investigated: SMAW with E7018 electrodes and FCAW process with E70T-6 electrodes.

- Effect of stiffener details on link web fracture.

    It was postulated that web fracture could be delayed or avoided by welding stiffeners to the web only or to the flanges only.

- Effect of stiffener spacing on link web fracture.

    In a final specimen, the role of the spacing between stiffeners was examined. It was postulated that stiffener spacing required under current code provisions might be a factor in the occurrence of web fractures. To investigate this possibility, one specimen was tested with stiffener spaced farther apart than that required by the *2002 AISC Seismic Provisions.*

5.2 RESULTS AND CONCLUSIONS

This section presents a brief description of the results obtained in this experimental program.

- Hardness tests on the k-area of the W10X33 sections from Mills A, B and C, were compared. Mill B exhibited the lowest hardness and Mill C exhibited the highest hardness. Also, tension coupons were taken from the k-area of each section. The k-area of the section from Mill B exhibited

145

better ductility than the k-area of the sections of Mills A and C. Therefore, it was postulated that the specimen built from Mill B would achieve a higher plastic rotation than those constructed using sections from Mills A and C. All three specimens ultimately failed by the development of web fracture in the k-area of the link sections, with fracture initiating at the termination of stiffener to link web welds. However, the specimen built using Mill B steel developed web fracture earlier than the others. Also, the specimen built using Mill C steel achieved a higher plastic rotation prior to web fracture. The results showed no clear correlation between k-area material properties and link rotation at web fracture.

- Even though k-area properties do not appear to change the mode of failure of the links, they appear to affect the maximum shear that a link can achieve. Specimens built from steel with higher ultimate stress in tension coupons taken from the k-area exhibited higher maximum link shear. This result suggests that there is a correlation between the strength of the k-area and the overall shear strength of the links. However, in deeper link sections the strength of the k-area may have less influence on the maximum link shear strength, since the k-area will likely represent a small fraction of the total web depth.

146

- The specimen built with two sided-stiffeners welded to its web and flanges did not develop web fracture earlier than the specimen which was built with one-sided stiffeners. In fact, the specimen with two-sided stiffeners sustained an additional loading cycle prior to failure. This result suggests that links with two-sided stiffeners are no more critical with respect to web fracture than links with one-sided stiffeners.

- The specimen built with stiffeners welded using the FCAW process exhibited web fractures earlier than the specimen built with stiffeners welded using the SMAW process. These results suggest that the higher heat input of the FCAW might prompt web fractures at an earlier stage resulting in lower plastic rotation. The welding procedure used for the stiffeners appear to be an important variable affecting the occurrence of web fractures. An additional specimen with stiffeners welded by FCAW was tested under the revised loading protocol and exceeded the plastic rotation required by the *2002 AISC Seismic Provisions*. Thus, even though the FCAW procedure proved to be detrimental to the link rotation capacity, the specimen still exceeded the 0.08 radian required by the *2002 AISC Seismic Provisions*.

- The specimen constructed with two-sided stiffeners welded to the flanges only did not develop web fractures in the k-area of the section. In addition,

the specimen reached a higher plastic rotation than similar specimens with stiffeners welded to the flanges and to the web. These results suggest that web fractures can be prevented by eliminating welding in the web of the specimen. This specimen was repeated and tested with the revised loading protocol. This specimen exceeded the plastic rotation requirement of 0.08 radian of the *2002 AISC Seismic Provisions*. The result suggests that links constructed with stiffeners welded to the flanges only can provide excellent cyclic performance, and merit further investigation.

- The specimen constructed with one-sided stiffeners welded to the web only failed earlier than the rest of the specimens. This specimen developed the same type of web fractures developed by the rest of the specimens. It appears that by eliminating the connection of the stiffeners to the flanges, web deformations help propagate cracks initiated at the termination of the stiffener welds.

- The specimen constructed with two stiffeners rather than three still developed web fractures. These results suggest that current stiffener spacing required by the *2002 Seismic Provisions* is not likely responsible for web fractures.

- Even though the specimen with only two stiffeners developed web fracture, it surpassed the required 0.08 radian plastic rotation. This result suggests the possibility of relaxing current stiffeners spacing requirements.

In conclusion, all specimens where stiffeners were welded to the web failed by web fracture initiated at the termination of the fillet welds. However, the specimens tested using the revised loading protocol met the required plastic rotation of 0.08 radian set by the *2002 AISC Seismic Provisions*.

The results from this program and other recent EBF research, i.e. Arce (2002) and Ryu (2004), indicate that shear links tested in recent years are exhibiting a fundamentally different failure mode compared to the many shear links tested in the 1980's. Recent tests on shear links consistently show link web fracture at or near the k-area as the dominant failure mode. Tests on many links conducted in the 1980's consistently showed web buckling as the dominant failure mode.

This test program has identified a number of factors that influence the occurrence of web fracture in shear links. However, the fundamental reason why web fracture has commonly been seen in recent shear link tests, and was not commonly seen in earlier shear link tests is still unclear.

This test program showed that the welding process used to connect the stiffeners to the link has an important effect on the occurrence of link web fracture. Links with stiffeners welded using the FCAW process developed web fractures significantly earlier in the loading sequence than links with stiffeners welded using the SMAW process. It appears that the higher heat input from the FCAW process contributed to the earlier development of web fracture. This suggests that a critical aspect of link web fracture may be as the as-welded properties of the k-area material. This test program showed no correlation between the occurrence of web fracture and the k-area material properties measured prior to welding. However, there is a possibility of a correlation between the occurrence of link web fracture and the material properties of the k-area as affected by welding. It is recommended that this possibility be explored in future research.

References

AISC(2002). "Seismic Provisions for Strucutral Steel Buildings," American Institute of Steel Construction,Inc., Chicago,IL.

AISC(2003). "Manual of Steel Construction", Third Edition. American Institute of Steel Construction, Inc., Chicago,IL.

ASTM A370-02 (2002), "Standard Tests Methods and Definitions for Mechanical Testing of Steel Products," American Society for Testing and Materials, West Conshohocken, Penssylvania.

Arce, Gabriela (2002) "Impact of Higher Strength Steels on Local Buckling and Overstrength of Links in Eccentrically Braced Frames," Department of Civil Engineering, The University of Texas at Austin

Hjelmstad, K.D and Popov, E.P. (1983). "Seismic Behavior of Active Beam Links in Eccentrically Braced Frames," *Report No*. UCB/EERC-83/15. Earthquake Engineering Research Center, University of California at Berkeley, Richmond, CA.

Malley, J.O and Popov, E.P (1984). "Shear Links in Eccentrically Braced Frames," Journal of Structural Engineering, ASCE Vol. 110, No 9, pp.2275-2295

McDanniel, CC., Uang, C.M. and Seible, F. (2002) "Cyclic Testing of Built-Up Steel Shear Links for the New Bay Bridge." Journal of Structural Engineering, American Society of Civil Engineering

Popov E.P. and Engelhardt, M.D. (1988) "Seismic Eccentrically Braced Frames," Journal of Constructional Steel Research, Vol. 10, 321-354

Richards, P. and Uang, CM (2003). "Development of Testing Protocol for Short Links in Eccentrically Braced Frames," Report No. SSRP-2003/08, Department of Structural Engineering, University of California at San Diego.

Tide R.H.R (2000) "Evaluation of Steel Properties and Cracking in "k-area of W Shapes." Engineering Structures, Vol. 22, 128-134

Vita

Pedro Gálvez was born in San Miguel, El Salvador on March 12, 1978, the son of Pedro Gálvez and Ana Julia Gálvez. He received his High School diploma in 1995 from Insituto Catolico de Oriente in San Miguel, El Salvador. Then, he attended Universidad Centroamericana "Jose Simeon Cañas" in San Salvador, El Salvador in 1996. In 1997, he entered Queens College in New York. Then, he transferred to St. John's University in New York in 1998. Finally, he transferred to Manhattan College in New York in May, 1999. He received the degree of Bachelor of Science from Manhattan College in May, 2002. In august, 2002, he entered the Graduate School at the University of Texas.

Permanent address: 155-01 90th Ave Apt 1-O
                      Jamaica, NY 11432

This Thesis was typed by the author.